Impact of water quality on UV disinfection of indigenous spores in surface, flocculated, and softened water from a drinking water treatment plant

By

Judith Straathof

In partial fulfillment of the requirements for the degree of

Master of Science
in Applied Earth Sciences

at Delft University of Technology,

Project duration:	February 2019 – July 2023	
Thesis Committee:	Prof. dr. ir. Natalie Hull,	Ohio State University
	Prof. dr. ir. Jan Peter van der Hoek,	TU Delft
	Prof. dr. ir. Merle de Kreuk,	TU Delft

Acknowledgements

I am deeply appreciative of the support that I have received from everyone around me who helped me finish my studies. I would not have been able to do this alone. Thank you to Dr. Natalie Hull, my advisor who guided me throughout every step of this thesis and gave me opportunities for invaluable experience that fostered my research interests. Without her continued support over many years, this report would never have been finished. Thank you to Dr. Zuzana Bohrerova, who guided me and gave me the skills necessary to excel in the laboratory, and the Ohio Water Resources Center that funded this research.

I also want to thank my teachers at Delft University of Technology who gave me the knowledge to pursue this research and supported me during unexpected circumstances that led me to be a visiting scholar at The Ohio State University. An extra thanks to Merle de Kreuk, Jan Peter van der Hoek, and Boris van Breukelen who went out of their way to ensure I could complete my studies and move on to the next chapter.

I am grateful to my classmates, especially Daniel Ma, Yijing Liu, Zanna Leciejewski, and Amanda Killian for their support, collaboration, and for creating an awesome environment in the lab. I am eternally thankful for the support and unconditional love I have received from my family and friends. This would not have been possible without any of you.

Abstract

UV disinfection is an efficient way to inactivate chlorine resistant protozoan pathogens such as *Cryptosporidium parvum* and *Giardia muris*. In the United States, regulatory UV disinfection credit is typically granted when turbidity is <1 NTU. However, studies show turbidity does not correlate well with UV dose responses and partial inactivation when turbidity is > 1 NTU should be considered to avoid certain violations while still protecting public health. The objective of this study was to examine the impact of worst-case scenarios at drinking water treatment plants on UV disinfection. Indigenous spores from unfiltered source water and samples taken during the flocculation and softening steps at the Dublin Road Water Treatment Plant in Columbus, Ohio were exposed to Low-Pressure mercury UV254 disinfection from July 2019 to January 2020. Raw source water and softened water had similar dose responses despite significantly different water quality parameters. Flocculated water had the worst dose response: significantly lower maximum inactivation rate and higher residual population density than the other two water types despite having a lower turbidity than softened water. The modeled Geeraerd-tail maximum inactivation rates (k_{max}) were 0.027, 0.021, and 0.030 cm^2/mJ for raw source, flocculated, and softened water, respectively. The modeled Geeraerd-tail residual population density values (N_{res}) were 1.168, 7.081, and 0.216 SFU/mL for raw source, flocculated, and softened water, respectively. Relationships between water quality parameters and modeled UV inactivation parameters were analyzed to determine and compare other potential indicators for UV disinfection to turbidity. Particle size and particle properties that govern the degree of particle-associated microorganisms best explained the differences in dose response between flocculated water and the other two water types. Larger particles are worse for UV disinfection. Microorganisms associated with particles are harder to disinfect with UV and lead to tailing. Climate change impacts on types, consistency, quantity, and quality of source waters for drinking water treatment make it especially important to understand UV disinfection kinetics under challenging scenarios. Informing regulatory changes to properly account for disinfection when turbidity is > 1 NTU could be especially useful for small or aged utilities that may not be as equipped to handle highly variable water qualities.

Table of Contents

List of Figures

List of Tables

List of Abbreviations

DOC	Dissolved organic carbon
DNA	Deoxyribonucleotide acid
DRWP	Dublin Road Water Plant
DWTP	Drinking water treatment plant
EPA	Environmental Protection Agency
IS	Integrating sphere
k_{max}	Maximum inactivation rate
N_0	Initial population density
N_{res}	Residual population density
NTU	Nephelometric turbidity unit
PP	Polypropylene
RED	Reduction equivalent dose
RNA	Ribonucleic acid
SFU	Spore forming unit
SUVA	Specific ultraviolet absorbance
TSS	Total suspended solids
UV	Ultraviolet
UVA	Ultraviolet absorbance
UVT	Ultraviolet transmission

Preface

Chapter 1 includes the background information and literature review. The next chapters and the appendix will be submitted in a manuscript for consideration for publication. Therefore, Chapter 2 has an abbreviated introduction, paraphrasing Chapter 1. Some material in Chapter 2 will be repetitive of Chapter 1. Chapter 3 details the methods section, Chapter 4 reports the results, Chapter 5 is the discussion, and Chapter 6 contains the conclusion and future recommendations.

1 Background

Ultraviolet (UV) light is widely used to disinfect water from drinking and wastewater treatment facilities. Advantages of UV disinfection over conventional chemical disinfection, such as chlorine disinfection, include effective inactivation of protozoan parasites, absence of harmful disinfection byproducts, and negligible disinfection by-product formation (Choi & Choi, 2010; Dotson et al., 2012; Masschelein & Rice, 2002). The main disadvantage of UV disinfection is the absence of residual disinfection, and other disadvantages include the electrical power requirement, photoreactivation and dark repair (Dotson et al., 2012). UV disinfection is especially effective against *Cryptosporidium parvum* and *Giardia muris*, which are protozoan pathogens whose (oo)cysts are difficult to remove or inactivate with coagulation, sedimentation, filtration, and chlorine disinfection (Betancourt & Rose, 2004). *Cryptosporidium* and *Giardia* cause gastrointestinal illnesses in humans, and infections can be extremely harmful for young children (Certad et al., 2017).

Regulation of UV disinfection is frequently based on conditions and doses to inactivate viruses and protozoa. Regulations and recommendations state that combined filter turbidity should not exceed the maximum value of 1 NTU and the 95th percentile monthly turbidity measurements should not exceed 0.3 NTU (Code of Federal Regulations §141.551 and Directive (EU) 2020/2184) at drinking water treatment plants (DWTP). Although turbidity is used to regulate UV disinfection because it is easy to measure and low-cost, utilities also monitor water quality with UV transmission (UVT) or UV absorbance (UVA) of the water because absorbance is used to calculate fluence for UV systems. Not meeting regulations in the United States leads to a tier 1 public notification where the utility must immediately notify the public. Public notifications erode consumers' trust in the utility, they should only be used when the drinking water may pose a risk to consumers' health. These regulations are in place because particles that contribute to turbidity can shield microorganisms during UV disinfection. Particulate matter in the water matrix can impact the effectiveness of UV disinfection by scattering, blocking, or absorbing UV light (Christensen & Linden, 2003) and by shielding microorganisms embedded within a particle from UV light. However, UV inactivation still occurs even when turbidity values are greater than 1 NTU (Amoah et al., 2005; Clancy et al., 2000; Passantino et al., 2004; Templeton et al., 2009).

One reason for reexamining the impact of turbidity on UV disinfection is that as climate change drives an increase in the frequency and intensity of extreme weather events, it causes changes in turbidity of source waters (Lee et al., 2015; Mi et al., 2019; Mukundan et al., 2018; Zhang et al., 2013). Multiple climate change factors project an increase in turbidity. Drought can increase turbidity and total suspended solids as there is less time and volume for settling and dilution of river source water into a reservoir before it is withdrawn for use (Hannoun et al., 2022). In other areas, climate change causes lakes to grow at unprecedented rates. Average lake turbidity increased significantly from climate-driven increase in sediment supply from source rivers and from sediment coming from erosion of recently submerged shorelines (Mi et al., 2019). For streams, global climate models forecast an increase in frequency and magnitude of hydrological

events that can generate high stream turbidity and cause water quality challenges for utilities in Northern America (Mukundan et al., 2018). With more frequent high-turbidity events, smaller and rural water utilities will disproportionately be impacted due to more frequent filter upset (Allaire et al., 2018). During filter upset particles go further downstream than designed, either through filter malfunction or issues with particles settling in the basin. As such, both small and larger utilities could benefit from a more accurate and updated understanding of how turbidity impacts UV disinfection and how it should be regulated. More research is needed to accurately determine if the disinfection credit at higher turbidity values can be increased.

1.1 UV inactivation

1.1.1 UV radiation

UV (Ultraviolet) light is a form of electromagnetic radiation with a wavelength between 100 to 400 nanometers. Common identification ranges of UV light are 315 – 400 nm (UV-A), 280 – 315 nm (UV-B), 280 – 200 nm (UV-C), and 100 – 200 nm (V-UV, vacuum ultraviolet). Light in the UV-C range is absorbed by proteins, ribonucleic acid (RNA), and deoxyribonucleic acid (DNA). Due to UV absorption by DNA/RNA, a chemical dimer is formed between two bases which inhibits formation of new DNA/RNA and inactivates organisms because they can no longer replicate (Bolton & Linden, 2003). The practical wavelength for UV disinfection is 200 to 300 nm (UVDGM, 2006). At water utilities, mercury lamps are commonly used. The wavelength of light emitted depends on the mercury vapor pressure. Low-pressure UV (LP-UV) lamps produce monochromatic UV light at 253.7 nm. Medium-pressure UV (MP-UV) lamps produce a broad spectrum (polychromatic) of light.

1.1.2 UV fluence

To study the response of microorganisms to UV in the laboratory bench scale apparatuses with collimated beams are used for experiments (Figure 1.1). The term “collimated beam” is commonly used in UV disinfection terminology, but the UV light beam does not have truly parallel rays. The UV light beam is collimated through multiple apertures. The sample is placed in a petri dish on a horizontal surface that allows for continuous stirring. Two apertures are used to create a homogenous irradiation field onto the sample in the petri dish. Not shown in Figure 1.1 is a physical shutter over one of the apertures used to regulate the exposure time.

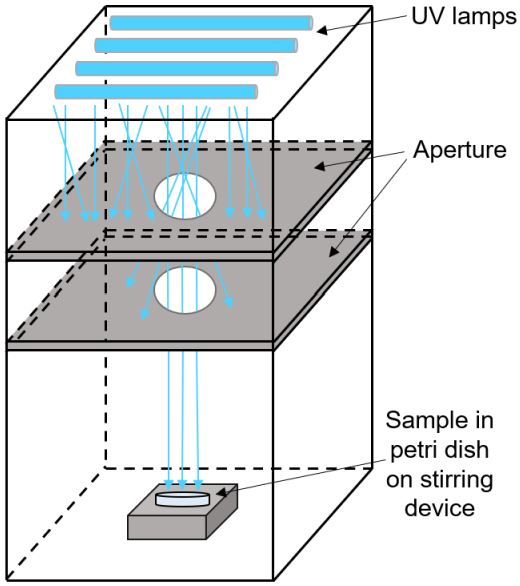

Figure 1.1. Example of bench scale UV device with a qausi-parallel/collimated beam. Not depicted is a physical shutter over one of the apertures used to regulate the exposure time. Modified from Bolton & Linden, 2003.

To determine how much UV light a microorganism in water has been exposed to, fluence rate and fluence need to be determined. "The fluence rate is defined as the total radiant power incident from all directions onto an infinitesimally small sphere of cross-sectional area *dA*, divided by *dA*" (Bolton & Linden, 2003). Fluence rate is dependent on the total radiant power incident from all directions, while the irradiance is defined as the total radiant power incident from all upward directions on a surface. Fluence rate and irradiance are effectively the same in well-designed UV experiments. In a UV collimated beam experiment, the fluence rate is constant and when multiplied by the exposure time it calculates the fluence. While dose is used to describe total absorbed energy, the fluence describes the total incident UV energy. (Bolton & Linden, 2003). Fluence usually has units of mJ/cm^2. Due to common terminology in literature, UV dose and UV fluence are used interchangeably.

A radiometer measures the irradiance incident on the water at the center of the UV light beam. There are corrections factors needed to calculate the average irradiance in the water, which provides the average fluence rate. The Reflection Factor accounts for when the beam of light passes from air into water. The refractive index changes and some amount of the light is reflected off the surface of the water sample. The Reflection Factor for air and water is 0.975 at 254 nm and represents the fraction of the UV incident beam that enters the water sample (Bolton & Linden, 2003). The Petri Factor accounts for the irradiance varying over the surface area of the water sample. The Petri Factor is defined as "the ratio of the average of the incident irradiance over the area of the petri dish to the irradiance at the center of the petri dish" (Bolton & Linden, 2003). It corrects the radiometer reading at the center of the dish to represent the average incident fluence rate more accurately over the entire surface area of the sample. The Water Factor corrects for the irradiance of the beam decreasing as it passes through the water sample due to being absorbed.

The absorbance of UV light in water through a one-centimeter path length and through the depth of the sample are used to calculate the Water Factor. The UV beam is quasi-parallel and not perfectly collimated, corrected by the Divergence Factor. The distance between the UV lamp and the surface of the water sample and the vertical path length of the water sample are used to calculate the Divergence Factor. For low pressure UV lamps the average fluence rate in the water is equal to the radiometer reading at the center of the petri dish and at the surface of the water level multiplied by the Petri Factor, Reflection Factor, Water Factor, and Divergence Factor. The average fluence is equal to the average fluence rate multiplied by the exposure time.

1.1.3 UV inactivation of microorganisms

Pathogenic microorganisms include bacteria, viruses, and protozoa including their (oo)cysts. The scope of this paper focuses on the inactivation of indigenous spores as a surrogate for oocysts. UV irradiation is an effective disinfection method against pathogenic protozoa in drinking water and wastewater treatment (Choi & Choi, 2010; Dotson et al., 2012; Masschelein & Rice, 2002). Microorganisms absorb UV light, leading to nucleic acid damage within the cells, ending its ability to reproduce and infect humans. The response to UV light varies among different microorganisms. A UV dose of 10 mJ/cm^2 achieved at least 4-log inactivation of five different *C. parvum* strains (Clancy et al., 2004) while a LP-UV dose of 159 to 337 mJ/cm^2 is needed for 4-log inactivation of adenoviruses (Augsburger et al., 2021). Drinking water treatment plants in the United States are required to use a minimum dose of 22 mJ/cm^2 for 4-log inactivation of *C. parvum* and *G. muris,* per US Federal Code of Regulations 40 CFR 141.720 (UVDGM, 2006). Most regulatory bodies recommend a fluence of 40 mJ/cm^2 during LP-UV inactivation and therefore it is commonly used by drinking water treatment plants.

Experiments are commonly performed with indicator organisms due to the impracticality of using pathogens in laboratory experiments. Drawbacks of using *Cryptosporidium* oocysts include high costs and difficulty producing and analyzing oocysts (Ryan & Hijjawi, 2015), low reproducibility of oocysts assays (Clancy et al., 1994), and low initial oocyst concentrations in raw or treated drinking water (Brown & Cornwell, 2007; Karanis et al., 2006). In this research, indigenous aerobic bacterial endospores and seeded *Bacillus subtilis* spores are used as surrogates of *Cryptosporidium* oocysts.

Aerobic bacterial endospores are very resistant to UV disinfection compared to *C. parvum* and also lab-strain spores, such as *Bacillus subtilis* ATCC 6633 (Mamane-Gravetz et al., 2005; Mamane-Gravetz & Linden, 2004, 2005). *Bacillus* species spores are 5 to 50 times more resistant to UV disinfection than their growing vegetative cells (Setlow, 2001). Aerobic spores are nonpathogenic, are simple and inexpensive to analyze (Mamane-Gravetz & Linden, 2004; Nieminski et al., 2000), and share similarities to oocysts, including an isoelectric point below pH 3, neutral to strongly negative zeta potentials, and glycoproteins on the exterior surface (Bradford et al., 2016). Aerobic bacterial spores are slightly smaller in size than oocysts. Aerobic bacterial spores are approximately 0.8 µm in width and range from 1 to 2 µm in length while *C. parvum* oocysts are 3.5 to 6 µm in size (Bradford et al., 2016; Feng et al., 2003). Due to being smaller and more resistant to UV disinfection, aerobic bacterial spores can serve as a conservative surrogate for *Cryptosporidium* oocysts. The main benefit of using indigenous aerobic bacterial spores as a

surrogate for *Cryptosporidium* in drinking water is that the indigenous spores from the source water undergo the same removal and mixing processes as *C. parvum* oocysts at the utility, possibly leading to similar proportions of attachment to particles and freely suspended. Multiple studies indicate that seeded indicator bacteria may be easier to inactivate than indigenous bacteria in unfiltered waters, not only due to the difference in resistance but also because free-floating bacteria are easier to inactivate than bacteria embedded in particles (Table 1.1). Meanwhile, "indigenous aerobic spores correlated to the removal of particles through coagulation, sedimentation, and filtration treatments" (Mamane-Gravetz & Linden, 2004; Rice et al., 1996) implying that they have particle associations during water treatment.

1.1.4 Dose response

UV dose response of microorganisms is expressed as log inactivation or log survival. The log inactivation is calculated as:

$$Log\ inactivation = log_{10}\frac{N_0}{N} \qquad \text{Eq 1.1}$$

where N_0 is equal to the concentration of microorganisms before UV irradiation and N is equal to the concentration of microorganisms after UV irradiation (N_t or N_F) at a given exposure time or fluence. When studying spores, both N_0 and N have units of spore-forming units per mL (SFU/mL). Many bacterial organisms exhibit shouldering at low UV fluence, a log-linear inactivation relationship at mid-range fluence and tailing at high fluence (Figure 1.2). The shoulder effect refers to an initial delay of inactivation before the log-linear region. The tailing effect refers to a decrease in inactivation after the log-linear region, nearing a plateau. It can indicate the presence of a residual population of microorganism(s) surviving at a high UV fluence.

The multi-target model is the accepted explanation for shouldering (Oguma et al., 2019; Severin et al., 1983). The multi-target model assumes that multiple critical targets in bacteria and spores must be hit by photons for complete inactivation, while viruses are completely inactivated by one single photon hit. There are multiple possible explanations for tailing. If there are multiple populations of microorganisms, one type of microorganism could be more resistant to UV than others (Mamane-Gravetz & Linden, 2004). Multiple studies show that one cause of tailing is due to the presence of bacteria associated with particles (Darby et al., 1993; Dietrich et al., 2003; Emerick et al., 2000; Farrell et al., 2018). The presence of self-aggregates where microbes are clumped together and protected from UV light is another possible explanation for tailing (Cerf, 1977; Kollu & Örmeci, 2015). Greater tailing is observed in effluents with larger flocs during UV disinfection (Azimi et al., 2014; Loge et al., 2001; Yong et al., 2008). Dormancy, strain resistance, strain variability, and cell growth status also affect tailing (Mofidi et al., 2002).

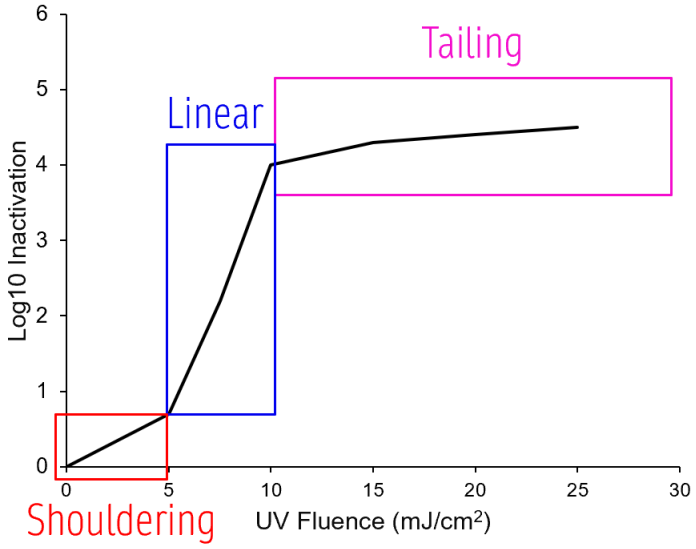

Figure 1.2. Example UV dose response with shouldering, tailing, and log-linear sections labeled.

The Geeraerd model (Geeraerd et al., 2000) is an inactivation kinetic model that can include shouldering and tailing. The Geeraerd model is a mechanistic model that includes biological parameters and is derived from:

$$N_t = (N_0 - N_{res}) \cdot e^{-k_{max}t} \cdot \left(\frac{e^{k_{max}S_1}}{1 + (e^{k_{max}S_1} - 1) \cdot e^{-k_{max}t}} \right) + N_{res} \qquad \text{Eq 1.2}$$

Where N is concentration (SFU/mL), t is UV exposure time, k_{max} is the maximum inactivation rate (time^{-1}), N_{res} is the residual population density (SFU/mL), and S_1 is the shoulder length in units of time. This equation has three phases: log-linear, shoulder, and tailing. To derive reduced models without shouldering or tailing, set S_1 or N_{res}, equal to zero, respectively. To transform this equation to eventually solve for inactivation, both sides of the equation were divided by N_0:

$$\frac{N_t}{N_0} = \left(1 - \frac{N_{res}}{N_0}\right) \cdot e^{-k_{max}t} \cdot \left(\frac{e^{k_{max}S_1}}{1 + (e^{k_{max}S_1} - 1) \cdot e^{-k_{max}t}} \right) + \frac{N_{res}}{N_0} \qquad \text{Eq 1.3}$$

Instead of using time as a variable, fluence, F (mJ/cm^2), will be used. S_1 is replaced by S_F (mJ/cm^2) and indicates shoulder length based on fluence instead of time. The maximum inactivation rate will have units cm^2/mJ:

$$\frac{N_F}{N_0} = \left(1 - \frac{N_{res}}{N_0}\right) \cdot e^{-k_{max}F} \cdot \left(\frac{e^{k_{max}S_F}}{1 + (e^{k_{max}S_F} - 1) \cdot e^{-k_{max}F}} \right) + \frac{N_{res}}{N_0} \qquad \text{Eq 1.4}$$

When applying the model to experimental data, the equation is log transformed to show log survival:

$$\log_{10}(\frac{N_F}{N_0}) = \log_{10}\left[\left(1 - 10^{log_{10}(\frac{N_{res}}{N_0})}\right) \cdot e^{-k_{max}F} \cdot \left(\frac{e^{k_{max}S_F}}{1 + (e^{k_{max}S_F} - 1) \cdot e^{-k_{max}F}}\right) + 10^{log_{10}(\frac{N_{res}}{N_0})}\right] \quad \text{Eq 1.5}$$

Without shouldering ($S_F = 0$):

$$\log_{10}(\frac{N_F}{N_0}) = \log_{10}\left[\left(1 - \frac{N_{res}}{N_0}\right) \cdot e^{-k_{max}F} + \frac{N_{res}}{N_0}\right] \quad \text{Eq 1.6}$$

Without tailing ($N_{res} = 0$):

$$\log_{10}(\frac{N_F}{N_0}) = \log_{10}\left[e^{-k_{max}F} \cdot \left(\frac{e^{k_{max}S_F}}{1 + (e^{k_{max}S_F} - 1) \cdot e^{-k_{max}F}}\right)\right] \quad \text{Eq 1.7}$$

For plotting, the equation was modified to log inactivation instead of log survival:

$$\log_{10}\left(\frac{N_F}{N_0}\right) = -\log_{10}\left[\left(1 - 10^{log_{10}(\frac{N_{res}}{N_0})}\right) \cdot e^{-k_{max}F} \cdot \left(\frac{e^{k_{max}S_F}}{1 + (e^{k_{max}S_F} - 1) \cdot e^{-k_{max}F}}\right) + 10^{log_{10}(\frac{N_{res}}{N_0})}\right] \quad \text{Eq 1.8}$$

For plotting without shouldering ($S_F = 0$):

$$\log_{10}\left(\frac{N_0}{N_F}\right) = -\log_{10}\left[\left(1 - \frac{N_{res}}{N_0}\right) \cdot e^{-k_{max}F} + \frac{N_{res}}{N_0}\right] \quad \text{Eq 1.9}$$

For plotting without tailing ($N_{res} = 0$):

$$\log_{10}\left(\frac{N_F}{N_0}\right) = -\log_{10}\left[e^{-k_{max}F} \cdot \left(\frac{e^{k_{max}S_F}}{1 + (e^{k_{max}S_F} - 1) \cdot e^{-k_{max}F}}\right)\right] \quad \text{Eq 1.10}$$

The mechanistic Geeraerd model was compared to the empirical quadratic model:

$$\log_{10}\left(\frac{N_0}{N_F}\right) = \mathrm{a} \cdot F^2 + b \cdot F + c \quad \text{Eq 1.11}$$

Where a is the quadratic coefficient, b is the linear coefficient, and c is the y-intercept, which is set to zero.

1.1.5 Reduction equivalent dose bias

The US EPA created a method to translate dose response information obtained from collimated beam testing to full-scale reactors. The reduction equivalent dose (RED) is "the UV dose derived by entering the log inactivation measured during full-scale rector testing into the UV dose-response curve that was derived through the collimated beam testing" (USEPA, 2006). The reduction equivalent dose is always specific to the challenge microorganism tested during experiments and the microorganism tested during validation test conditions in full-scale reactors. When the challenge microorganism (e.g., indigenous bacterial spores) is different from the target microorganism (e.g., *Cryptosporidium* oocysts), a RED bias value is included in the RED calculation. The RED bias is a correction that accounts for differences in microorganisms' inactivation kinetics (USEPA, 2006). RED bias tables are provided in the UV Disinfection Guidance Manual. When one microorganism is more sensitive than the other, non-perfect hydraulic conditions in UV reactors could have a more significant impact on the log reduction and therefore RED for the more sensitive microorganism. As an example of RED bias, consider a UV reactor operating at a dose of 22 mJ/cm^2, achieving 1 log inactivation for the challenge microorganism and 4 log inactivation for the more sensitive target microorganism, both with initial concentrations of 10^6 microorganisms/mL. In a worst-case scenario, with less than ideal hydraulic conditions, 1% of the water may not receive UV radiation. In that case, 0.999 log inactivation is achieved for the challenge microorganism, but 1.999 log inactivation is achieved for the more sensitive target microorganism, a difference of nearly two logs demonstrating a greater impact of RED bias on the more sensitive organism. RED bias factors are dependent on UV transmission and the UV sensitivity of microorganisms. The UV sensitivity is dependent on the log inactivation at a specific dose:

$$\text{UV sensitivity} = \frac{UV\ Fluence\ \frac{mJ}{cm^2}}{Log\ inactivation} \qquad \text{Eq 1.12}$$

1.2 Factors affecting UV inactivation

1.2.1 UV absorbance and scattering

UV absorbance is used for the design and operation of UV treatment units. The UV operating conditions depend on the absorption coefficient of the water that needs to be treated. The water itself and anything in the water, such as microorganisms or particles, absorb UV light. As stated in Section 1.1.2, the Water Factor accounts for the absorbance through the sample. Suspended particles can absorb, scatter, or reflect UV light away from the detector, which could lead to an incomplete absorbance measurement from a direct spectrophotometer. In a direct spectrophotometer (Figure 1.3a), reflected light may be registered as absorbed light, which incorrectly increases the absorbance measurement (Linden & Darby, 1998). Scattered light might still be available for inactivating microorganisms. Integrating sphere (IS) spectroscopy (Figure 1.3b) accounts for scattering due to particles (Christensen & Linden, 2003). Scattered light remains in the highly reflective sphere so that it can be detected as transmitted light by the instrument.

Integrating spheres are made of a material that exhibits high diffuse reflectance. Depending on the integrating sphere type, samples are placed inside the center of the sphere or on the outside against the sphere. There are four ports present on the integrating sphere: the transmittance port, reference port, sample reflectance port, and the reference beam entrance beam port (PerkinElmer, Inc, 2004). Ports can be closed depending on what needs to be measured. The sample beam enters the sphere through the transmittance port. To measure reflectance, samples can be placed inside of the sphere or mounted on the sample reflectance port on the outside of the sphere (Figure 1.3b).

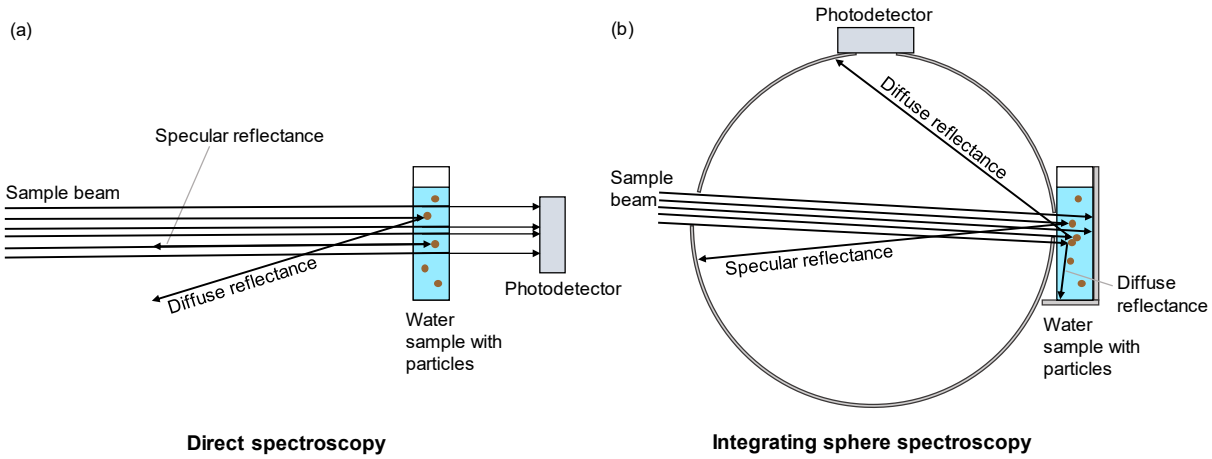

Figure 1.3. Direct spectroscopy (a) compared to integrating sphere spectroscopy (b). Not pictured is an 8° wedge at the sample reflectance port that angles the sample so that the specular reflectance is reflected within the integrating sphere. All specular reflectance and some diffuse reflectance is measured during integrating sphere spectroscopy in the set-up shown. Direct spectroscopy does not measure specular reflectance.

An 8° wedge is used to place the sample against the integrating sphere. With the wedge, specular reflectance is reflected into the sphere. Without a wedge to place the sample at an angle against the sphere, the specular reflectance would reflect out of sphere through the transmittance port it entered through originally and it would not be measured. Specular reflectance occurs when light rays reflect at the same angle to the surface normal as the incident light rays (sample beam) on the opposing side of the surface. While specular reflectance is often referred to as mirror-like reflection, diffuse reflectance scatters the light in a range of directions (Figure 1.4). Diffuse reflectance occurs when the surface is rough at a microscopic level, while specular reflectance occurs when the surface is smooth at a microscopic level. If the sample is placed on the inside of the integrating sphere, both specular and diffuse reflectance are measured. If the sample is placed on the outside of the integrating sphere with an 8° wedge, the specular and some of the diffuse reflectance is measured. Not all diffuse reflectance is measured because some of it may be scattered further into or out of the cuvette instead of into the integrating sphere. To correct for the absorbance overestimation during direct spectroscopy, the absorbance measured during integrating sphere spectroscopy should be subtracted from the direct spectroscopy absorbance measurement when measurements are taken with the sample on the outside of the integrating sphere.

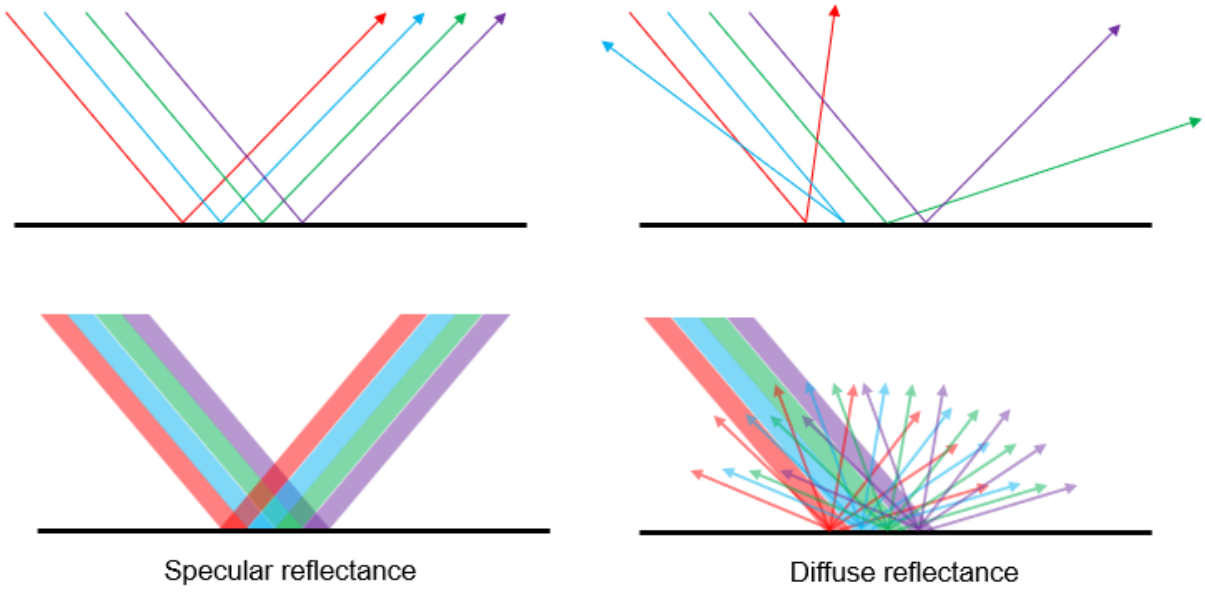

Figure 1.4. Comparison of specular reflectance and diffuse reflectance. When light is reflected at one definite angle it is defined as specular reflectance, occurring when the surface is smooth at a microspopic level. When light is reflected at many angles it is defined as diffuse reflectance, occuring when the surface is rough at a microscopic level.

Besides the surface of particles, the wavelength of light can also impact the intensity of scattering. Known as the Tyndall effect, or Tyndall scattering, shorter wavelengths are more diffusely reflected than longer wavelengths (He et al., 2009). Although commonly it is mentioned in relation to visible light with wavelengths of 400 to 750 nm and not a concern for UV sources with monochromatic light, it should be considered for polychromatic UV light. The Tyndall effect is present when particles range in size from approximately 40 to 900 nm (He et al., 2009).

1.2.2 Turbidity

Turbidity is the cloudiness or haziness of the water. Turbidity is caused by both suspended and dissolved solids, such as clays, silts, organic and inorganic matter. It is an optical property of the liquid, measured by the amount of light scattered. Correlation between turbidity with the particle number concentration or weight is complex because the shape, size, and refractive index of the particles affect light scattering. It is easy and affordable to measure turbidity for water utilities. Turbidity is used to regulate UV disinfection. Water treatment plants in the United States do not get inactivation credit for *Giardia* or *Cryptosporidium* when the combined filter turbidity exceeds the maximum value of 1 NTU or when the 95th percentile monthly turbidity measurements is above 0.3 NTU. There are studies that show turbidities higher than 1 NTU do not impact UV disinfection (Table 1.1). If turbidity is below 10 NTU it is does not impact the UV inactivation of spiked organisms when correcting for light scattering (Amoah et al., 2005; Batch et al., 2004; Christensen & Linden, 2003; Clancy et al., 2000; Oppenheimer et al., 2002; Passantino et al., 2004). Although turbidity is used by regulatory agencies to set restrictions and guidelines for UV disinfection as well as monitor the quality of UV disinfection, there are other water quality parameters that could have an impact on and provide an indication of the effectiveness of UV

disinfection. For example, results from Madge & Jensen (2006) showed that turbidity and total suspended solids did not correlate with the disinfection rate and tailing. Using turbidity as the only measurement for UV disinfection regulation is insufficient to account for the impact of particle shielding (Caron et al., 2007). Table 1.1 summarizes the effect of turbidity on UV disinfection.

1.2.3 Particles

Particles can scatter, absorb, or block UV light from reaching a microorganism. Any matter suspended or dissolved in water is referred to as solids. Total solids are the material residue left behind after evaporation and drying. Total suspended solids (TSS) are the solids retained by a 0.45 µm filter (Rice et al., 2012). Particles that passed through the filter are called dissolved solids.

Particle size analysis of the water can provide information on the size distribution of the particles present in the water. Particle size parameters include surface area moment mean, volume moment, mean, percentiles of the volume weighted particle size distributions (10%, 50%, 90%), and cumulative particle size fractions. The surface area moment mean, also known as the Sauter Mean Diameter, is sensitive to the presence of fine particles. The volume moment mean, also known as the De Brouckere Mean Diameter, reflects the size of the particles that make up the bulk of the sample volume. It is sensitive to the presence of large particles. The 50^{th} percentile is the median particle size by volume, the value of the 50^{th} percentile is the maximum particle diameter below which 50% of the sample volume exists.

Particle shielding decreases the level of inactivation of microorganisms (Emerick et al., 1999; Jolis et al., 2001; Loge et al., 1999, 2001; Madge & Jensen, 2006; Örmeci & Linden, 2002; Parker & Darby, 1995; Qualls et al., 1983, 1985). Amount, size distribution, and chemical nature and structure of the particles are better predictors for potential shielding of microorganisms during UV disinfection than turbidity (Liu et al., 2007; Mamane & Linden, 2006b; Qualls et al., 1985; Templeton et al., 2005). The number and size of particles, the degree of association between microorganisms and particles, and the nature of the particles determine the extent of influence that particles have on UV inactivation (Caron et al., 2007).

Multiple studies have researched for size thresholds of particle impact on microorganism shielding during UV disinfection (Table 1.1). Shielding of coliform and indigenous surface water aerobic bacterial spores during UV disinfection has been mainly attributed to particles larger than 7 – 10 µm (Cantwell et al., 2010; Caron et al., 2007; Jolis et al., 2001; Madge & Jensen, 2006; Qualls et al., 1983) and particles smaller than 20 µm did not impact UV inactivation of *Mycobacterium terrae* (Bohrerova & Linden, 2006). In Amoah, et al. (2005), turbidity below 10 NTU did not have a measurable effect on *C. parvum* and *G. muris* and the naturally occurring particles from lake water contributing to the turbidity were mainly 5 to 25 µm in size. Particle size had a significant effect on *E. coli* inactivation at high UV fluence, with 25 µm particles shielding *E. coli* more than 3.5 and 11 µm sized particles (Kollu & Örmeci, 2012). One study showed that particles did not have an adverse effect on UV disinfection, but authors noted that the concentration of particles above 10 µm may not have been high enough to offer protection (Templeton et al., 2009). Particles over 20 and 40 µm provided more coliform protection than particles smaller than 20 µm even though there was a larger number of the smaller particles (Qualls et al., 1985). Winward et al. (2008) showed that UV disinfection efficacy is linked to particle size fractions.

Although a size threshold has not been determined, larger particles have a greater negative impact on UV disinfection. Table 1.1 summarizes the effect of turbidity and particle size on UV disinfection.

Microorganisms can be free-floating and dispersed in the water or attached to or embedded within particles. Microorganisms can also form self-aggregates. The degree of association microorganisms have with particles affects the impact of particle shielding during UV disinfection (Caron et al., 2007). For the same UV fluence, self-aggregates and particle-associated microorganisms are inactivated less than microorganisms freely suspended with particles in the water sample (Mamane & Linden, 2006a; Örmeci & Linden, 2002). The proportion of microorganisms freely dispersed, attached to or embedded within particles varies for different particles, water sample types, and for different types of microorganisms. Microorganisms attached on the outside of a particle or loosely attached within a particle are less likely to be shielded than microorganisms located deep within a particle. The size of self-aggregates can also impact the amount of shielding, depending on how dense the aggregate is. (Mamane & Linden, 2006a). Depending on the structure, porosity, and density of the particle and the location of the microorganism within a particle, UV light can still inactivate microorganisms if light-accessible pathways are present within the particle (Emerick et al., 2000). Therefore, studies that use seeded or spiked microorganisms are not representative of the level of association between indigenous microorganisms and particles of their source water.

Just like turbidity, determining a well-defined particle size threshold is difficult. An explanation for this is the proportion of free-floating microorganisms to particle-associated microorganisms. Free-floating microorganisms are considered to be easily disinfected, while the particle-associated microorganisms attached to or enmeshed within the particle affects shielding and are considered difficult to disinfect (Caron et al., 2007), resulting in the majority of tailing effects (Tan et al., 2017). For the same UV fluence, self-aggregates and particle-associated microorganisms are inactivated less than freely suspended microorganisms when particles are present (Mamane & Linden, 2006a; Örmeci & Linden, 2002). Microorganisms attached on the outside of a particle or loosely attached within a particle are less likely to be shielded than microorganisms located deep within a particle. The size of self-aggregates can also impact shielding, depending on aggregate density (Mamane & Linden, 2006a). Degree of association are dependent on particle size, structure, amount, surface charge, and hydrophobicity (Cantwell & Hofmann, 2008; Templeton et al., 2008), with zeta potential having a higher significant impact on degree of tailing than turbidity and absorbance (Soleimanpour Makuei et al., 2022). Depending on the structure, porosity, and density of the particle and the location of the microorganism within a particle, UV light can still inactivate microorganisms if light-accessible pathways are present (Emerick et al., 2000). Seeded and indigenous microorganisms may also have variable proportion and degree between free suspension and particle-attachment if lab mixing and timing parameters are not the same as the sample source. In one study, 30% of seeded *C. parvum* and *G. lambia* attached to particles during the first few minutes of mixing, and increased to 75% after 24 hours (Medema et al., 1998).

The nature of the particle can impact the level of microorganism shielding during UV disinfection. Composition, structure, porosity, and surface charge impacts the relationship between

microorganism and particles (Mamane & Linden, 2006a). Hydrophobicity and surface charge can impact microbial surface adhesion to particles and microbes (Mamane-Gravetz & Linden, 2005). Flocculated particles have a different impact on UV disinfection than natural surface water particles (Liu et al., 2007). Different mixing parameters (flow speed, width of channel) at water treatment plants introduce variable shear forces that can also impact the amount of particle-microorganism attachment. Additionally, it can be difficult to replicate attachment of spores to particles from water treatment plant in bench scale experiments at a lab. Flocculated particles are made at a water treatment plant when coagulants are added to the water to combine ions and smaller particles into larger, heavier particles (flocs or flocculated particles) that will settle. Aluminum sulfate [$XAl(SO_4)_2 \cdot 12H_2O$], or alum, is a commonly used coagulant. Alum coagulation flocs are porous with a lot of surface area (Gorczyca & Ganczarczyk, 2001).

With the presence of particles, microbes may need to be extracted before enumeration. Previous research for need of bacterial extraction prior to enumeration widely differs (Liu, 2005) (Table 1.1), ranging from physical processes and chemical extractants to not using an extractant method. This suggests that the need for bacterial extraction prior to enumeration is dependent on the water, particle, and organism types.

Table 1.1. Impact of turbidity and particles on microorganisms during UV disinfection

Literature source	**Water type**	**Water Matrix Change**	**Target Organisms**	**Microbial Method**	**Extraction Method**	**UVA (cm^{-1}) or UVT (%) at 254 nm**	**Turbidity (NTU)**	**Particle size (µm)**	**Impact on UV inactivation**
(Amoah et al., 2005)	Untreated lake water	Concentrate lake particles	Seeded *G. muris*, *C. parvum*	Mouse infectivity assay	Centrifugation	Not specified	0.3–20	Majority 5–25	No (when turbidity < 10 NTU)
(Batch et al., 2004)	DWTP effluent (GW, lake, river)	Dechlorinated	Seeded MS2 coliphage	Top agar assay	NA	<0.4, except one utility ~0.7	0.3	Majority < 10, but > 10 present	No
(Bohrerova & Linden, 2006)	Wastewater effluent	100, 41, 20 µm nylon net filtered	Seeded Myco-bacteria	Spot plating	NA	0.03–0.16 (0.45 with spiked Myco-bacteria)	1.00–15.56	Majority 0.06–4.5, but on average at least 15 particles/mL >41	Yes (when self-aggregates or particles are > 41 µm)
(Cantwell et al., 2010)	Unfiltered surface water	NA	Total coliforms and total aerobic spores	MF (coliforms), agar plate enumeration (spores)	NA	mostly ~90% (max 97%, min 82%)	0.13-17.9, 99% <5.6	<10, 10–100	Yes (when particles > 10 µm)
(Caron et al., 2007)	Two surface waters	Unfiltered and 8 µm filtered	Indigenous aerobic spore-forming bacteria	MF - Barbeau method	Chemical extractant, blending at 8000 rpm for 4 min	River 1 88-94%, River 2 40-55%	10–35, <1.5	5-10, 10–20, >20, majority 5-10	Yes (amount of particles > 8 µm correlated when trying to achieve > 2 log inactivation)
(Carré et al., 2018)	Activated-sludge effluent	Addition of mixed liquor from aeration tank	Total coliforms, *E. coli*, enterococci	MPN	NA	Unfiltered 57–71.6%, filtered 70.2–71.2%	0.6–23.3	>2, 2–5, 5–25, >25	Yes (strong correlation between tailing and particles > 25 µm)

Table 1.1 (continued). Impact of turbidity and particles on microorganisms during UV disinfection

Literature source	Water type	Water Matrix Change	Target Organisms	Microbial Method	Extraction Method	UVA (cm^{-1}) or UVT (%) at 254 nm	Turbidity Value (NTU)	Particle size (µm)	Impact on UV inactivation
(Christensen & Linden, 2003)	Raw water (DWTP)	Filtered to make size fractions, diluted to vary turbidity	NA (tested UV dose)	NA	NA	<40 µm: 0.044-0.27, 54-90% (IS 0.021-0.23, 58-95%), <11 µm: 0.044-0.25, 57-90% (IS 0.014-0.18, 66-97%), <5 µm 0.051-0.27, 53-89% (IS 0.035-0.24, 57-92%)	<40 µm: 0.057-16.2 <11 µm: 0.057-10.1 <5 µm: 0.046-10.1	0–5, 0–11, 0–40	Yes (when turbidity > 3 NTU, can account for it with proper IS absorbance measurement)
(Clancy et al., 2000)	DI water, backwash recycle water	NA	Seeded *C. parvum* oocysts	Mouse infectivity assay	NA	Not specified	DI: < 1, backwash water: up to 11	Not specified	No
(Darby et al., 1993)	Activated sludge secondary effluent	Unfiltered and filtered (0.9mm sand filter)	Total coliforms	MTF/MPN	NA	Unfiltered: 78.0 (4.4)% filtered: 75.6 (6.9)%	unfiltered: 3.8 (1.5) filtered: 1.1 (0.4)	Peaks at 1 and 35	Yes (but filtering increased UV disinfection efficacy)
(Emerick et al., 1999)	Wastewater influent	Unfiltered, 80 and 11 µm filtered	Total coliforms	MTF, fluorescent microscopy	NA	Activated sludge: 69.4–76.2%, Trickling filter: 68.6%, Aerated lagoon: 51.6%, Facultative lagoon: 27.2%	Not specified	up to 200	Yes (particles > 10 µm increase tailing effect)

Table 1.1. (continued) Impact of turbidity and particles on microorganisms during UV disinfection

Literature source	Water type	Water Matrix Change	Target Organisms	Microbial Method	Extraction Method	UVA (cm^{-1}) or UVT (%) at 254 nm	Turbidity Value (NTU)	Particle size (µm)	Impact on UV inactivation
(Guo & Hu, 2012)	DWTP (pre/post coagulation & MF/UF filtration)	Alum addition	MS2 bacterio-phage	Double agar layer enumeration	NA	Not specified	1–5	Not specified	Yes (inactivation rate increased with alum addition)
(Jolis et al., 2001)	Filtered secondary effluent	Alum and polymer addition, 8 µm filtered	Total coliforms	Not specified	NA	Not specified	0.2–4.8	Wide range, but majority < 7	Yes (when particles > 7 µm)
(Kollu & Örmeci, 2012)	DI water	Alginate, calcium, latex particles	Seeded *E. coli*	MF	Vortex (45 s)	Not specified	Not specified	1, 3.2, 11, 25, 45	Yes (at high doses only)
(Liu et al., 2007)	River water and WTP process water (floc/coag)	NA	Seeded *E. coli*	MF	None	River: 0.24–0.34 Process: 0.31–0.38	River: 12–32 Process: 5.3–17	River: 0.5–8.1, Process: 5.4–38.2	No (river water), Yes (when floc particles present)
(Madge & Jensen, 2006)	Wastewater (2 WWTPs)	NA	Fecal coliform	MPN	Chemical extractant with blending on some samples	Pre-chem A: 59.7 (4.5)%, B: 38.2 (7.3)%, Post-chem A: 39.6 (3.9)% B: 24.5 (4.7)%	A: 5.4 (1.3) B: 8.0 (2.9)	Not specified	Yes (when particles > 20 µm)
(Mamane & Linden, 2006a)	Simulated drinking water	Addition of montmorillo-nite clay, NOM, alum, varied pH	seeded *B. subtilis* spores	Pour plating	Blending	Not specified	0.46–17.8 (additions of 0, 5, 10 NTU clay particles)	Average up to 2.47, most averages ~1	Yes (< 0.3 log inactivation decrease for spore-clay aggregates)

Table 1.1. (continued) Impact of turbidity and particles on microorganisms during UV disinfection

Literature source	Water type	Water Matrix Change	Target Organisms	Microbial Method	Extraction Method	UVA (cm^{-1}) or UVT (%) at 254 nm	Turbidity Value (NTU)	Particle size (µm)	Impact on UV inactivation
(Mamane & Linden, 2006b)	Natural raw water, simulated drinking water	Montmorillo-nite added to simulated drinking water	Seeded *B. subtilis* spores	Pour plating	NA	5 NTU clay + spores: ~0.28 (direct) ~0.17 (IS)	natural: 6.3–15.8, simulated: 0, 5, and 10	0.5–10.5	Yes (when turbidity > 5 NTU)
(Oppenheimer et al., 2002)	Raw, unfiltered water (DWTP)	NA	Seeded *C. parvum*, *G. muris*, MS2 coliphage	Mouse infectivity assay, MS2: ATCC 15597 B1 & *E. coli* (Adams 1959)	NA	Not specified	0.65–7.00	NA	No
(Örmeci & Linden, 2002)	Secondary wastewater effluent	Unfiltered and 5 µm filtered	Non- & Particle-associated coliform	MF	EGTA extraction, filtration, blending	Not specified	Not specified	2–5, 5–10, >10 (majority 2–5)	Yes (inactivation rate of non-particle > particle-associated coliform)
(Parker & Darby, 1995)	Secondary wastewater effluent	NA	Total coliforms, fecal coliforms	MTF/MPN	Blending and sonication with chemical extractant	Unfiltered: 60.9–72.4%, filtered: 66.5–73.9% (avgs)	1.30–3.95	Majority 1, particles >10 also present, peaks at 1, 8, and 35	Yes (particle-associated total coliforms are shielded)
(Passantino et al., 2004)	Natural unfiltered water and DI water	Addition of montmorillo-nite clay, algae to DI water	Seeded MS2 bacterio-phage	Double agar layer method, *E. coli* host (Adams, 1959)	NA	0.075–0.125 (74–84%)	3.0–12	Not specified	No
(Qualls et al., 1983)	Secondary wastewater effluent	Unfiltered, 8 and 70 µm filtered	Total coliforms, fecal coliforms	MPN	NA	Unfiltered: 0.179 (0.031), filtered: 0.161 (0.029)	Unfiltered: 4.9 (1.8) filtered: 2.1 (1.4)	<8, <70, >70	Yes (when particles > 8 µm)

Table 1.1. (continued) Impact of turbidity and particles on microorganisms during UV disinfection

Literature source	**Water type**	**Water Matrix Change**	**Target Organisms**	**Microbial Method**	**Extraction Method**	**254 nm UVA (cm^{-1}) or UVT (%)**	**Turbidity Value (NTU)**	**Particle size (µm)**	**Impact on UV inactivation**
(Qualls et al., 1985)	Secondary wastewater effluent	Unfiltered, 10 and 0.45 µm filter	Total coliforms	MF	NA	Unfiltered: 0.233 (0.073)	1.9 - 14 (unfiltered)	< 0.45, <10, > 10 (but particles classified in groups of 5-10, 10-20, >20	Yes (when particles > 40 µm, no significant impact for particles < 10 µm)
(Soleimanpour Makuei et al., 2022)	2 DWTPs prior UV disinfection, raw intake	NA	Seeded MS2 bacterio-phage, E. coli host	Pour plating (plaque counting)	NA	Raw intake: ~0.29-0.48, A: ~0.04-0.07, B: ~0.03-0.06	Raw intake: 1-3.5, A: 0.38 (0.09), B: 0.61 (0.33)	Raw intake: peaks at 0.69 & 5.17, A: 2-6, peak at 4.95, B: NA	Yes (30 min mixing to encourage potential particle-microorganism association)
(Templeton et al., 2009)	2 DWTPs with worst-case scenario conditions	Alum, activated silica, chemical coagulants	Total coliforms	MF	Chemical extractant with blending (20,000 rpm, 3 min)	A: 48-81%, B: 73-81%	Up to 2.9	Mainly 2–10, < ~5% particles >10	No
(Winward et al., 2008)	Treated wastewater effluent, treated grey water	NA	E. coli and total coliforms, Enterocci	MPN (E. coli & total coliforms) and MF (Enterocci)	Blending (4000 rpm for 60s)	grey: 47%, wastewater: 57%, treated grey: 62% (avgs)	grey: 18, wastewater: 10, treated grey: 6	Wide range, mainly 1–1233 for grey water	Yes (due to larger particle size)
Straathof Thesis 2023	Raw, Flocculated, Softened water from DWTP	NA	Indigenous spores and seeded *B. subtilis* spores	Pour plating	Manual shaking	See results section	See results section	See results section	Yes (impact due to larger particles and degree of microorganism particle-association)

1.2.4 Other water quality impacts

Dissolved organic carbon (DOC) is defined as the organic matter that passes through a 0.45 µm filter. DOC is degraded by UV radiation (Paul et al., 2012). DOC can have an impact on the final UV fluence. Specific ultraviolet absorbance (SUVA) is an indicator of water quality. SUVA provides a general characterization of the nature of natural organic matter (NOM) in a sample. SUVA is equal to the absorbance at 254 nm divided by the DOC.

1.3 Objective and research questions

The objective of this research is to determine the impact of filtration failure before or after coagulation and flocculation on LP UV disinfection of surface water, and to investigate relationships between the inactivation and various water quality characteristics. UV disinfection was performed on DWTP samples collected throughout one year at various stages of treatment using a LP UV bench scale apparatus to determine the log inactivation of indigenous bacterial endospores. Another goal is to translate the indigenous spore dose responses in the three water types to predict *Cryptosporidium* inactivation in similar scenarios as tested. Based on the purpose of this study, these questions are asked:

1. Is turbidity the best water quality parameter to govern UV disinfection regulations and standards? If not, what water quality parameter is better?
2. Is the best water quality parameter to govern UV disinfection different depending on water type?
3. Is a maximum turbidity value of 1 NTU during UV disinfection too conservative?

1.4 Research need

Other studies have analyzed the relationships between water quality parameters and UV disinfection. This study differs in that it more closely resembles potential reality at DWTP. One differentiating aspect is that indigenous spores from a DWTP are tested. It is more common to spike microorganisms than to use indigenous spores or pathogens. Seeded organisms can have different proportions of particle-associations, both due to the different nature of particles and mixing parameters/shear forces. Additionally, the water is collected from a DWTP and not simulated in a lab. To control turbidity value ranges and/or particle size fractions, some previous studies add particles or turbidity causing materials in the lab. In this study particles and turbidity will not be simulated in the lab, but naturally present from the flocculation/coagulation step and softening step. We expect that the source of turbidity and particles will have an impact on UV disinfection and therefore it is crucial to use water collected from the DWTP. This study will compare the water qualities between different turbidity sources present at a DWTP.

1.5 Thesis overview

Chapter 1 included background information and literature review. The next chapters and the appendix will be submitted in a manuscript for consideration for publication, therefore, Chapter 2 has an abbreviated introduction, paraphrasing Chapter 1. Chapter 3 details the methods section, Chapter 4 reports the results, Chapter 5 is the discussion, and Chapter 6 contains the conclusion and future recommendations.

2 Introduction

As climate change drives an increase in the frequency and intensity of extreme weather events, turbidity of source waters will increase in frequency and magnitude (Lee et al., 2015; Mi et al., 2019; Mukundan et al., 2018; Zhang et al., 2013). Multiple different climate change factors are projected to increase turbidity. Drought can increase turbidity and total suspended solids as there is less time and volume for settling and dilution of river source water into a reservoir (Hannoun et al., 2022). In other areas, climate change causes lakes to grow at unprecedented rates. Average lake turbidity increased significantly from climate-driven increase in sediment supply from source rivers and from sediment coming from erosion of recently submerged shorelines (Mi et al., 2019). For streams, global climate models forecast an increase in frequency and magnitude of hydrological events that can generate high stream turbidity and cause water quality challenges for utilities (Mukundan et al., 2018). More frequent high-turbidity events and lower source water quality pose challenges for unit processes at drinking water treatment plants, especially for smaller water utilities or aged utilities that may be less adept or funded to handle it. Coagulation is used to adjust turbidity. If an increase in alum or iron dosage and/or cationic polymer is not enough to remove turbidity-causing particles, particles can negatively impact other processes downstream, such as filtration and disinfection. Sometimes filters are operated under upset conditions which create opportunities for particle breakthrough to occur (Cantwell & Hofmann, 2008).

Ultraviolet (UV) light is widely used to disinfect drinking water and treated wastewater. Advantages of UV disinfection over conventional chemical disinfection, such as chlorine disinfection, include effective inactivation of protozoan parasites and negligible disinfection by-product formation (Choi & Choi, 2010; Dotson et al., 2012; Masschelein & Rice, 2002). The main disadvantage of UV disinfection is the absence of residual disinfection, and other disadvantages include the electrical power requirement, photoreactivation and dark repair (Dotson et al., 2012). Although UV disinfection is especially effective against protozoa, including *Cryptosporidium parvum* and *Giardia muris*, that are difficult to remove or inactivate with coagulation, sedimentation, filtration, and chlorine disinfection (Betancourt & Rose, 2004), water treatment plants in the United States do not get protozoan inactivation credit when the combined filter effluent turbidity exceeds the maximum value of 1 NTU or when the 95^{th} percentile monthly turbidity measurements is greater than 0.3 NTU during UV disinfection (as per Code of Federal Regulations § 141.551). Turbidity is used as a water quality indicator and can be easily, inexpensively, rapidly, and accurately measured (USEPA, 2006). Tier 1 violations require immediate notice to the public, through both media outlets and personally delivered notices to consumers. Tier 1 violations can be detrimental to public trust in the utility and should only be used when human health will be impacted. Small utilities especially could benefit from a more accurate and updated turbidity regulation value. The US EPA's Safe Drinking Water Information System database shows small water systems with financial difficulties are more likely to have violations (Eskaf, 2015). Safe consumption is the focus of water treatment plants, but it must be done in a cost-effective manner.

Although UV disinfection is regulated by turbidity, the UV system is designed and monitored by absorbance/transmission. The absorbance of the water sample is used to calculate the fluence. Particles can shield microorganisms from UV light, but they can also scatter the light, possibly leading to an apparent increase in absorbance. The current regulations are in place to account for potential water quality and particle shielding that can lead to microbial survival during UV disinfection. Particulate matter in the water matrix can impact the effectiveness of UV disinfection by scattering, blocking, or absorbing UV light (Christensen & Linden, 2003) and by shielding microorganisms embedded within a particle from UV light (Emerick et al., 1999; Jolis et al., 2001; Loge et al., 1999, 2001; Madge & Jensen, 2006; Örmeci & Linden, 2002; Parker & Darby, 1995; Qualls et al., 1983, 1985). Although regulations stipulate that turbidity values should remain below 1 NTU to avoid violations, partial inactivation has been observed (Amoah et al., 2005; Clancy et al., 2000; Passantino et al., 2004; Templeton et al., 2009) (Table 1.1).

Water quality characteristics, including turbidity, do not correlate well with UV inactivation or UV absorption (Cantwell & Hofmann, 2011; Soleimanpour Makuei et al., 2022). While some studies confirm absorbance as the most important process quality control and having a relationship with dose response (Tan et al., 2017; Wright et al., 2011), others show UVA and turbidity do not explain results (Farrell et al., 2018; Soleimanpour Makuei et al., 2022). Amount, size distribution, surface charge, chemical nature and structure of the particles charge have been shown to be better predictors for potential shielding of microorganisms during UV disinfection than turbidity (Farrell et al., 2018; Liu et al., 2007; Mamane & Linden, 2006b; Qualls et al., 1985; Soleimanpour Makuei et al., 2022; Templeton et al., 2005). The number and size of particles, the degree of association between microorganisms and particles, and the nature of the particles determine the extent of influence that particles have on UV inactivation (Caron et al., 2007; Farrell et al., 2018). This is further explained in Table 1.1.

Multiple studies have investigated size thresholds of particle impacts on microorganism shielding during UV disinfection (Table 1.1), indicating that larger particles tend to impact UV disinfection more negatively. Shielding of coliform and indigenous aerobic bacterial spores in surface water during UV disinfection has mainly been attributed to particles $\geq 7 – 10$ µm (Cantwell et al., 2010; Caron et al., 2007; Jolis et al., 2001; Madge & Jensen, 2006; Qualls et al., 1983). However, in some cases particles > 10 µm did not impact UV inactivation. Particles ≤ 20 µm did not impact UV inactivation of *Mycobacterium terrae* (Bohrerova & Linden, 2006). In Amoah, et al. (2005), turbidity < 10 NTU had no measurable effect on *C. parvum* and *G. muris* disinfection in lake water with naturally occurring 5 to 25 µm particles. Larger particles (≥ 25 µm) more significantly affected *E. coli* inactivation at high UV fluence than smaller (3.5 and 11 µm) particles (Kollu & Örmeci, 2012). One study showed that particles had no adverse effect on UV disinfection of coliforms, but the concentration of particles > 10 µm may have been inadequate for shielding (Templeton et al., 2009). Particles > 20 and 40 µm provided more coliform shielding than particles < 20 µm even though there were more smaller particles (Qualls et al., 1985). Winward et al. (2008) showed that UV disinfection efficacy of *E. coli*, total coliforms, and *Enterococci* is linked to particle size.

Attempts at determining a general particle size threshold impacting UV disinfection are further complicated by the degree of particle association of microorganisms. Free-floating microorganisms are considered to be easily disinfected, while the particle-associated microorganisms attached to or enmeshed within the particle affects shielding and are considered difficult to disinfect (Caron et al., 2007), resulting in the majority of tailing effects (Tan et al., 2017). For the same UV fluence, self-aggregates and particle-associated microorganisms are inactivated less than freely suspended microorganisms when particles are present (Mamane & Linden, 2006a; Örmeci & Linden, 2002). Microorganisms attached on the outside of a particle or loosely attached within a particle are less likely to be shielded than microorganisms located deep within a particle. The size of self-aggregates can also impact shielding, depending on aggregate density (Mamane & Linden, 2006a). Degree of association is dependent on particle size, structure, amount, surface charge, and hydrophobicity (Cantwell & Hofmann, 2008; Templeton et al., 2008), with zeta potential having a higher significant impact on degree of tailing than turbidity and absorbance (Soleimanpour Makuei et al., 2022). Depending on the structure, porosity, and density of the particle and the location of the microorganism within a particle, UV light can still inactivate microorganisms if light-accessible pathways are present (Emerick et al., 2000). Seeded and indigenous microorganisms may also have variable proportion and degree between free suspension and particle-attachment if simulated lab mixing and timing parameters are not the same as the DWTP. In one study, 30% of seeded *C. parvum* and *G. lambia* attached to particles during the first few minutes of mixing, and increased to 75% after 24 hours (Medema et al., 1998).

More research is needed to accurately reevaluate the 1 NTU turbidity threshold for receiving no credit for UV disinfection, and to explore potential alternative water quality parameters for ensuring regulatory compliance for UV disinfection efficacy of protozoan pathogens. This study builds on previous research to more closely approximate potential real-world worst case scenario conditions by investigating UV disinfection of indigenous rather than seeded microorganisms, and in DWTP source and unfiltered treatment process waters with extremely high turbidity rather than simulated water.

3 Methods

3.1 Dublin Road Water Treatment plant

Water samples were collected from Dublin Road Water Treatment plant (DRWP) in Columbus, OH (Figure 3.1). Dublin Road Water Treatment plant treats raw surface water from the Griggs and O'Shaughnessy Reservoirs on the Scioto River. After passing through rotating screens, aluminum sulfate [$XAl(SO_4)_2 \cdot 12H_2O$], (alum) is added for flocculation to cause coagulation. After rapid mixing, the flocculated particles settle in the sedimentation basin before proceeding to softening where sodium hydroxide, sodium carbonate (soda ash), and hydrated lime are added to the water. After settling, carbon dioxide and ozone are added separately before biologically active filtration and dual media rapid sand filtration to remove particles and dissolved organic matter. Chlorine, fluoride, and corrosion inhibitor are added before distribution. (City of Columbus, 2022).

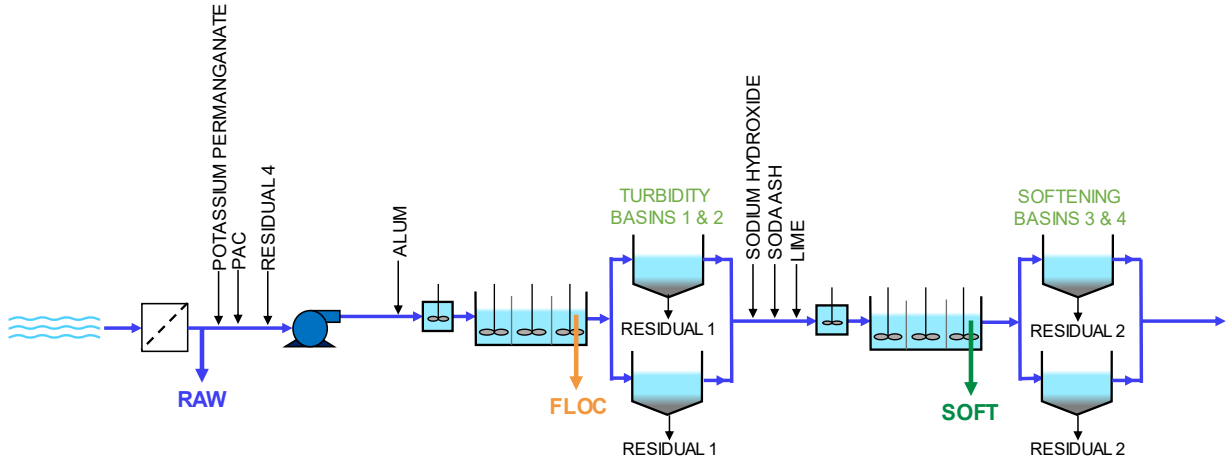

Figure 3.1. Treatment schematic of Dublin Road Water Treatment Plant with sample collection locations labeled with arrows for raw source water (raw), unsettled flocculated water (floc), and unsettled softened water (soft).

3.2 Water sample collection

On each collection date from April 2019 to January 2020, three water types were collected. Two (biological duplicate) one-liter plastic bottles (Nalgene, PP) were filled with raw river water, flocculated water collected from the end of the flocculated rapid mixing channel before settling, and softened water collected from the end of the softened rapid mixing channel before settling (Figure 3.1). Flocculated water and softened water were collected as grab samples with a dipper. For most water quality measurements, technical duplicates were taken from each biological replicate, resulting in four total replicates per water type. The only exception was January 6, 2020 when one biological replicate of each water type was collected, with three technical replicates. Alum dosing to the flocculated water varied from 60 – 93 ppm (Figure A 1). Usually the dosing was 90 ppm, but in July DRWP lowered alum dosing by 10 ppm each week before increasing it later in summer. Samples were transported in a cooler with ice and stored at 4°C. To maximize turbidity consistency with the DRWP and between analyses (Text A 1 and Table A 1), all samples were stirred for 125 rpm for at least 60 seconds before measurements and UV exposure.

3.3 Water characterisation

3.3.1 *UV absorbance*

The LAMBDA 950 UV/Vis Spectrophotometer was used to take UV absorbance measurements. Measurements were taken according to the instrument manual. A one-centimeter path length cuvette (Azzota Corp Q204) with four clear windows was filled with 3.2 mL of sample (or total liquid volume if diluted with DI) and rinsed with DI between measurements. Direct absorbance through the samples was measured, and integrating sphere absorbance accounting for reflectance was measured with the cuvette placed against the 60 mm integrating sphere with 8° wedge at the reflectance port (Figure 1.3). The cuvette container was raised to the reflectance port on a 24 mm platform. To calculate "corrected" UV absorbance, integrating sphere absorbance was subtracted from direct absorbance.

3.3.2 Particle size analysis

The Malvern Panalytical Mastersizer S was used to measure the particle size distribution of the samples. Measurements were taken according to the instrument manual. 50 mL of samples were dispersed at 1200 rpm (the lowest mixing rate for the wet sample dispersion unit). DI was run in between each measurement to flush the container and tubing.

3.3.3 Turbidity

Turbidity measurements were taken according to standard method 2130B (APHA, 2012). The Mirco 100 Turbidimeter (HF scientific, inc) was used. 25 mL of sample was placed in the clear sample cell that was rinsed 3 times with the respective sample. The sample cell was also rinsed with DI in between each water type.

3.3.4 Total suspended solids

Total suspended solids (TSS) was measured according to the standard method 2540D (Rice et al., 2012). 0.7 mm glass-fiber filter disks (Whatman 1825-047) were used along with aluminum weighing dishes (Fisherband, 08-732-102).

3.3.5 Dissolved organic carbon

Dissolved organic carbon (DOC) was measured according to the 5310B combustion-infrared method (Rice et al., 2012) and the instrument manual in a Shimadzu TOC-V_{CSN} analyzer. Clear borosilicate glass bottles were washed with DI three times, sealed with aluminum foil, and baked at 550°C for at least 4 hours. 25-30 mL of sample was filtered through a 0.45 µm Polypropylene membrane syringe filter (Foxx Life Sciences, 37B-3216-OEM). DI water was measured between each water type. The instrument was set to do a 50 µL injection three times of each sample cell, two-minute sparging time, and 1.5% acid injection.

Specific ultraviolet absorbance (SUVA) provides a general characterisation of the natural organic matter (NOM) in the water. SUVA is calculated by dividing the UV absorbance at 254 nm by DOC:

$$SUVA\ (\frac{L}{mg \cdot m}) = \frac{UV_{254}(cm^{-1})}{DOC\ \frac{mg}{L}} \cdot 100(\frac{cm}{m}) \qquad \text{Eq 3.1}$$

3.4 UV disinfection and enumeration

3.4.1 Surrogate microorganism selection

Indigenous aerobic bacterial spores were selected as a conservative surrogate for pathogenic protozoan *Cryptosprodium* (oo)cysts because spores are slightly smaller and have a similar surface charge (Bradford et al., 2016). Experiments are commonly performed with indicator organisms due to the impracticality of using pathogens in laboratory experiments. Drawbacks of using *Cryptosporidium* oocysts include high costs and difficulty producing and analyzing oocysts (Ryan & Hijjawi, 2015), low reproducibility of oocysts assays (Clancy et al., 1994), and low initial oocyst concentrations in raw or treated drinking water (Brown & Cornwell, 2007; Karanis et al., 2006).

Indigenous aerobic bacterial endospores are very resistant to UV disinfection compared to *C. parvum* and also lab-strain spores, such as *Bacillus subtilis* ATCC 6633 (Mamane-Gravetz et al., 2005; Mamane-Gravetz & Linden, 2004, 2005). *Bacillus* species spores are 5 to 50 times more resistant to UV disinfection than their growing vegetative cells (Setlow, 2001). Aerobic spores are nonpathogenic, are simple and inexpensive to analyze (Mamane-Gravetz & Linden, 2004; Nieminski et al., 2000), and share similarities to oocysts, including an isoelectric point below pH 3, neutral to strongly negative zeta potentials, and glycoproteins on the exterior surface (Bradford et al., 2016). Aerobic bacterial spores are slightly smaller in size than oocysts. Aerobic spores are approximately 0.8 µm in width and range from 1 to 2 µm in length while *C. parvum* oocysts are 3.5 to 6 µm in size (Bradford et al., 2016; Feng et al., 2003). Due to being smaller and more resistant to UV disinfection, aerobic spores can serve as a conservative surrogate for *Cryptosporidium* oocysts. The main benefit of using indigenous aerobic spores as a surrogate for *Cryptosporidium* in drinking water is that the indigenous spores undergo the same removal and mixing processes as *C. parvum* oocysts at the utility, possibly leading to similar proportions of attachment to particles and freely suspended. Multiple studies indicate that seeded indicator bacteria may be easier to inactivate than indigenous bacteria in unfiltered waters, not only due to the difference in resistance but also because free-floating bacteria are easier to inactivate than bacteria embedded in particles (Table 1.1). Meanwhile, "indigenous aerobic spores correlated to the removal of particles through coagulation, sedimentation, and filtration treatments" (Mamane-Gravetz & Linden, 2004; Rice et al., 1996) implying that they have particle associations during water treatment.

3.4.2 Pasteurisation and pour plating

Pasteurisation was conducted to enumerate only spores and not vegetative cells. Samples were placed in a sterile plastic tube incubated at 35-37°C for 30 minutes, and then pasteurized for 15 minutes at 65°C in a water bath (Barbeau et al., 1997; Mamane-Gravetz & Linden, 2005). Samples were placed on ice until enumeration when 1 mL to 10 mL sample was inoculated on 100 mm petri dish (VWR, 25384-342) after which approximately 25 mL of sterile nutrient agar

(Tryptic Soy Broth (TSB) (BD, 211825) containing 1.5% agar (BD, 214010)) at 55°C was poured over it. This pour plating method maximized spore recovery from samples compared to vacuum filtration, and swirl, and spread plating (Text A 2 and Table A 2).

3.4.3 Releasing spores from particles

Spores attached to or embedded within particles must be released or extracted before enumeration. If trapped within the particle or aggregated with other spores, the spore will not grow individual colonies and the count will not be accurate. The P-value from t-testing indicated that the mean for aggressive methods (vortex, tissue homogenizer, grinder, bath sonicator, detergent) was significantly less than or not significantly different than the method for manual shaking (Table A 3). All tubes were therefore shaken manually for approximately three seconds to ensure that particles were suspended to maximize spore recovery.

3.4.4 Association of spores with particle size fractions

A filtrate experiment was performed to determine the ratio of indigenous spores attached to size fractions of flocculated particles. Flocculated water with low and high turbidity (June 04, 2019, and June 18, 2019) was filtered with 100 µm (pluriStrainer), 70 µm (pluriStrainer), 12 µm (Whatman, 7060-2516), and 1.2 µm (Scientific Tisch, SF17970) filters. Filter sizes were chosen based on availability in the lab and size ranges that were previously mentioned in literature (Table 1.1). UV absorbance, particle size, and spore counts were measured for each size fraction.

3.4.5 UV inactivation

UV exposure was performed on water samples collected from July, 2019 to January, 2020. The UV inactivation process was performed according to the standard methods (Bolton & Linden, 2003) using a bench scale UV box with four 6 Watts Low Pressure lamps emitting monochromatic light at the 254 nm wavelength (6W CNLIGHT CO., LTD.UV Linear Germicidal Lamp, ozone free). The apparatus has a quasi-parallel/collimated beam with a shutter (

Figure 1.1 1.1). The distance between the sample surface and the UV lamps was measured each time and used to calculate the divergence factor. An ILT5000 Research Radiometer was used to measure the irradiance at the center of the petri dish and the petri factor. Jim Bolton's values from 2016 were used for the reflection factor (Bolton et al., 2015). The average fluence rate in the water is equal to the radiometer reading at the center of the petri dish and at the surface of the water level multiplied by the Petri Factor, Reflection Factor, Water Factor, and Divergence Factor. The average fluence is equal to the average fluence rate multiplied by the exposure time. 12 mL of sample was placed in a 60 mm petri dish with a flea stir bar under the quasi-parallel beam on a magnetic stirring plate. The exposure times needed for a pre-determined fluence (0, 10, 20, 40, 80, 160, and 200 mJ/cm^2) was calculated by dividing the UV fluence by the average UV irradiance. Timing started when the shutter was pulled out and ended when the shutter was returned. Exposures were performed in duplicate on biological duplicate sample bottles for each water type.

3.4.6 Seeded Bacillus subtilis

For water collected on January 6, 2020, *Bacillus subtilis* subsp. *Spizizenii* (ATCC 6633) were spiked into each water type to compare the dose responses for indigenous spores to commercial lab strains. ATCC 6633 was reconstituted according to the ATCC method. After

plating, a colony was scraped and added to a flask with 25 mL of TSB from which freezer stocks were made by centrifuging the overnight culture (shaking 24 hours at 30°C) and washing with sterile DI and resuspending in 20% glycerol and TSB. Freezer stocks (1mL each) were stored at -80°C. To propagate spores, one freezer stock was added to 25 mL of 2xSG medium (Leighton & Doi, 1971) at 35°C for 72 hours, shaking at 180 rpm in a baffled flask, achieving a spore concentration of 10^8 SFU/mL. This was spiked into each water type and phosphate-buffered saline (PBS) targeting an initial spore *B. subtilis* concentration of 10^6 SFU/mL for inactivation as described in section 3.4.3 and enumeration method as mentioned in section 3.4.1.

3.5 Statistical analysis and modelling

The Geeraerd model (Geeraerd et al., 2000) is a mechanistic inactivation kinetic model that can include biological parameters like shouldering and tailing. Below, is the log-transformed Geeraerd model:

$$\log_{10}\left(\frac{N_F}{N_0}\right) = \log_{10}\left[\left(1 - 10^{log_{10}\left(\frac{N_{res}}{N_0}\right)}\right) \cdot e^{-k_{max}F} \cdot \left(\frac{e^{k_{max}S_F}}{1 + (e^{k_{max}S_F} - 1) \cdot e^{-k_{max}F}}\right) + 10^{log_{10}\left(\frac{N_{res}}{N_0}\right)}\right] \quad \text{Eq 3.2}$$

Where N_0 is the initial spore concentration before any UV disinfection (SFU/mL), N_F is the spore concentration post UV disinfection (SFU/mL), F is UV exposure in fluence (mJ/cm^2), k_{max} is the maximum inactivation rate (cm^2/mJ), N_{res} is the residual population density (SFU/mL), and S_F is the shoulder length in units of fluence (mJ/cm^2). This equation has three phases: log-linear, shoulder, and tailing. To derive reduced models without shouldering or tailing, set S_F or N_{res}, equal to zero, respectively.

Without shouldering ($S_F = 0$):

$$\log_{10}\left(\frac{N_F}{N_0}\right) = \log_{10}\left[\left(1 - \frac{N_{res}}{N_0}\right) \cdot e^{-k_{max}F} + \frac{N_{res}}{N_0}\right] \quad \text{Eq 3.3}$$

Without tailing ($N_{res} = 0$):

$$\log_{10}\left(\frac{N_F}{N_0}\right) = \log_{10}\left[e^{-k_{max}F} \cdot \left(\frac{e^{k_{max}S_F}}{1 + (e^{k_{max}S_F} - 1) \cdot e^{-k_{max}F}}\right)\right] \quad \text{Eq 3.4}$$

For plotting, the equation was modified to log inactivation instead of log survival:

$$\log_{10}\left(\frac{N_F}{N_0}\right) = -\log_{10}\left[\left(1 - 10^{log_{10}\left(\frac{N_{res}}{N_0}\right)}\right) \cdot e^{-k_{max}F} \cdot \left(\frac{e^{k_{max}S_F}}{1 + (e^{k_{max}S_F} - 1) \cdot e^{-k_{max}F}}\right) + 10^{log_{10}\left(\frac{N_{res}}{N_0}\right)}\right] \quad \text{Eq 3.5}$$

For plotting without shouldering ($S_F = 0$):

$$\log_{10}\left(\frac{N_0}{N_F}\right) = -\log_{10}\left[\left(1 - \frac{N_{res}}{N_0}\right) \cdot e^{-k_{max}F} + \frac{N_{res}}{N_0}\right] \quad \text{Eq 3.6}$$

For plotting without tailing ($N_{res} = 0$):

$$\log_{10}\left(\frac{N_F}{N_0}\right) = -\log_{10}\left[e^{-k_{max}F} \cdot \left(\frac{e^{k_{max}S_F}}{1 + (e^{k_{max}S_F} - 1) \cdot e^{-k_{max}F}}\right)\right] \quad \text{Eq 3.7}$$

The mechanistic Geeraerd model was compared to the empirical quadratic model:

$$\log_{10}\left(\frac{N_0}{N_F}\right) = \mathrm{a} \cdot F^2 + b \cdot F + c \quad \text{Eq 3.8}$$

Where a is the quadratic coefficient, b is the linear coefficient, and c is the y-intercept, which was set to zero.

Analysis was performed on uncorrected and corrected dose responses. Uncorrected dose responses used direct spectroscopy for the absorbance measurement. Corrected dose responses had modified fluences based on the corrected spectroscopy (integrating sphere absorbance value subtracted from direct absorbance value). Excel add-in tool GInaFiT (Geeraerd et al., 2005) was used to obtain Geeraerd inactivation model parameters for dose responses (Equations 3.2–3.4). The model parameters were then used to calculate the dose responses as log inactivation (Equations 3.5–3.7). (GInaFiT only allows log survival). RStudio v 3.6.3 (geom_smooth function, method "lm") was used to model the quadratic equation for the dose responses (Equation 3.8). The mechanistic Geeraerd model parameters were compared to the empirical quadratic model parameters.

Pearson-wise correlation was performed between the model parameters and water quality characteristics. The R-functions "aov" and "TukeyHSD" were used to perform analysis of variance (ANOVA) on model parameters and post-hoc testing to determine significant differences. A nested ANOVA was used to test the difference in corrected versus uncorrected model parameters.

3.5.1 Data omission

On August 27th visible dirt in the raw river water sample due to high rainfall and pump malfunction led to uncharacteristic and extremely high turbidity (215 ± 6.24 NTU). Therefore, raw water UV inactivation data for August 27th was omitted. To ensure accuracy of particle size analysis, when concentration of particles was low (based on obscuration values) and/or when variance between replicate measurements was high, potential outlier data was identified and omitted. If a replicate had an obscuration value above 75%, it was excluded from data analysis. If the obscuration value was outside of the 7 – 60% range, a replicate would be excluded if at least two of the coefficients of variation of D(v, 0.1), D(v, 0.5), and D(v, 0.9) without that replicate were

at least 10% less than the coefficient of variation of all four replicates. If the obscuration value was inside the 7 – 60% range, a replicate would be excluded if all three of the coefficients of variation of D(v, 0.1), D(v, 0.5), and D(v, 0.9) without that replicate were 10% less than the coefficients of variation of all four replicates.

4 Results

4.1 Water characteristics

Over a 10-month sampling period from April 2019 to January 2020, average turbidity ranged from 0.978 – 258 NTU for raw river water, 6.49 – 430 NTU for flocculated water, and 229 – 603 NTU for softened water. During UV exposure experiments from July 9, 2019 to January 6, 2020, the average turbidity similarly ranged from 0.978 – 215 NTU for raw river water, 6.49 – 164 NTU for flocculated water, and 318 – 495 NTU for softened water (Figure 4.1a). Softened water turbidity was the greatest, and raw water turbidity was usually the lowest.

TSS measurements followed a similar trend to turbidity measurements (Figure 4.1b). Softened water had the highest TSS measurements, while raw river water had the lowest TSS measurements. From April 2, 2019 to July 30, 2019 TSS averages ranged from 1.35 – 163 mgTSS/L for raw river water, 32.3 – 302 mgTSS/L for flocculated water, and 248 – 664 mgTSS/L for softened water. During UV exposure experiments in the month of July, TSS measurements ranged from 1.35 – 26.6 mgTSS/L for raw river water, 32.3 – 72.1 mgTSS/L for flocculated water, and 274 – 435 mgTSS/L for softened water. Because turbidity and TSS measurements for each water type had a significant positive relationship ($p<0.05$, $R^2>0.9$, Table A 4, Tables 4.1 – 4.4) labor- and resource-intensive TSS measurements were discontinued. Because regulations are based on turbidity, turbidity measurements continued.

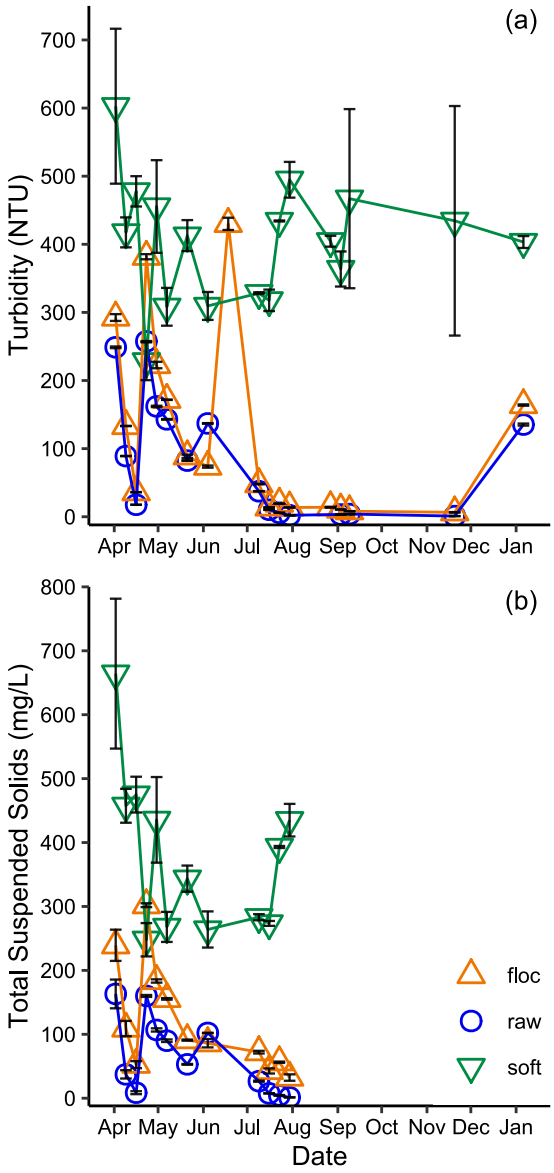

Figure 4.1. (a) Turbidity and (b) total suspended solids results of the three water types. Points represent the average across four total technical replicates from both biological replicates. Error bars represent the standard error of the mean.

DOC results in Figure 4.2a show that unlike TSS and turbidity, raw river water had the highest DOC concentration and softened water has the lowest DOC concentration. DOC measurements ranged from 4.09 – 9.14 mg/L for raw river water, 3.41 – 5.50 mg/L for flocculated water, and 1.92 – 3.87 mg/L for softened water. During UV exposure experiments, DOC measurements ranged from 4.09 – 9.14 mg/L for raw river water, 3.41 – 5.35 mg/L for flocculated water, and 2.57 – 3.87 mg/L for softened water.

SUVA at 254 nm ranged from 2.84 – 23.7 L/mg-m for raw river water, 5.37 – 21.3 L/mg-m for flocculated water, and 8.38 – 20.2 L/mg-m for softened water. During the UV exposure

experiments, SUVA at 254 nm ranged from 2.84 – 15.7 L/mg-m for raw river water, 5.37 – 16.8 L/mg-m for flocculated water, and 9.53 – 17.5 L/mg-m for softened water (Figure 4.2b). At times SUVA for flocculated water and raw river water followed similar trends, but not as closely as turbidity and TSS. Softened water SUVA at 254 mm varied less than raw river water and flocculated water. A high SUVA value indicates that there is a large portion of humic matter in the sample.

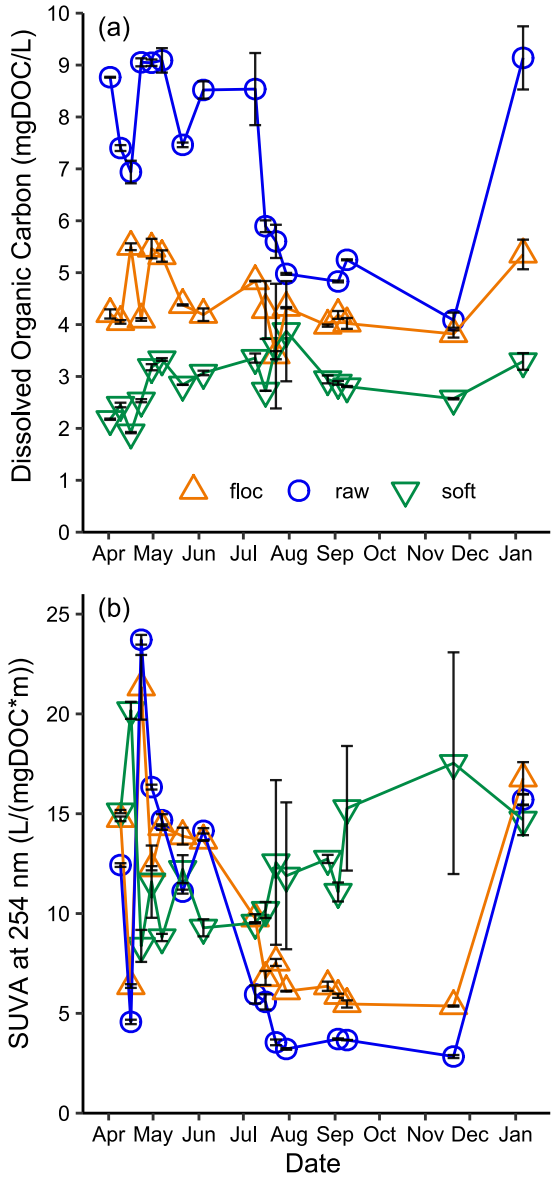

Figure 4.2. (a) Dissolved organic carbon and (b) specific ultraviolet absorbance at 254 nm in samples of unsettled flocculated water (floc), raw river water (raw), and softened water (soft) at DRWP. Points represent the average across four total technical replicates from both biological replicates. Error bars represent the standard error of the mean.

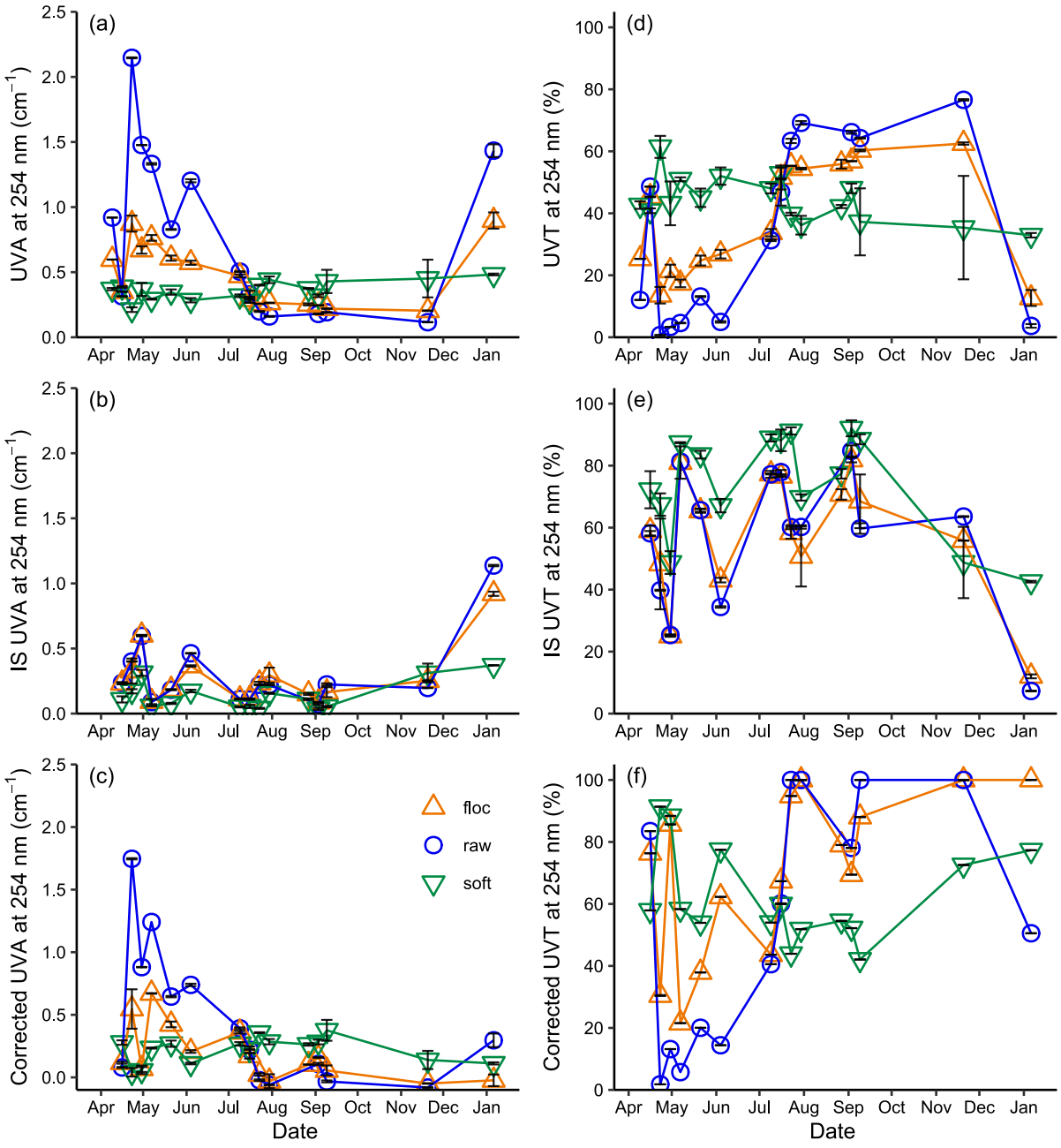

Figure 4.3. (a) Direct UV absorbance, (b) integrating sphere UV absorbance, and (c) corrected UV absorbance measurements and (d) direct UV transmission, (e) integrating sphere UV transmission, and (f) corrected UV transmission measurements at 254 nm in samples of unsettled flocculated water (floc), raw river water (raw), and softened water (soft) at DRWP. Points represent the average across four total technical replicates from both biological replicates. Error bars represent the standard error of the mean.

Direct absorbance and integrating sphere absorbance measurements were taken from wavelengths 200 – 350 nm (Figure A 2 and Figure A 3). Average 254 nm absorbance ranged from 0.116 – 2.15 cm^{-1} for raw river water, 0.204 – 0.897 cm^{-1} for flocculated water, and 0.212 – 0.483 cm^{-1} for softened water at 254 nm (Figure 4.3). During UV exposure experiments, the average absorbance ranged from 0.116 – 1.43 cm^{-1} for raw river water, 0.204 – 0.897 cm^{-1} for flocculated water, and 0.277 – 0.483 cm^{-1} for softened water. Softened water absorbance at 254 nm varied less than flocculated water and raw river water. There is no visible trend between the three water types, because raw river water and flocculated water absorbance measurements were sometimes greater and sometimes less than the softened water. Corrected absorbance averages ranged from 0.0718 – 1.14 cm^{-1} for raw river water, 0.0871 – 0.920 cm^{-1} for flocculated water, and 0.0360 – 0.371 cm^{-1} for softened water. The integrating sphere absorbance measured the reflectance, and the three types of water followed a similar trend, with raw river water usually having the highest reflectance and softened water having the lowest reflectance. UV transmission at 254 nm ranged widely for all three water types.

Various metrics were used to analyze particle size distribution: percent of particles present at a specific size ranges (Figure 4.4), the 10^{th}, 50^{th}, and 90^{th} percentile particle diameter (Figure 4.5a-c), and the De Brouckere (D[4,3]) and Sauter (D[3,2]) mean diameters (Figure 4.5d-e). De Brouckere mean diameter is the volume moment mean and reflects the size of those particles which constitute the bulk of the sample volume. Although raw river particle size distributions were more variable between sampling dates, flocculated water had more larger particles with a narrower distribution than softened water (Figure 4.4). The most common size range with the highest percentage of flocculated particles was 30.5253 – 35.5618 μm. The most common size range with the highest percentage of softened particles was 26.2020 – 30.5252 μm. T-test results showed that there was a significant difference in the size range with the highest percentage of particles between softened and flocculated particles (p-value 0.0305) Full range (up to 817 μm) particle size distributions (percent and cumulative) are in the appendix (Figure A 4 and Figure A 5).

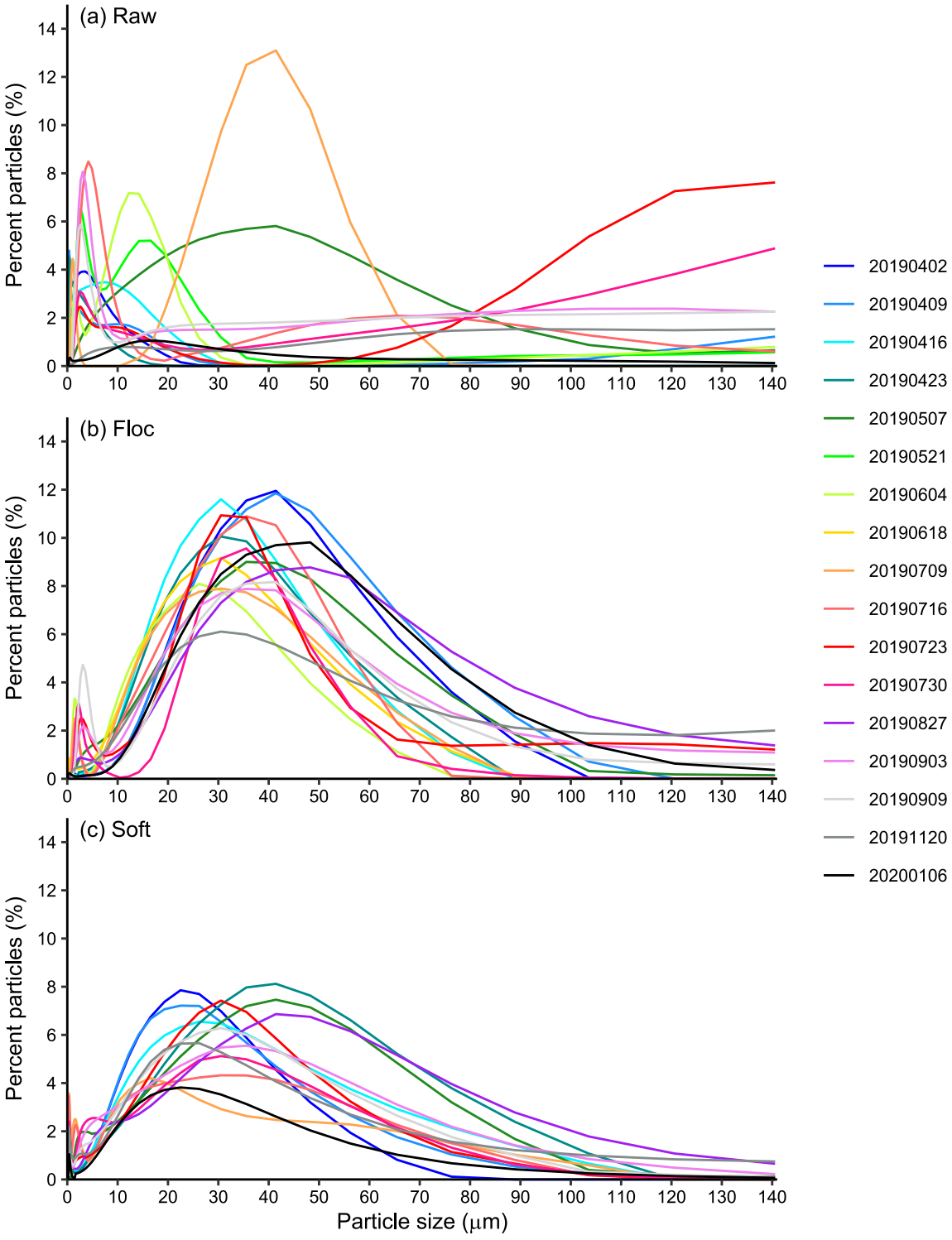

Figure 4.4. Percent of total particles for (a) raw river water, (b) flocculated water, and (c) softened water. Lines represent the average of four total technical replicates from two biological replicates for each water type on each collection date.

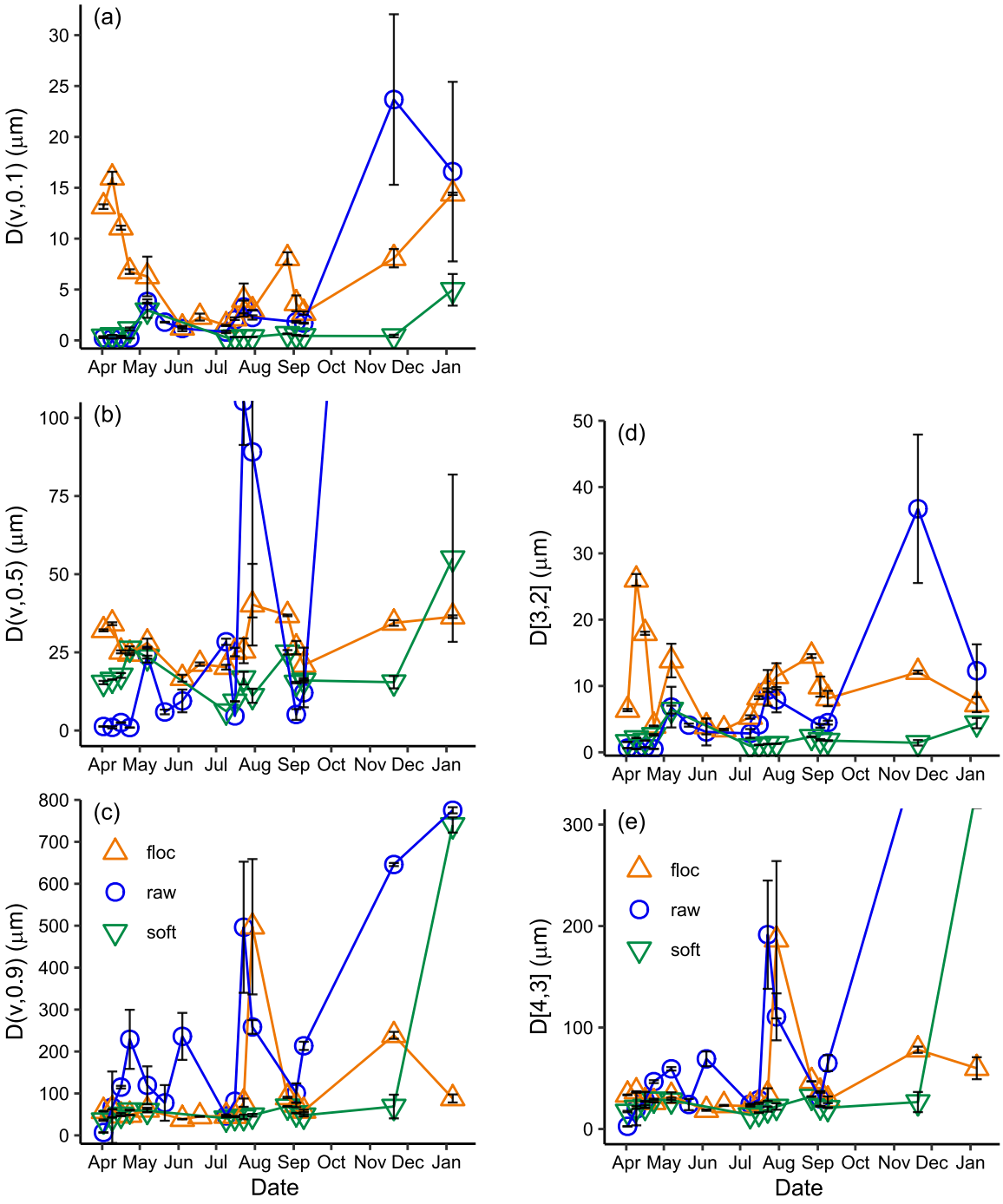

Figure 4.5. (a) 10th, (b) 50th, (c) and 90th percentile particle diameter in samples of flocculated water, raw river water, and softened water at DRWP. (d) The Sauter mean diameter (D[3,2]) and (e) the De Brouckere mean diameter (D[4,3]) in samples of flocculated water, raw river water, and softened water. Points represent the average across four total technical replicates from both biological replicates. Error bars represent the standard error of the mean.

The median particle diameter (50^{th} percentile particle diameter) ranged from 0.935 – 610 μm for raw river water, 16.7 – 40.3 μm for flocculated water, and 6.18 – 55.12 μm for softened water from April 2, 2019 to January 6, 2020 and ranged from 4.66 – 610 μm for raw river water, 20.3 – 40.3 μm for flocculated water, and 6.18 – 55.12 μm for softened water during UV exposure experiments (July 2019 – January 2020). Raw river water often had no or very few particles, leading to frequent data omission as described in Section 3.5.1. Overall, flocculated water had a larger median particle diameter size than raw and softened water (Figure 4.5b).

D(v, 0.1) or D10 is the particle diameter size at which 10% of total particles are smaller than it. D10 ranged from 0.197 – 23.7 μm for raw river water, 1.23 – 16.0 μm for flocculated water, and 0.29 – 4.97 μm for softened water from April 2, 2019 to January 6, 2020 and ranged from 0.823 – 23.7 μm for raw river water, 1.47 – 14.4 μm for flocculated water, and 0.290 – 4.97 μm for softened water during UV exposure experiments (July 2019 – January 2020) (Figure 4.5a). On most sample dates, flocculated water had the highest D10 diameter, indicating a lower percentage of small particles than raw river water and softened water.

D(v, 0.9) or D90 is the particle diameter size at which 90% of total particles are smaller than it. D90 ranged from 6.89 – 775 μm for raw river water, 38.7 – 498 μm for flocculated water, and 36.2 – 740 μm for softened water from April 2, 2019 to January 6, 2020 and ranged from 46.4 – 775 μm for raw river water, 45.7 – 498 μm for flocculated water, and 40.9 – 740 μm for softened water during UV exposure experiments (July 2019 – January 2020) (Figure 4.5c).

D[4,3] or the De Brouckere mean diameter the volume moment mean and reflects the size of those particles which constitute the bulk of the sample volume. The De Brouckere mean diameter is more sensitive to the larger particles than the smaller particles of the sample. The De Brouckere mean diameter ranged from 2.62 – 519 μm for raw river water, 18.6 – 187 μm for flocculated water, and 13.9 – 336 μm for softened water. During UV exposure, it ranged from 24.5 – 519 μm for raw river water, 22.6 – 187 μm for flocculated water, and 13.9 – 336 μm for softened water during UV exposure experiments (July 2019 – January 2020) (Figure 4.5). On most sample collection days, flocculated water and softened water had similar De Brouckere mean diameter values, but the values were higher for flocculated water.

D[3,2] or the Sauter mean diameter is the surface area mean and is more sensitive to the presence of fine or small particulates in the size distribution. The Sauter mean diameter ranged from 0.503 – 36.7 μm for raw river water, 3.42 – 26.0 μm for flocculated water, and 0.95 – 6.44 μm for softened water from April 2, 2019 to January 6, 2020 and ranged from 2.84 – 36.7 μm for raw river water, 5.32 – 14.5 μm for flocculated water, and 0.950 – 4.40 μm for softened water during UV exposure experiments (July 2019 – January 2020) (Figure 4.5). On most sample collection days, flocculated water has a significant greater Sauter mean diameter than the softened water Sauter mean diameter, which agrees with the D10 results (Figure 4.5) that softened water has proportionally more smaller particles than flocculated water.

Pearson correlation coefficients were used to determine relationships between water quality characteristics. Raw river water indicated a strong, positive correlation among non-particle size analysis water quality characteristics and among particle size analysis water quality characteristics, but not between particle and non-particle characteristics (Table 4.1). The trend for flocculated water is similar but not as strong (Table 4.1). Softened water had strong positive correlation between different particle size water quality characteristics (Table 4.1). Noticeably, TSS and abs254 IS had strong positive correlations between almost all water quality characteristics for softened water. When comparing the water quality characteristics across water types (Table 4.1), there was strong positive correlation between turbidity and TSS, SUVA and TSS, SUVA and turbidity, and between different particle size water quality characteristics. P-values are in the appendix (Table A 5).

Table 4.1. Pearson's r correlation coefficient between water quality characteristics (* indicates P-value < 0.05)

		TSS	Turbidity	DOC	UVA254	UVA254 IS	UVA254 C	SUVA	D[4,3]	D[3,2]	D(v,0.1)	D(v,0.5)	D(v,0.9)
Raw	Turbidity	*1.00											
	DOC	*0.95	*0.80										
	UVA254	*0.96	*0.99	*0.81									
	UVA254 IS	-0.7	*0.88	0.48	*0.86								
	UVA254 C	*0.91	*0.60	*0.85	*0.64	0.15							
	SUVA	*0.78	*0.98	*0.76	*0.99	*0.86	*0.62						
	D[4,3]	-0.67	0.5	0.03	0.46	*0.73	-0.22	0.48					
	D[3,2]	*-0.82	-0.07	-0.39	-0.12	0.13	-0.44	-0.11	*0.70				
	D(v,0.1)	*-0.82	0.25	-0.16	0.21	0.42	-0.24	0.22	*0.82	*0.94			
	D(v,0.5)	-0.64	*0.62	0.16	*0.58	*0.78	-0.05	*0.59	*0.97	*0.67	*0.84		
	D(v,0.9)	-0.66	0.31	-0.12	0.27	*0.61	-0.4	0.29	*0.95	*0.66	*0.71	*0.85	
Floc	Turbidity	*0.87											
	DOC	0.24	*0.68										
	UVA254	*0.79	*0.98	*0.77									
	UVA254 IS	-0.44	*0.84	0.41	*0.76								
	UVA254 C	0.7	0.02	0.4	0.17	*-0.51							
	SUVA	*0.93	*0.98	*0.64	*0.98	*0.76	0.14						
	D[4,3]	*-0.71	-0.07	0.05	-0.09	0.17	-0.38	-0.13					
	D[3,2]	*-0.72	-0.39	-0.41	-0.46	-0.11	-0.44	-0.46	0.47				
	D(v,0.1)	-0.22	*0.55	0.14	0.45	*0.73	*-0.51	0.45	0.05	0.4			
	D(v,0.5)	*-0.74	0.06	-0.01	0.01	0.28	-0.41	-0.01	*0.84	*0.74	0.45		
	D(v,0.9)	*-0.71	-0.15	-0.01	-0.17	0.13	-0.42	-0.21	*0.99	0.47	0.01	*0.79	
	Alum	*0.77	*0.52	0.45	*0.57	0.25	0.38	*0.56	-0.45	*-0.50	0.27	-0.31	-0.44
Soft	Turbidity	*0.99											
	DOC	0.31	0.09										
	UVA254	*0.98	*0.91	0.07									
	UVA254 IS	0.65	0.33	-0.06	*0.63								
	UVA254 C	0.68	*0.50	0.14	0.21	*-0.63							
	SUVA	0.47	*0.72	*-0.54	*0.79	*0.54	0.12						
	D[4,3]	0.66	-0.03	0.08	0.27	*0.59	-0.47	0.11					
	D[3,2]	*0.86	-0.1	-0.04	0.15	0.44	-0.4	0.07	*0.88				
	D(v,0.1)	*0.80	-0.05	0.05	0.25	*0.57	-0.46	0.11	*1.00	*0.90			
	D(v,0.5)	0.47	0.01	0.08	0.28	*0.53	-0.38	0.13	*0.91	*0.96	*0.92		
	D(v,0.9)	0.32	-0.05	0.06	0.26	*0.59	-0.48	0.1	*1.00	*0.87	*1.00	*0.91	
All	Turbidity	*1.00											
	DOC	*-0.54	*-0.50										
	UVA254	0.37	*0.34	*0.39									
	UVA254 IS	*-0.53	-0.1	*0.40	*0.72								
	UVA254 C	*0.51	*0.59	0.03	*0.46	-0.28							
	SUVA	*0.79	*0.82	*-0.36	*0.66	*0.28	*0.55						
	D[4,3]	-0.43	-0.21	*0.32	0.27	*0.57	*-0.36	-0.1					
	D[3,2]	*-0.73	*-0.53	0.11	-0.21	0.2	*-0.56	*-0.44	*0.62				
	D(v,0.1)	*-0.68	*-0.34	0.21	0.17	*0.53	*-0.45	-0.16	*0.68	*0.88			
	D(v,0.5)	*-0.51	-0.19	*0.40	*0.41	*0.59	-0.18	-0.05	*0.86	*0.63	*0.76		
	D(v,0.9)	-0.42	-0.26	0.27	0.1	*0.48	*-0.47	-0.2	*0.96	*0.57	*0.56	*0.71	

4.2 Filtrate experiment

The filtrate experiment was performed on three flocculated water samples: low turbidity (6.49 ± 0.248 NTU), medium turbidity (73.6 ± 1.58 NTU), and high turbidity (430 ± 9.00 NTU). Approximately 27.7% (±5.28%) of indigenous spores were associated with flocculated particles equal to or larger than 12 µm (Figure 4.6). Approximately 72.2% (±5.28%) of indigenous spores were either associated with flocculated particles between 1.2 and 12 µm or free-floating. Approximately 0.153% (±0.188%) of indigenous spores from flocculated water passed through the 1.2 µm filter. No indigenous spores were present in the flocculated water 0.45 µm filtrate. The filtrate experiment was also performed once on softened water and raw river water (Figure A 6). There were no significant differences in the raw water indigenous spores for the unfiltered, 70 µm, and 12 µm size fractions, while there were almost no spores present in the 1.2 µm size fraction. There were no significant differences in the softened water indigenous spores for the unfiltered and 70 µm size fractions, while there were almost no spores present in the 12 and 1.2 µm size fractions.

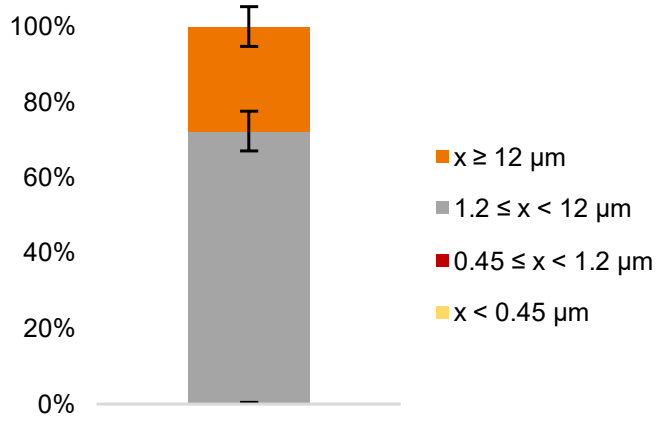

Figure 4.6. Percentage of indigenous spores in flocculated water filtrate. Error bars represent standard deviation between average of three dates sampling dates with variable turbidity values (low, medium, and high), with four total replicates for each filtrate level for two sample dates and two replicates for each filtrate level for one sample date. X is particle size.

T-tests were performed between spore concentrations in different filtrates. The spore concentration between the unfiltered sample and 70 µm filtrate was indistinguishable: there was no significant difference for the low, medium, and high turbidity flocculated water samples (Figure A 6, P – values 0.1107, 0.3595, and 0.0502, respectively). There was a significant difference between the unfiltered sample and 12 µm filtrate for the low, medium, and high turbidity flocculated water samples (P – values 0.0010, 0.0086 and 0.0477, respectively). There was a very significant difference between 70 µm filtrate and 12 µm filtrate for both medium turbidity and high turbidity flocculated water samples (P – value 0.0086 and 0.0054, respectively) but there was not a significant difference for the low turbidity flocculated water sample (P – value 0.1011). There was a very significant difference between the 12 µm filtrate and 1.2 µm filtrate for the low, medium, and high turbidity flocculated water samples (P – values 0.0029, 0.0006, and 0.0069,

respectively). There were zero spores in the 0.45 µm filtrate and less than three spores per milliliter in the 1.2 µm filtrate (Figure 4.6, Figure A 6).

Integrating sphere (IS) absorbance scans showed that for both June 4, 2019 (medium turbidity, 73.6 NTU) and June 18, 2019 (high turbidity, 430 NTU) the filtrate from the 70 µm filter had a higher IS absorbance than the unfiltered sample (Figure 4.7). For June 4, 2019, the filtrate from the 12 µm filter also had a higher IS absorbance than the unfiltered sample. The larger particles had higher reflectance than the overall sample. Absorbance and corrected absorbance scans are in the appendix (Figure A 7).

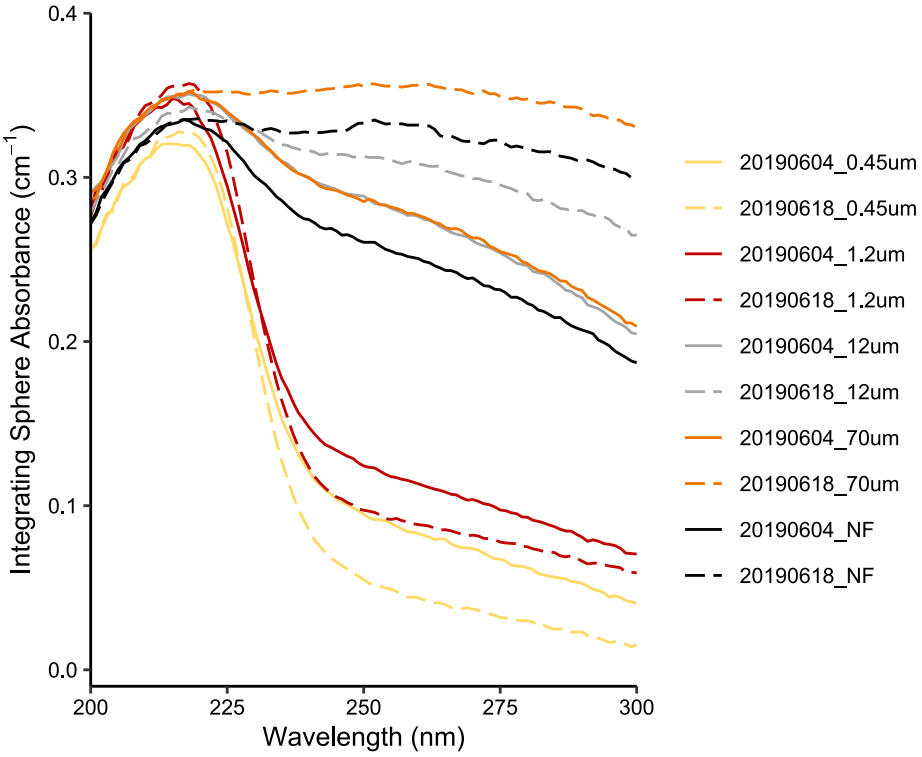

Figure 4.7. Integrating sphere absorbance measurements of various filtrate from two sample dates with variable turbidity values (medium and high). Lines represent the average of 3 technical replicates from one biological water sample.

4.3 UV disinfection of spores

4.3.1 Indigenous spore dose responses

Initial indigenous spore concentrations results showed that all three water types had similar trends, but flocculated water and raw river water had consistently higher values than softened water. Flocculated water had slightly higher initial spore concentrations than raw river water.

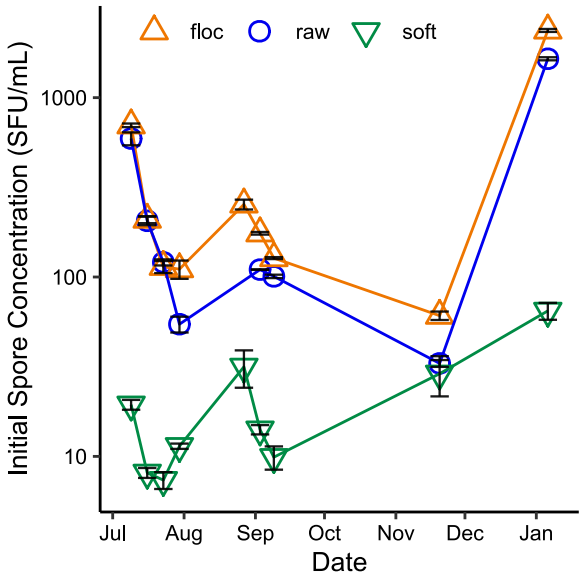

Figure 4.8. Initial indigenous spore concentration in raw river water, flocculater water, and softened water. Points represent the average across four to eight total technical replicates from both biological replicates for each type. Error bars represent the standard error of the mean.

UV exposure experiments in the three different water types showed that raw river water and softened water had a similar dose response, while flocculated water had a lower dose response for both uncorrected and corrected fluences (Figure 4.9a–f). The absorbance measured with the integrating sphere was used to correct the dose received (Figure 4.9, d – f). Correcting UV fluence increased the overall fluence for all types of water.

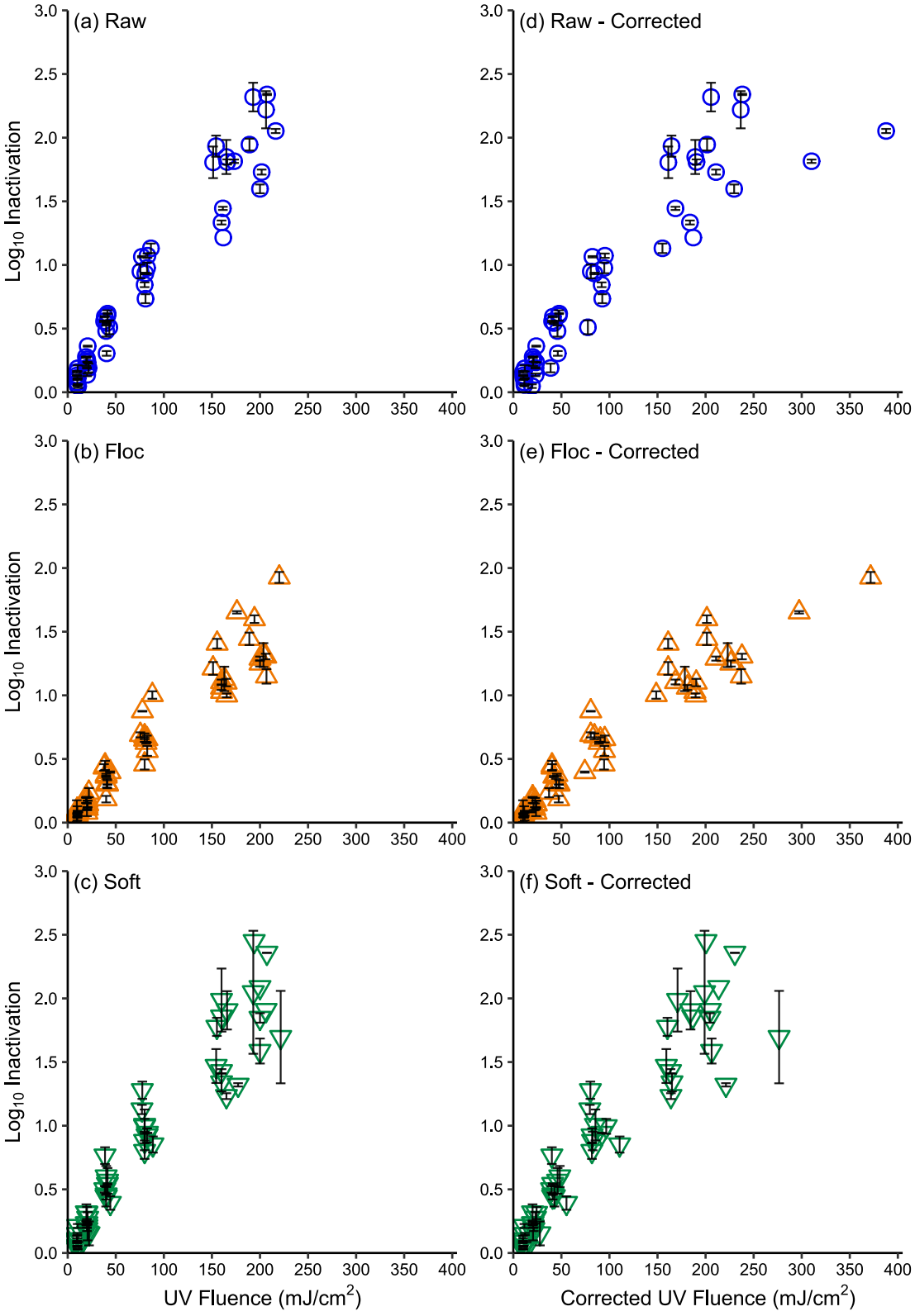

Figure 4.9. Subfigures a – c on the left side depict dose responses for indigenous, aerobic spores in samples of raw river water, unsettled flocculated water, and unsettled softened water. In

comparison, subfigures d – f on the right side depict UV exposure results corrected for absorbance and reflectance for the same samples of raw river water, unsettled flocculated water, and unsettled softened water. For every collection date, each type of water was collected with two biological replicates. During UV exposure, each biological replicate had two technical replicates at every dose. Dose replicates were plated in two technical replicates. The average was calculated between the biological replicates. Error bars represent SEM of two biological replicates.

4.3.2 Modeled dose responses

In this paper, the model resulting from the average of each biological replicate for each water type and collection date will be called the super model (Figure 4.10). Goodness of fit (RMSE, R^2) values showed similarities between the three Geeraerd models (shoulder, tailing, shoulder + tailing) (Table 4.2). However, because modeled shoulder lengths were small to negative, the tailing model was chosen. Previous research on indigenous spores also reported no shouldering (Mamane-Gravetz & Linden, 2004). The goodness of fit can not be compared between quadratic and Geeraerd models because the quadratic model used log inactivation and the Geeraerd model used log survival data. Super Geeraerd-tail models and super quadratic models were fit to data for both uncorrected and corrected fluence responses, and demonstrated that raw river water and softened water had similar and greater dose responses than flocculated water (Figure 4.10). When comparing differences in Geeraerd model parameters, flocculated water had the lowest k_{max} (maximum inactivation rate) (Figure 4.11a, Table A 6) and highest N_{res} (residual population density, or tailing parameter) (Figure 4.11b, Table A 6) indicating slower disinfection kinetics and more surviving spores. Flocculated water has the highest initial population density and the values were significantly different. Softened water had the lowest initial concentration (Figure 4.8 and Figure 4.11). When comparing differences in quadratic model parameters, the linear coefficients of flocculated water were one order of magnitude smaller than raw river water and softened water (Figure 4.12b, Table A 7). RMSE, R^2, and adjusted R^2 values for models in Figure 4.10 are in the appendix (Table A 8).

A dose response was also modeled on the average of each biological replicate for each type for every collection date. Analysis of variance was performed on this data set for both corrected and uncorrected water types to determine statistical significance of trends observed in the super models. For both corrected and uncorrected models, ANOVA results showed significant differences for flocculated water compared to both softened water and raw river water: for k_{max}, N_{res}, and the linear coefficient (Figure 4.11 and Figure 4.12). No differences were observed for N_0. Between softened water and flocculated water, the quadratic coefficient was also significantly different (Figure 4.12). P-values are in the appendix (Table A 11). ANOVA results further confirmed that there were no significant differences between corrected and uncorrected model parameters for each water type (Table A 12).

Table 4.2. Goodness of fit for uncorrected and corrected super models on the different water types

Water Type	Model Type	Uncorrected			Corrected		
		RMSE	R^2	R^2 adjusted	RMSE	R^2	R^2 adjusted
Raw	Geeraerd tail	0.456	0.702	0.696	0.484	0.664	0.657
	Geeraerd shoulder	0.455	0.703	0.697	0.514	0.620	0.612
	Geeraerd shoulder-tail	0.457	0.703	0.694	0.486	0.664	0.654
	Quadratic	0.167	0.979	0.978	0.205	0.968	0.967
Floc	Geeraerd tail	0.345	0.665	0.659	0.362	0.631	0.624
	Geeraerd shoulder	0.346	0.662	0.656	0.374	0.605	0.598
	Geeraerd shoulder-tail	0.346	0.665	0.656	0.363	0.632	0.622
	Quadratic	0.137	0.972	0.971	0.122	0.978	0.977
Soft	Geeraerd tail	0.321	0.810	0.806	0.337	0.790	0.786
	Geeraerd shoulder	0.325	0.804	0.800	0.351	0.772	0.768
	Geeraerd shoulder-tail	0.322	0.810	0.805	0.338	0.790	0.784
	Quadratic	0.196	0.970	0.969	0.208	0.966	0.965

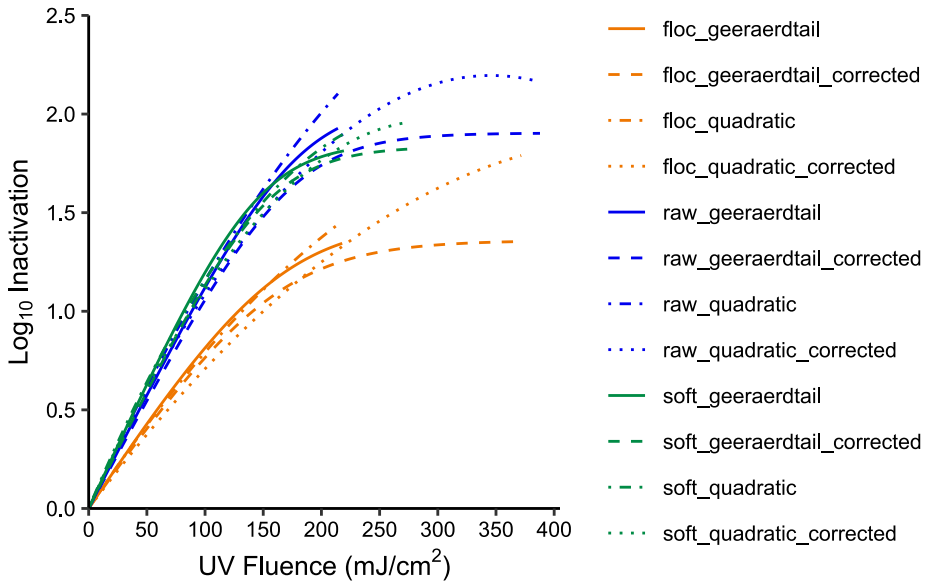

Figure 4.10. The lines represent the super Geeraerd-tail model and the super quadratic model for each water type. Super models were calculated from the average of each biological replicate for each water type and collection date.

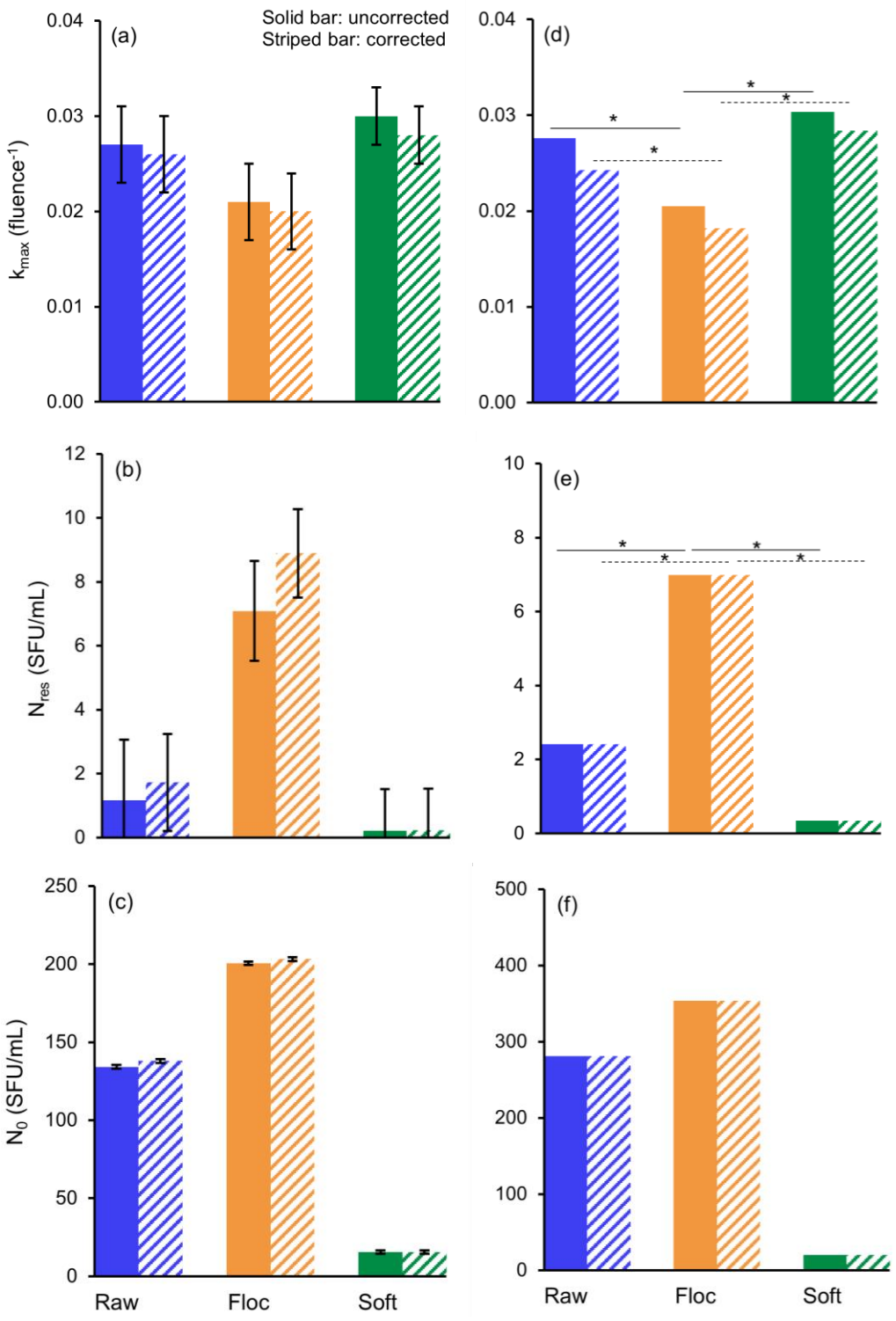

Figure 4.11. Subfigures on the left are from the super Geeraerd-tail model, with (a) k_{max} (fluence units mJ/cm^2), (b) N_{res}, and (c) N_0. Subfigures on the right are parameters from averaged individual Geerared tail model dose responses on each average biological replicate for every collection date, with (d) k_{max} (fluence units mJ/cm^2), (e) N_{res}, and (f) N_0. Significant different parameters between water types are indicated by asterisks. Error bars excluded on right-side figures due to it being a different subset of data.

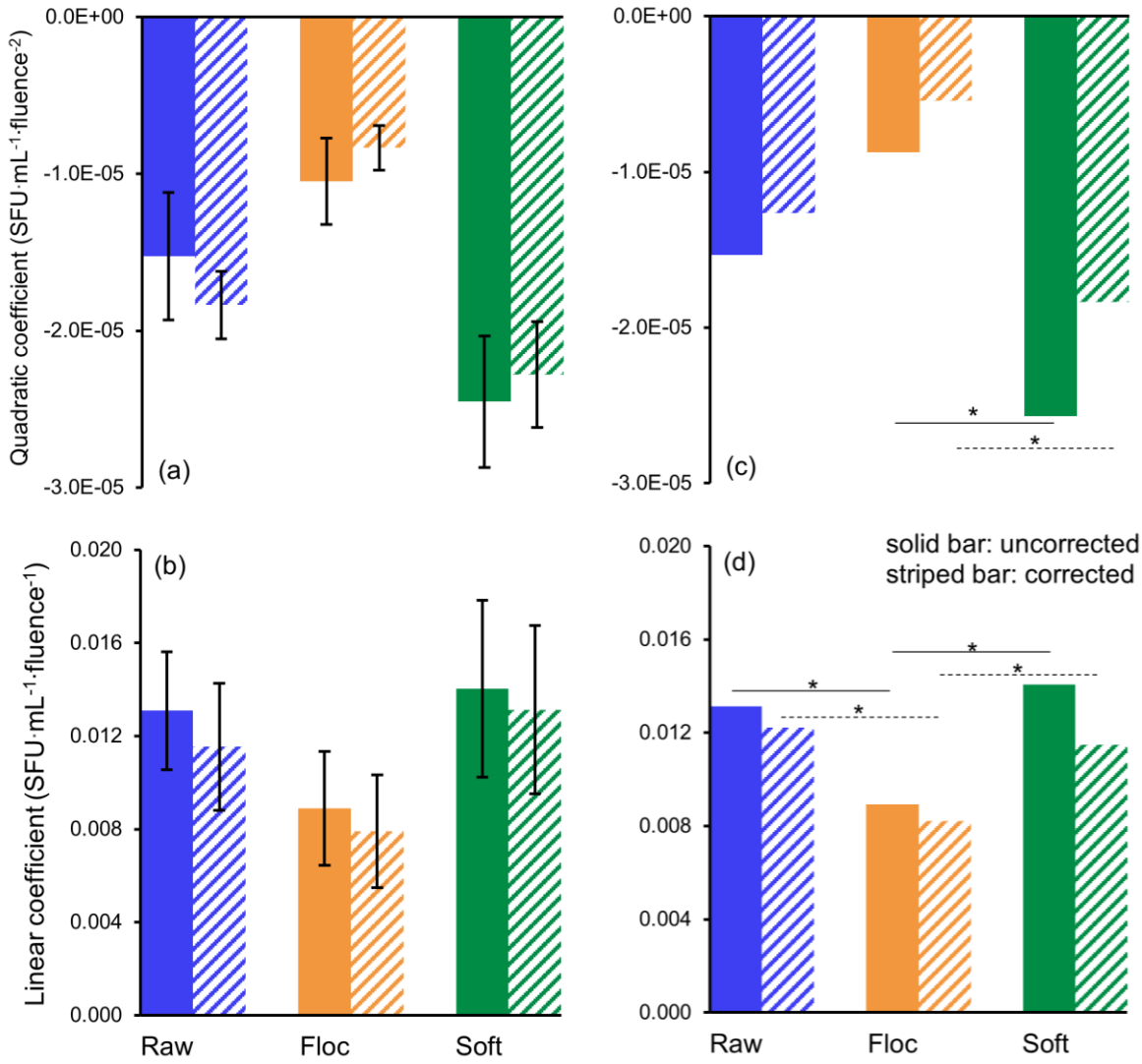

Figure 4.12. Subfigures on the left are from the super quadratic model, with (a) k_{max} (fluence has units of mJ/cm^2), (b) N_{res}, and (c) N_0. Subfigures on the right are parameters from averaged individual quadratic model dose responses on each average biological replicate for every collection date, with (d) k_{max} (fluence has units of mJ/cm^2), (e) N_{res}, and (f) N_0. Significant different parameters between water types are indicated by asterisks. Error bars excluded on right-side figures due to it being a different subset of data.

4.3.3 Seeded B. subtilis spore dose responses

When using an indicator microbe as a surrogate, the UVDGM uses Reduction Equivalent Dose (RED) bias values to account for different inactivation kinetics between challenge and target microorganisms (USEPA, 2006). However, the increased UV resistance of indigenous spores compared to *C. parvum* was above the range of the RED bias factor tables provided in the UVDGM. Therefore, we spiked less resistant lab-spores into the three water types to calculate the RED for *C. parvum*. Integrating sphere absorbance measurements were not taken on the spiked water as there was no significant difference between uncorrected and corrected model parameters.

Results from spiking *B. subtilis* endospores into raw river water, flocculated water, softened water from January, 6, 2020 sample date containing indigenous spores at 1648 ± 33, 2370 ± 45, and 65 ± 7 SFU/mL, respectively, and into sterile PBS showed that the flocculated water had the lowest dose response (Figure 4.13).The Geeraerd shoulder-tail model fit best (Table 4.3), shouldering was expected for the lab-type *B. subtilis* spores based on previous research (Mamane-Gravetz et al., 2005; Mamane-Gravetz & Linden, 2004; Sommer & Cabaj, 1993). Model parameters confirmed that flocculated water had the lowest k_{max} and the highest N_{res} (Figure 4.14). Flocculated model parameters k_{max} and N_{res} are significantly different from raw, soft, and PBS model parameters (Figure 4.14, Table A 9). PBS and raw water had similar k_{max} values, but significantly different N_{res} values. Softened water had the lowest N_{res}. Flocculated water also had the lowest linear coefficient for the quadratic model (Figure 4.15, Table A 9). Water quality values for the spiked water are in the Appendix (Table A 10). k_{max} for all water types in the spiked experiment was one order of magnitude greater than indigenous spores without spiked *B. subtilis*.

Table 4.3. A comparison of models' goodness of fit for water types from the spiked experiment (bold values indicate best Geeraerd model fit for each water type)

Water Type	Model Type	RMSE	R2	R2 adjusted
Raw	Geeraerd tail	0.437	0.973	0.959
	Geeraerd shoulder	0.943	0.873	0.810
	Geeraerd shoulder-tail	**0.417**	**0.981**	**0.963**
	Quadratic	0.420	0.986	0.979
Floc	Geeraerd tail	0.239	0.990	0.986
	Geeraerd shoulder	0.678	0.924	0.886
	Geeraerd shoulder-tail	**0.194**	**0.995**	**0.991**
	Quadratic	0.321	0.989	0.983
Soft	Geeraerd tail	0.271	0.993	0.989
	Geeraerd shoulder	1.095	0.879	0.818
	Geeraerd shoulder-tail	**0.207**	**0.997**	**0.994**
	Quadratic	0.430	0.988	0.982
PBS	Geeraerd tail	0.358	0.985	0.977
	Geeraerd shoulder	1.331	0.792	0.688
	Geeraerd shoulder-tail	**0.181**	**0.997**	**0.994**
	Quadratic	0.493	0.983	0.974

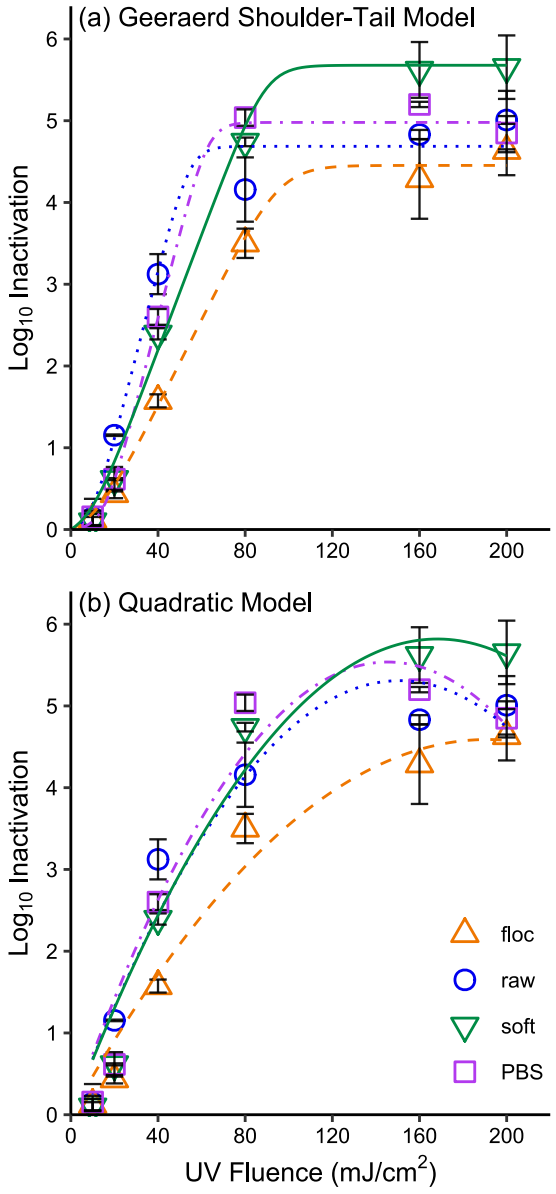

Figure 4.13. Average dose response for indigenous and spiked *B. subtilis* ATCC 6633 endospores spiked into flocculated water, raw river water, softened water collected on January 6, 2020, and PBS. (a) Geeraerd shoulder-tail model and (b) quadratic model. Error bars represent standard deviation values between the technical dose replicates.

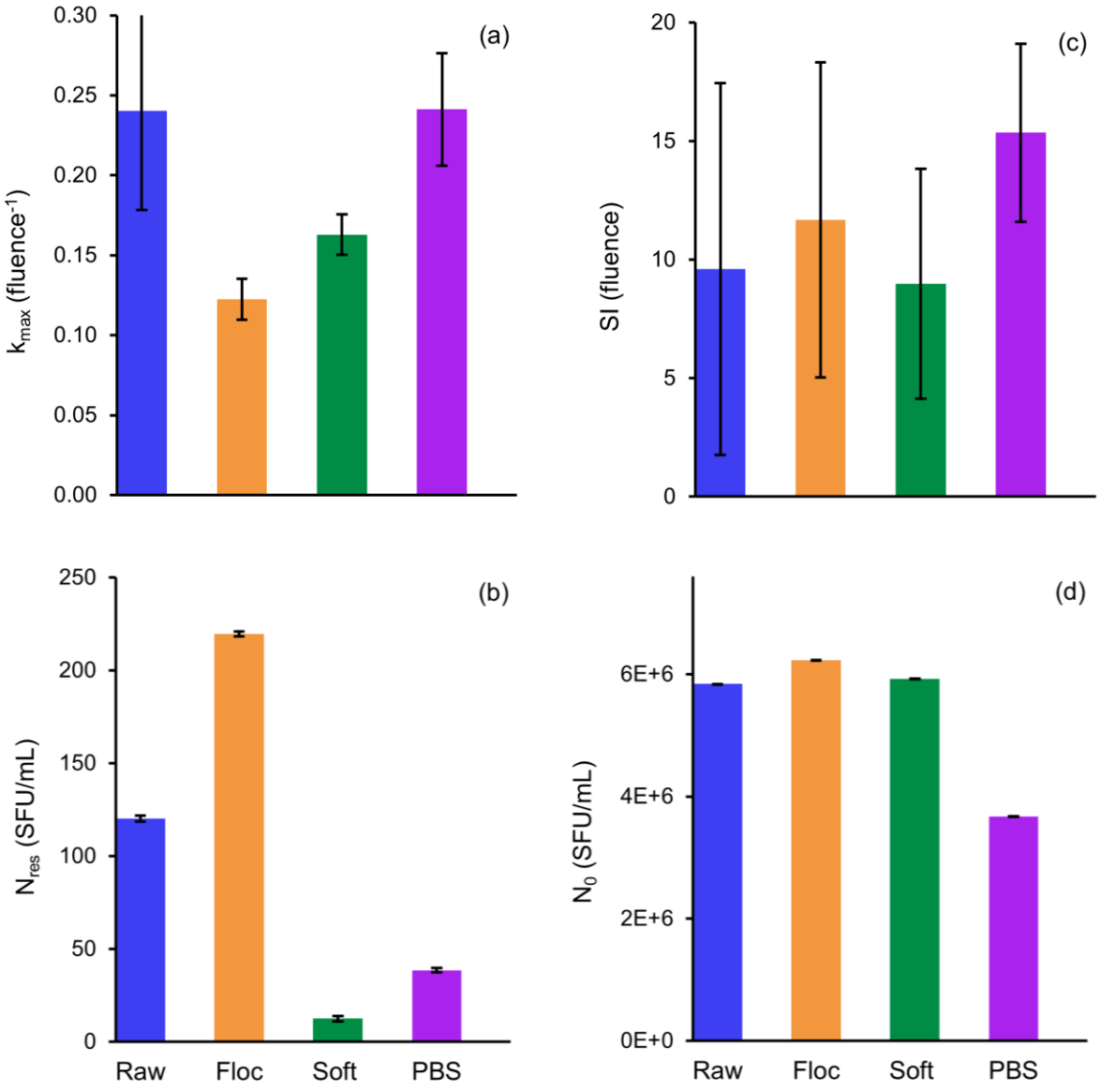

Figure 4.14. Geeraerd shoulder-tail model coefficients from the spiked experiment: (a) the maximum inactivation rate, (b) the residual population density, (c) the shoulder length, and (d) the initial population density.

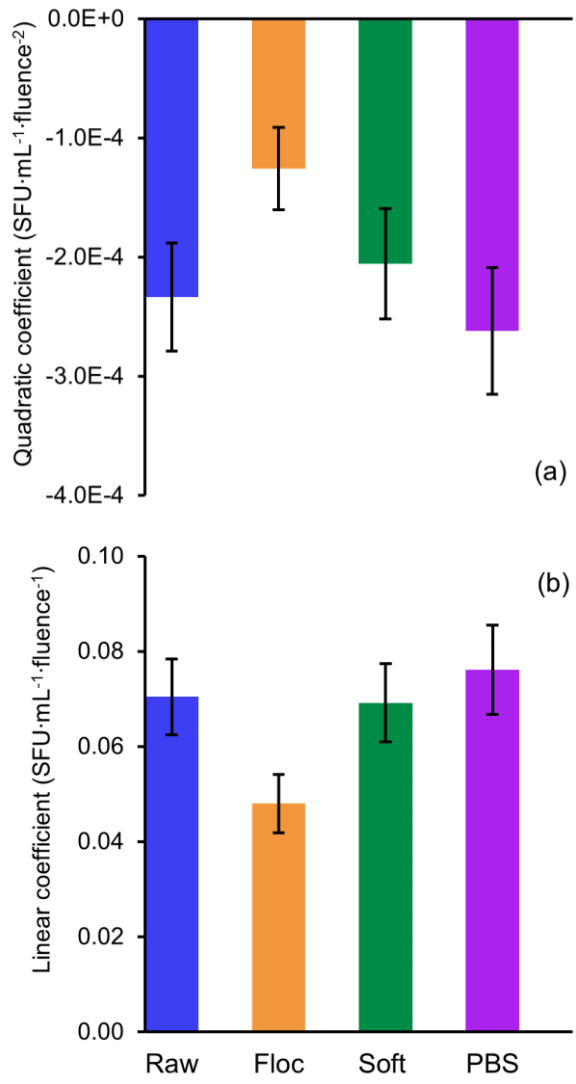

Figure 4.15. Quadratic model coefficients from the spiked experiment

Although indigenous and spiked *B. subtilis* spores were used as a surrogate for *Cryptosporidium*, the difference in UV sensitivity between *B. subtilis* measured here and *Cryptosporidium* known from the literature can be used to calculate the dose (known as the reduction equivalent dose or RED) and estimate the level of disinfection of *Cryptosporidium* in DRWP water types. RED bias factors account for the impact on full scale UV disinfection reactors caused by the difference in inactivation kinetics between the challenge surrogate and the target pathogen. The UV sensitivity of *B. subtilis* was calculated by dividing the fluence of 40 mJ/cm^2 by the value of log inactivation at that fluence from the spiked Geeraerd model for each type (Equation 1.12). The UV sensitivity of *B. subtilis* in raw, floc, and soft water is 12.7, 26.4, and 18.2 mJ/cm^2/log I, respectively. "Table G.1. RED Bias values for 4.0-log *Cryptosporidium* Inactivation Credit as a Function of UVT and UV Challenge Microorganism Sensitivity" from the UV Disinfection Guidance Manual (2006), partially shown below (Table 4.4), and the calculated UV sensitivity of *B. Subtilis* in each water type based on the Geeraerd shoulder-tail model k_{max}, were used to calculate the dose that *Cryptosporidium* would have experienced in full scale reactors if it was in the different water types during the *B. subtilis* spiking experiment (Table 4.5). The RED bias values are a function of challenge organism and target pathogen UV sensitivities and UV transmission. The tables provide bias factors for UVT above 65%, but the UVT during this experiment was below 65% (Table A 10). After accounting for RED bias, *Cryptosporidium* would receive a calculated fluence above 22 mJ/cm^2, which is the dose required for 4-log inactivation, in raw, floc, or soft water if the UVT is $\geq$ 65%, 90%, or 80%, respectively.

Table 4.4. RED bias values, points of interest copied from Table G.1. (USEPA, 2006)

Cryptosporidium log inactivation credit		4.0						
Required UV dose (mJ/cm^2)		22						
Cryptosporidium UV sensitivity (mJ/cm^2/log I)		5.5						
UVT (%)		≥98	≥95	≥90	≥85	≥80	≥75	≥65
Challenge UV sensitivity (mJ/cm^2/log I)		RED Bias						
Lower	Upper							
>12	≤14	1.13	1.24	1.37	1.44	1.49	1.53	1.60
>18	≤20	1.17	1.34	1.55	1.69	1.78	1.87	1.99
>26	≤28	1.21	1.41	1.74	1.98	2.14	2.28	2.48

Table 4.5. The calculated dose (mJ/cm^2) for *Cryptosporidium* in each water type based on the UV sensitivity of *B. subtilis* in the spiking experiment for a UV transmission range of 65 to 100% and a fluence of 40 mJ/cm^2

Water type	UVT (%)						
	≥98	≥95	≥90	≥85	≥80	≥75	≥65
Raw	35.4	32.3	29.2	27.8	26.8	26.1	25
Soft	34.2	29.9	25.8	23.7	22.5	21.4	20.1
Floc	33.1	28.4	23	20.2	18.7	17.5	16.1

4.4 Relationships between water characteristics and UV disinfection

Impacts of water quality measurements on dose responses are visualized with different point sizes in the appendix (Figure A 8 through Figure A 13) and statistically quantified in Table 4.6 and Table 4.7. There was strong, positive linear correlation between some water quality characteristics and model parameters for raw river water (Table 4.6 and Table 4.7). N_{res} and N_0 had the most significant correlations compared to k_{max}, linear coefficient, and quadratic coefficient. N_{res}, N_0, and the quadratic coefficient did not have strong correlations with most of the particle size characteristics. For k_{max}, corrected absorbance at 254 nm and DOC had the strongest positive correlations. For the uncorrected model, k_{max} and the linear coefficient are negatively related to the particle size characteristics. For the corrected model, the negative correlation became stronger and significant between k_{max} and the linear coefficient and the particle size characteristics. The quadratic coefficient had a very strong, negative correlation with TSS.

Table 4.6. Pearson's r correlation coefficient between water quality characteristics and parameters from modeled uncorrected dose response (n=8 for TSS, n=15 for raw, and n=17 floc and soft for other characteristics, * indicates P-value < 0.05). P-values are in Table A 13.

Uncorrected Model & Parameter		TSS	Turbidity	DOC	abs254 Direct	abs254 IS	abs254 Corrected	SUVA	D[4,3]	D[3,2]	D(v,0.1)	D(v,0.5)	D(v,0.9)
Raw	k_{max}	0.66	0.50	*0.76	*0.56	0.16	*0.84	*0.56	-0.30	-0.52	-0.33	-0.19	-0.44
	N_{res}	*0.99	*0.96	*0.76	*0.94	*0.82	*0.59	*0.92	0.40	-0.11	0.22	0.53	0.19
	N_0	*1.00	*1.00	*0.81	*1.00	*0.87	*0.62	*0.98	0.48	-0.09	0.23	*0.60	0.29
	Linear coef	0.66	0.25	*0.57	0.31	-0.02	*0.62	0.31	-0.49	*-0.65	-0.54	-0.42	*-0.57
	Quad coef	*-0.86	-0.20	-0.38	-0.23	0.00	-0.43	-0.22	0.42	0.40	0.29	0.37	0.51
Flocculated	k_{max}	0.12	0.40	*0.51	0.47	0.10	0.48	0.44	-0.42	*-0.51	-0.13	-0.38	*-0.50
	N_{res}	*0.72	*0.80	*0.77	*0.86	0.43	*0.49	*0.83	-0.18	*-0.48	0.19	-0.13	-0.27
	N_0	*0.79	*0.99	*0.71	*0.98	*0.82	0.05	*0.96	-0.10	-0.37	*0.58	0.06	-0.19
	Linear coef	0.22	0.39	*0.50	0.47	0.05	*0.55	0.45	-0.41	*-0.57	-0.27	-0.43	*-0.50
	Quad coef	-0.07	-0.17	-0.34	-0.25	0.13	*-0.52	-0.23	0.26	0.44	0.46	0.37	0.35
Softened	k_{max}	-0.57	0.09	-0.12	0.08	0.13	-0.08	0.18	-0.29	-0.45	-0.30	-0.34	-0.28
	N_{res}	-0.15	*0.50	-0.08	*0.70	*0.72	-0.21	*0.67	0.29	0.07	0.27	0.23	0.29
	N_0	-0.37	0.13	-0.07	0.39	*0.68	-0.46	0.32	*0.73	*0.73	*0.74	*0.77	*0.73
	Linear coef	*-0.73	-0.01	-0.02	-0.08	0.06	-0.15	-0.03	-0.33	*-0.50	-0.35	-0.43	-0.32
	Quad coef	*0.72	-0.22	-0.02	-0.22	-0.21	0.04	-0.22	0.23	0.49	0.25	0.35	0.23
All	k_{max}	0.31	*0.44	0.04	0.27	-0.03	*0.40	*0.37	-0.16	*-0.40	-0.25	-0.03	-0.22
	N_{res}	-0.32	*-0.31	*0.38	*0.53	*0.52	0.07	0.14	0.08	0.13	0.28	0.16	-0.02
	N_0	*-0.46	-0.16	*0.54	*0.77	*0.79	0.06	0.26	0.25	0.07	*0.41	*0.37	0.12
	Linear coef	0.25	*0.40	0.12	0.23	-0.08	*0.42	0.27	-0.23	*-0.49	*-0.36	-0.10	-0.28
	Quad coef	*-0.41	*-0.40	0.03	-0.22	0.06	*-0.39	*-0.36	0.28	*0.39	0.32	0.20	0.33

Table 4.7 Pearson's r correlation coefficient between water quality characteristics and parameters from modeled corrected dose response (n=8 for TSS, n=15 for raw, and n=17 floc and soft for other characteristics, * indicates P-value < 0.05). P-values are in

Table A 14

Corrected Model & Parameter		TSS	Turbidity	DOC	abs254 Direct	abs254 IS	abs254 Corrected	SUVA	D[4,3]	D[3,2]	D(v,0.1)	D(v,0.5)	D(v,0.9)
Raw	k_{max}	0.69	-0.25	0.25	-0.18	*-0.62	*0.57	-0.18	*-0.83	-0.53	*-0.60	*-0.78	*-0.85
	N_{res}	*0.99	*0.96	*0.76	*0.94	*0.82	*0.59	*0.92	0.40	-0.11	0.22	0.53	0.19
	N_0	*1.00	*1.00	*0.81	*1.00	*0.87	*0.62	*0.98	0.48	-0.09	0.23	0.60	0.29
	Linear coef	*0.73	-0.19	0.28	-0.12	-0.50	0.51	-0.13	*-0.80	*-0.63	*-0.68	*-0.76	*-0.81
	Quad coef	*-0.91	0.00	-0.28	-0.03	0.24	-0.42	-0.02	*0.59	0.44	0.40	0.55	*0.66
Flocculated	k_{max}	0.11	-0.09	0.28	0.03	-0.42	*0.67	-0.01	-0.39	-0.37	*-0.49	-0.43	-0.44
	N_{res}	*0.72	*0.80	*0.77	*0.86	0.43	*0.49	*0.83	-0.18	*-0.48	0.19	-0.13	-0.27
	N_0	*0.79	*0.99	*0.71	*0.98	*0.82	0.05	*0.96	-0.10	-0.37	*0.58	0.06	-0.19
	Linear coef	0.20	0.02	0.34	0.13	-0.35	*0.71	0.11	-0.41	-0.47	*-0.55	-0.48	-0.47
	Quad coef	-0.07	-0.01	-0.29	-0.11	0.31	*-0.61	-0.08	0.28	0.42	*0.57	0.41	0.36
Softened	k_{max}	-0.59	-0.03	-0.04	-0.09	-0.12	0.06	-0.01	-0.38	*-0.51	-0.39	-0.42	-0.37
	N_{res}	-0.15	*0.50	-0.08	*0.70	*0.72	-0.21	*0.67	0.29	0.07	0.27	0.23	0.29
	N_0	-0.37	0.13	-0.07	0.39	*0.68	-0.46	0.32	*0.73	*0.73	*0.74	*0.77	*0.73
	Linear coef	*-0.76	-0.12	0.05	-0.25	-0.2	-0.01	-0.22	-0.42	*-0.56	-0.43	*-0.51	-0.41
	Quad coef	0.69	-0.08	-0.13	-0.04	0.00	-0.04	-0.01	0.28	*0.53	0.30	0.39	0.27
All	k_{max}	0.36	*0.44	-0.08	0.02	*-0.36	*0.49	0.23	*-0.34	*-0.44	*-0.41	-0.22	*-0.36
	N_{res}	-0.32	*-0.31	*0.38	*0.53	*0.52	0.07	0.14	0.08	0.13	0.28	0.16	-0.02
	N_0	*-0.46	-0.16	*0.54	*0.77	*0.79	0.06	0.26	0.25	0.07	*0.41	*0.37	0.12
	Linear coef	0.31	*0.40	0.01	0.02	*-0.36	*0.49	0.16	*-0.38	*-0.52	*-0.49	-0.27	*-0.40
	Quad coef	*-0.44	*-0.40	0.07	-0.10	0.24	*-0.44	-0.27	*0.36	*0.42	*0.40	0.29	*0.40

There was strong, positive linear correlation between some water quality characteristics and model parameters for flocculated water (Table 4.6 and Table 4.7). N_{res} and N_0 had the most significant and strong correlations compared to k_{max}, linear coefficient, and quadratic coefficient. N_{res} and N_0 were well correlated with TSS, turbidity, DOC, absorbance at 254 nm, and SUVA. N_0 also had a strong, positive correlation with IS absorbance at 254nm. For both corrected and uncorrected models, the particle size water quality characteristics had mostly negative correlation with the model parameters.

There were a few strong, positive linear correlations between some water quality characteristics and model parameters for unsettled softened water (Table 4.6 and Table 4.7). N_{res} had the most significant positive correlations for non-particle size water quality characteristics, including SUVA, absorbance, and IS absorbance at 254 nm. The correlation with turbidity was significant, but it was only 0.50. N_0 had strong positive correlations with particle size characteristics. The linear coefficient had a significantly strong, negative relationship with TSS. Although it is not strong, k_{max} and linear coefficient are negatively related with particle size characteristics. Overall, there were less strong correlations for k_{max}, N_{res} and the linear coefficient for softened water than for raw river water and flocculated water.

When comparing the water quality characteristics to the model parameters independent of water type, a lot of the strong, positive correlations disappeared (Table 4.6 and Table 4.7 (labeled "all")). The strongest correlation was between N_0 and absorbance and IS absorbance at 254 nm. N_{res} and N_0 had the most significant correlations compared to k_{max}, linear coefficient, and quadratic coefficient. For both corrected and uncorrected models, the particle size water quality characteristics had mostly negative correlations with k_{max} and the linear coefficient.

For all three water types, k_{max} has a negative relationship with particle size characteristics. Larger particles lead to a lower k_{max}. Raw river non-particle size water quality characteristics had stronger correlations with the Geeraerd model parameters than flocculated and softened water. For both softened and flocculated water, N_{res} had stronger positive correlations with non-particle size water quality parameters than k_{max}, including turbidity, direct UVA_{254}, and SUVA. There was no significant correlation (p-values > 0.05) between the most common particle size range and the model parameters for flocculated and softened water (Table 4.8).

Table 4.8. Pearson's r between modeled inactivation parameters and the particle size range with the highest amount of particles.

		Floc	Soft
Uncorrected	k_{max}	0.36	-0.04
	N_{res}	0.38	-0.41
	N_0	0.41	-0.15
	linearcoef	0.38	-0.01
	quadcoef	-0.35	0.22
Corrected	k_{max}	0.15	0.03
	N_{res}	0.38	-0.41
	N_0	0.41	-0.15
	linearcoef	0.21	0.06
	quadcoef	-0.25	0.19

5 Discussion

5.1 Overall impacts

Model parameters and dose responses were repeatable despite extremely varying water quality conditions and initial spore concentrations over the sampling period, both for indigenous spores and spiked *B. subtilis* spores, and even for different types (raw and soft). The final supermodel parameters combine data from experiments with extremely variable water qualities and times of year, with other unmeasured factors that could have impacted results. For example, the population of indigenous spores may have varied in resistance over the collection period. Even in the worst-case scenario conditions with extreme water quality fluctuations tested in this study, disinfection became very predictable.

The dose response in flocculated water was significantly different than dose responses for raw river water and softened water, confirmed by ANOVA on model parameters. Neither turbidity, absorbance, nor any particle size parameter had a definitive impact on dose response parameters across water types. For a given water type, stronger correlations were apparent especially for N_{res} and k_{max} in raw river water and flocculated water. The maximum specific inactivation rate, which is usually the main parameter used to describe dose response kinetics, does not have strong correlation with water quality parameters for softened water and flocculated water. While Carré et al., 2018 reported a strong correlation between inactivation rate constant and turbidity, UV_{254} transmission, and total suspended solids and Loge et al., 1996 stated that UV transmission and suspended solids concentration significantly impacted tailing, other studies did not report a correlation between inactivation and those water quality characteristics (Darby et al., 1993; Madge & Jensen, 2006). Instead, many studies reported a correlation between inactivation, particle size, and particle amount (Caron et al., 2007; Carré et al., 2018; Emerick et al., 1999, 2000; Jolis et al., 2001; Liu et al., 2007; Madge & Jensen, 2006; Qualls et al., 1985; Winward et al., 2008), which agrees with our results. There is a negative correlation between k_{max} and particle size characteristics for all water types, indicating that larger particles lead to a lower k_{max}. Additionally, particle size data did not correlate well with turbidity or total suspended solids, which was also noted by other studies (Cantwell et al., 2010; Qualls et al., 1983). Losing the strong correlations between model parameters and water quality characteristics when calculating it independent of water type indicates that numerous water quality characteristics are needed to accurately describe the relationship between UV disinfection and water parameters, and most likely different water qualities have a variable impact on UV disinfection for different water types. Although raw and soft dose responses were overall repeatable, it is likely that a different water quality parameter for raw and soft were making the biggest impact.

5.2 Particle size

Presence of flocculated particles could still explain the difference in UV inactivation between flocculated water and soft and raw river water. The distribution in the overall particle size graphs show that flocculated water had larger particles that were also more narrowly distributed than softened water. Larger particles have a stronger negative impact on UV disinfection, often through tailing, than smaller particles (Carré et al., 2018; Madge & Jensen, 2006; Winward et al.,

2008). For all three water types, the maximum inactivation rate and the linear coefficient had a negative correlation with particle size water quality characteristics, indicating that larger particle sizes and fractions correspond with a lower inactivation rate and linear coefficient. Studies where turbidity (up to 10 NTU) did not significantly impact UV inactivation reported small particle sizes (Amoah et al., 2005; Cantwell et al., 2010; Templeton et al., 2009). Commonly, larger than 7-10 µm has been regarded as a critical size for negative impact on UV disinfection, with a few studies showing slightly larger at 20 or 25 µm. Both softened and flocculated water contained mostly particles above 7-10 µm, with flocculated water having larger particles.

5.3 Microorganism-particle interactions

From the filtrate experiment, we know that at least 30.2% of indigenous spores are associated with flocculated particles greater than 12 microns. The rest of the indigenous spores are either free-floating or associated with particles smaller than 12 microns. Free-floating spores are mostly present as self-aggregates and not as individual cells because of the extremely low concentration in the 1.2-micron filtrate. It is easier to disinfect free-floating microorganisms and spores than particle associated microorganisms (Emerick et al., 2000; Mamane & Linden, 2006a; Örmeci & Linden, 2002). If the spores in the softened water were mainly free-floating instead of associated with particles, it could be a second explanation for the difference in dose response between flocculated water and softened water. The lower initial concentration of softened water compared to raw river water and flocculated water implies that most of the indigenous spores were associated with the flocculated particles and settled in the flocculation basin. The free-floating spores moved on to the softening channel. Most of the indigenous spores and microorganisms present in the raw river water and softened water are likely free-floating while the majority bacteria present in flocculated water is particle-associated. Knowing the degree of microorganism-particle association might improve predictions of water quality impact on UV disinfection.

Using an integrating sphere for measuring absorbance should correct for the effects of turbidity and particles during UV disinfection (Christensen & Linden, 2003), but there were no significant differences between corrected or uncorrected model parameters for all three types. Only for raw river water did there appear to be a difference in the strength of correlation from uncorrected to corrected between particle size water quality characteristics and maximum inactivation rate and the linear coefficient. Even though the absorbance was corrected for the presence of particles, there was no significant difference between corrected and uncorrected dose response because the integrating sphere cannot account for the proportions of free-floating microorganisms and particle associated organisms in flocculated water and softened water. Therefore, the negative correlation between particle size characteristics for flocculated water did not change significantly between uncorrected and corrected model parameters. Since raw river water did not have a lot of particles, it did show a stronger negative relationship between corrected maximum inactivation rate and corrected linear coefficient for particle-size water quality characteristics. If flocculated water had a larger percentage of particle associated microorganisms, as well as overall larger particles, it could explain the difference between softened water and flocculated water, and no significant difference between softened water and raw river water.

The flocculated particles have a different structure than softened particles. Different particle composition characteristics, such as surface charge and porosity, can impact the effect on UV disinfection. In agreement with our study, (Liu et al., 2007) noted that even at a turbidity of 32 NTU, surface water particles essentially had no influence on spiked *E. coli* UV inactivation, while the presence of flocculated particles in lower turbidity waters led to significantly lower *E. coli* UV inactivation. Additionally, (Templeton et al., 2005) reported that humic acid flocculated particles enmeshed and protected viral surrogates at extremely high turbidity levels, while inorganic kaolin clay particles did not provide protection under the same turbidity conditions. Flocculated particles have a porosity and structure conducive to trapping microorganisms (Gorczyca & Ganczarczyk, 2001) while softening particles do not. Results from the filtrate experiment also indicated that the filtrate with larger flocculated particles are more reflective than the filtrate with smaller particles or no particles. Recent studies show a strong correlation between surface charge of particles and negative impact on tailing (Farrell et al., 2018; Soleimanpour Makuei et al., 2022; Tan et al., 2017). UV dose response differences between flocculated and softened water were not explained by turbidity and are more likely due to differences in particle size and structure.

5.4 Spiked spores

The combined spiked *B. subtilis* and indigenous spores (mixed) had similar dose responses across the three water types compared to indigenous spores only. Flocculated water had a significantly lower maximum inactivation rate, significantly higher residual population density, and linear coefficient. The mixed maximum inactivation rate is one order of magnitude greater than the maximum inactivation rate of the indigenous spores only for all three water types. The main reason for this is likely that *B. subtilis* is a lab-type spore, which is less resistant than wild spores (Mamane-Gravetz et al., 2005; Mamane-Gravetz & Linden, 2004, 2005). We did not test the attachment proportions of the spiked *B. subtilis.* Although some of the *B. subtilis* spores could have formed spore-particle aggregates or spore-spore aggregates, it is likely that most of the *B. subtilis* spores would be free-floating in the water (Mamane-Gravetz & Linden, 2005). Free-floating spores, even in the presence of particles, are easier to disinfect than spore-particle aggregates (Farrell et al., 2018; Mamane & Linden, 2006a; Örmeci & Linden, 2002). Within the spiked experiment, turbidity did not explain the lowered dose response for flocculated water. In this case, it would still likely be due to the presence of larger particles and particle structure, because larger particles cause more shielding and result in a greater residual population density.

RED bias values are derived from real-word worst case UV reactors and the calculation is therefore considered to be overly conservative. Additionally, the calculated dose for *Cryptosporidium* is linked to UV transmission, even though our results show that turbidity and UVT were not well correlated with changes in disinfection kinetics, which makes the RED even more conservative than it already is. Although results showed 4-log *Cryptosporidium* inactivation for UVT above 65, 90, or 80% in raw, floc, or soft water, it's possible to expect 4-log inactivation in water with worse UVT values if other water quality factors, such as particle size or degree of microorganism-particle associations, are quantified.

6 Conclusion

Although turbidity can be a good indicator of water quality, it may not be the best water quality parameter to regulate UV disinfection. Raw water and softened water had very different water qualities including turbidity, but their indigenous spore UV dose responses were similar to each other, and UV disinfection of spiked spores in both raw and softened water was similar to lab water. In this and other studies, particle size may be a better indicator of UV disinfection than turbidity. Particle size and the degree of particle-associated microorganisms impacted the maximum inactivation rate and tailing, especially in flocculated water which was negatively impacted by adverse water quality while raw and softened water were not. Particle-associated microorganisms are more difficult to disinfect with UV. However, with very poor water quality, there was still significant and repeatable inactivation of indigenous spores and seeded *B. subtilis*. This means significant and predictable inactivation would be expected of *Cryptosporidium parvum* (oo)cysts even under variable water quality including high turbidity conditions. *C. parvum* is more sensitive than indigenous wild spores and lab spores, and would likely have higher inactivation than spores at the doses reported in this study. With climate change driving lower and more variable water quality of source waters, filter upset may occur more often and current regulations may be too conservative and inefficient for managing and responding to these issues.

This study shows how the source that contributes to the turbidity or particles should be taken into account when considering UV regulations. We recommend building on this study by testing UV disinfection on indigenous pathogens from filtered drinking process water and water that passed through during filter upset. Worst-case scenarios for flocculated water and softened water tested in this study would likely never actually occur at the UV disinfection step at a DWTP, even during filter upset, because our samples were collected pre-settling. Ideally, this would be tested at the pilot level with higher initial concentration of pathogens in the raw water and filter upset for flocculated water and softened water to determine if UV disinfection water quality regulations can be updated in the United States. Additionally, testing more variables, such as different source waters, types of flocculants, and other unit process worst case scenarios could provide valuable information that we were not able to investigate in this research.

7 References

Allaire, M., Wu, H., & Lall, U. (2018). National trends in drinking water quality violations. *Proceedings of the National Academy of Sciences*, *115*(9), 2078–2083. https://doi.org/10.1073/pnas.1719805115

Amoah, K., Craik, S., Smith, D. W., & Belosevic, M. (2005). Inactivation of Cryptosporidium oocysts and Giardia cysts by ultraviolet light in the presence of natural particulate matter. *Journal of Water Supply: Research and Technology - AQUA*, *54*(3), 165–178. https://doi.org/10.2166/aqua.2005.0016

Augsburger, N., Rachmadi, A. T., Zaouri, N., Lee, Y., & Hong, P.-Y. (2021). Recent Update on UV Disinfection to Fulfill the Disinfection Credit Value for Enteric Viruses in Water. *Environmental Science & Technology*, *55*(24), 16283–16298. https://doi.org/10.1021/acs.est.1c03092

Azimi, Y., Allen, D. G., Seto, P., & Farnood, R. (2014). Effect of Activated Sludge Retention Time, Operating Temperature, and Influent Phosphorus Deficiency on Floc Physicochemical Characteristics and UV Disinfection. *Industrial & Engineering Chemistry Research*, *53*(31), 12485–12493. https://doi.org/10.1021/ie5012068

Barbeau, B., Boules, L., Desjardins, R., Coallier, J., Prevost, M., & Duchesne, D. (1997). A modified method for the enumeration of aerobic spore-forming bacteria. *Canadian Journal of Microbiology*, *43*, 976–980. https://doi.org/10.1139/m97-140

Batch, L. F., Schulz, C. R., & Linden, K. G. (2004). Evaluating Water Quality Effects on UV Disinfection of MS2 Coliphage. *Journal - American Water Works Association*, *96*(7), 75–87. https://doi.org/10.1002/j.1551-8833.2004.tb10651.x

Betancourt, W. Q., & Rose, J. B. (2004). Drinking water treatment processes for removal of Cryptosporidium and Giardia. *Veterinary Parasitology*, *126*(1–2), 219–234. https://doi.org/10.1016/J.VETPAR.2004.09.002

Bohrerova, Z., & Linden, K. G. (2006). Ultraviolet and chlorine disinfection of mycobacterium in wastewater: Effect of aggregation. *Water Environment Research: A Research Publication of the Water Environment Federation*, *78*(6), 565–571. https://doi.org/10.2175/106143006x99795

Bolton, J. R., Beck, S. E., & Linden, K. G. (2015). *Protocol for the Determination of Fluence (UV Dose) Using A Low-Pressure or Low-Pressure High-Output UV Lamp in Bench-Scale Collimated Beam Ultraviolet Experiments*. IUVA Board of Directors.

Bolton, J. R., & Linden, K. G. (2003). Standardization of Methods for Fluence (UV Dose) Determination in Bench-Scale UV Experiments. *Journal of Environmental Engineering*, *129*(3), 209–215. https://doi.org/10.1061/(ASCE)0733-9372(2003)129:3(209)

Bradford, S. A., Kim, H., Headd, B., & Torkzaban, S. (2016). Evaluating the Transport of *Bacillus subtilis* Spores as a Potential Surrogate for *Cryptosporidium parvum* Oocysts. *Environmental Science & Technology*, *50*(3), 1295–1303. https://doi.org/10.1021/acs.est.5b05296

Brown, R. A., & Cornwell, D. A. (2007). Using spore removal to monitor plant performance for *Cryptosporidium* removal. *Journal - American Water Works Association*, *99*(3), 95–109. https://doi.org/10.1002/j.1551-8833.2007.tb07892.x

Cantwell, R. E., & Hofmann, R. (2008). Inactivation of indigenous coliform bacteria in unfiltered surface water by ultraviolet light. *Water Research, 42*(10), 2729–2735. https://doi.org/10.1016/j.watres.2008.02.002

Cantwell, R. E., & Hofmann, R. (2011). Ultraviolet absorption properties of suspended particulate matter in untreated surface waters. *Water Research, 45*(3), 1322–1328. https://doi.org/10.1016/j.watres.2010.10.020

Cantwell, R. E., Hofmann, R., Rand, J. L., Devine, P. M., & VanderMarck, M. (2010). Case Study of Particle-Related UV Shielding of Microorganisms When Disinfecting Unfiltered Surface Water. *Water Quality Research Journal, 45*(3), 343–351. https://doi.org/10.2166/wqrj.2010.030

Caron, E., Chevrefils, G., Barbeau, B., Payment, P., & Prévost, M. (2007). Impact of microparticles on UV disinfection of indigenous aerobic spores. *Water Research, 41*(19), 4546–4556. https://doi.org/10.1016/j.watres.2007.06.032

Carré, E., Pérot, J., Jauzein, V., & Lopez-Ferber, M. (2018). Impact of suspended particles on UV disinfection of activated-sludge effluent with the aim of reclamation. *Journal of Water Process Engineering*, *22*, 87–93. https://doi.org/10.1016/j.jwpe.2018.01.016

Cerf, O. (1977). Tailing of survival curves of bacterial spores. *Journal of Applied Bacteriology*, *42*(1), 1–19. https://doi.org/10.1111/j.1365-2672.1977.tb00665.x

Certad, G., Viscogliosi, E., Chabe, M., & Caccio, S. M. (2017). Pathogenic Mechanisms of *Cryptosporidium* and *Giardia*. *Trends in Parasitology*, *33*(7), 561–576. https://doi.org/10.1016/j.pt.2017.02.006

Choi, Y., & Choi, Y.-J. (2010). The effects of UV disinfection on drinking water quality in distribution systems. *Water Research, 44*(1), 115–122. https://doi.org/10.1016/j.watres.2009.09.011

Christensen, J., & Linden, K. G. (2003). How particles affect UV light in the UV Disinfection of Unfiltered Drinking Water. *Journal - American Water Works Association, 95*(4), 179–189. https://doi.org/10.1002/j.1551-8833.2003.tb10344.x

City of Columbus. (2022). *Drinking Water Consumer Confidence Report*. https://www.columbus.gov/utilities/water-protection/CCR/

Clancy, J. L., Bukhari, Z., Hargy, T. M., Bolton, J. R., Dussert, B. W., & Marshall, M. M. (2000). Using UV to inactivate Cryptosporidium. *Journal - American Water Works Association, 92*(9), 97–104. https://doi.org/10.1002/j.1551-8833.2000.tb09008.x

Clancy, J. L., Gollnitz, W. D., & Tabib, Z. (1994). Commercial labs: How accurate are they? *Journal - American Water Works Association, 86*(5), 89–97. https://doi.org/10.1002/j.1551-8833.1994.tb06198.x

Clancy, J. L., Marshall, M. M., Hargy, T. M., & Korich, D. G. (2004). Susceptibility of five strains of *Cryptosporidium parvum* oocysts to UV light. *Journal - American Water Works Association, 96*(3), 84–93. https://doi.org/10.1002/j.1551-8833.2004.tb10576.x

Darby, J. L., Snider, K. E., & Tchobanoglous, G. (1993). Ultraviolet Disinfection for Wastewater Reclamation and Reuse Subject to Restrictive Standards. *Water Environment Research, 65*(2), 169–180. https://www.jstor.org/stable/25044282

Dietrich, J. P., Başağaoğlu, H., Loge, F. J., & Ginn, T. R. (2003). Preliminary assessment of transport processes influencing the penetration of chlorine into wastewater particles and

the subsequent inactivation of particle-associated organisms. *Water Research*, *37*(1), 139–149. https://doi.org/10.1016/S0043-1354(02)00239-7

Dotson, A. D., Rodriguez, C. E., & Linden, K. G. (2012). UV disinfection implementation status in US water treatment plants. *Journal - American Water Works Association*, *104*(5), 318–324. https://doi.org/10.5942/jawwa.2012.104.0075

Emerick, R. W., Loge, F. J., Ginn, T., & Darby, J. L. (2000). Modeling the Inactivation of Particle-Associated Coliform Bacteria. *Water Environment Research*, *72*(4), 432–438. https://doi.org/10.2175/106143000x137969

Emerick, R. W., Loge, F. J., Thompson, D., & Darby, J. L. (1999). Factors Influencing Ultraviolet Disinfection Performance Part II: Association of Coliform Bacteria with Wastewater Particles. *Water Environment Research*, *71*(6), 1178–1187. https://doi.org/10.2175/106143097X122004

Eskaf, S. (2015, January 28). Small Water Systems with Financial Difficulties are More Likely to Violate EPA Regulations. *Environmental Finance Blog*. https://efc.web.unc.edu/2015/01/28/small-water-systems-financial-difficulties-likely-violate-epa-regulations/

Farrell, C., Hassard, F., Jefferson, B., Leziart, T., Nocker, A., & Jarvis, P. (2018). Turbidity composition and the relationship with microbial attachment and UV inactivation efficacy. *Science of The Total Environment*, *624*, 638–647. https://doi.org/10.1016/j.scitotenv.2017.12.173

Feng, Y. Y., Ong, S. L., Hu, J. Y., Song, L. F., Tan, X. L., & Ng, W. J. (2003). Effect of Particles on the Recovery of *Cryptosporidium* Oocysts from Source Water Samples of Various

Turbidities. *Applied and Environmental Microbiology*, *69*(4), 1898–1903. https://doi.org/10.1128/AEM.69.4.1898-1903.2003

Geeraerd, A. H., Herremans, C. H., & Van Impe, J. F. (2000). Structural model requirements to describe microbial inactivation during a mild heat treatment. *International Journal of Food Microbiology*, *59*(3), 185–209. https://doi.org/10.1016/S0168-1605(00)00362-7

Geeraerd, A. H., Valdramidis, V. P., & Van Impe, J. F. (2005). GInaFiT, a freeware tool to assess non-log-linear microbial survivor curves. *International Journal of Food Microbiology*, *102*(1), 95–105. https://doi.org/10.1016/j.ijfoodmicro.2004.11.038

Gorczyca, B., & Ganczarczyk, J. (2001). Fractal Analysis of Pore Distributions in Alum Coagulation and Activated Sludge Flocs. *Water Quality Research Journal of Canada*, *36*(4), 687–700. https://doi.org/10.2166/wqrj.2001.036

Guo, H., & Hu, J. (2012). Effect of hybrid coagulation–membrane filtration on downstream UV disinfection. *Desalination*, *290*, 115–124. https://doi.org/10.1016/j.desal.2012.01.015

Hannoun, D., Belding, J., Tietjen, T., & Devaney, R. (2022). Assessing treatability with simulated lake drawdown: Quantifying drought-driven turbidity in source water. *AWWA Water Science*, *4*(4), e1295. https://doi.org/10.1002/aws2.1295

He, G. S., Qin, H.-Y., & Zheng, Q. (2009). Rayleigh, Mie, and Tyndall scatterings of polystyrene microspheres in water: Wavelength, size, and angle dependences. *Journal of Applied Physics*, *105*(2), 023110. https://doi.org/10.1063/1.3068473

Jolis, D., Lam, C., & Pitt, P. (2001). Particle effects on ultraviolet disinfection of coliform bacteria in recycled water. *Water Environment Research: A Research Publication of the*

Water Environment Federation, *73*(2), 233–236. https://doi.org/10.2175/106143001x139218

Karanis, P., Sotiriadou, I., Kartashev, V., Kourenti, C., Tsvetkova, N., & Stojanova, K. (2006). Occurrence of *Giardia* and *Cryptosporidium* in water supplies of Russia and Bulgaria. *Environmental Research*, *102*(3), 260–271. https://doi.org/10.1016/j.envres.2006.05.005

Kollu, K., & Örmeci, B. (2012). Effect of particles and bioflocculation on ultraviolet disinfection of *Escherichia coli*. *Water Research*, *46*(3), 750–760. https://doi.org/10.1016/j.watres.2011.11.046

Kollu, K., & Örmeci, B. (2015). UV-induced self-aggregation of *E. coli* after low and medium pressure ultraviolet irradiation. *Journal of Photochemistry and Photobiology B: Biology*, *148*, 310–321. https://doi.org/10.1016/J.JPHOTOBIOL.2015.04.013

Lee, H. W., Kim, E. J., Park, S. S., & Choi, J. H. (2015). Effects of Climate Change on the Movement of Turbidity Flow in a Stratified Reservoir. *Water Resources Management*, *29*, 4095–4110. https://doi.org/10.1007/s11269-015-1047-2

Leighton, T. J., & Doi, R. H. (1971). The Stability of Messenger Ribonucleic Acid during Sporulation in *Bacillus subtilis*. *Journal of Biological Chemistry*, *246*(10), 3189–3195. https://doi.org/10.1016/S0021-9258(18)62213-6

Linden, K. G., & Darby, J. L. (1998). Ultraviolet Disinfection of Marginal Effluents: Determining Ultraviolet Absorbance and Subsequent Estimation of Ultraviolet Intensity. *Water Environment Research*, *70*(2), 214–223. https://www.jstor.org/stable/25045029

Liu, G. (2005). *An investigation of UV disinfection performance under the influence of turbidity & particulates for drinking water applications* [Master's Thesis, University of Waterloo]. http://hdl.handle.net/10012/823

Liu, G., Slawson, R. M., & Huck, P. M. (2007). Impact of flocculated particles on low pressure UV inactivation of *E. coli* in drinking water. *Journal of Water Supply: Research and Technology - AQUA*, *56*(3), 153–162. https://doi.org/10.2166/AQUA.2007.104

Loge, F. J., Bourgeous, K., Emerick, R. W., & Darby, J. L. (2001). Variations in Wastewater Quality Parameters Influencing UV Disinfection Performance: Relative Impact of Filtration. *Journal of Environmental Engineering*, *127*(9), 832–837. https://doi.org/10.1061/(ASCE)0733-9372(2001)127:9(832)

Loge, F. J., Emerick, R. W., Heath, M., Jacangelo, J., Tchobanoglous, G., & Darby, J. L. (1996). Ultraviolet Disinfection of Secondary Wastewater Effluents: Prediction of Performance and Design. *Water Environment Research*, *68*(5), 900–916. https://www.jstor.org/stable/25044788

Loge, F. J., Emerick, R. W., Thompson, D. E., Nelson, D. C., & Darby, J. L. (1999). Factors Influencing Ultraviolet Disinfection Performance Part I: Light Penetration to Wastewater Particles. *Water Environment Research*, *71*(3), 377–381. https://doi.org/10.2175/106143097X122176

Madge, B. A., & Jensen, J. N. (2006). Ultraviolet Disinfection of Fecal Coliform in Municipal Wastewater: Effects of Particle Size. *Water Environment Research*, *78*(3), 294–304. https://doi.org/10.2175/106143005x94385

Mamane, H., & Linden, K. G. (2006a). Impact of Particle Aggregated Microbes on UV Disinfection. I: Evaluation of Spore-Clay Aggregates and Suspended Spores. *Journal of Environmental Engineering*, *132*(6), 596–606. https://doi.org/10.1061/(ASCE)0733-9372(2006)132:6(596)

Mamane, H., & Linden, K. G. (2006b). Impact of Particle Aggregated Microbes on UV Disinfection II: Proper Absorbance Measurement for UV Fluence. *Journal of Environmental Engineering*, *132*(6), 607–615. https://doi.org/10.1061/(ASCE)0733-9372(2006)132:6(607)

Mamane-Gravetz, H., & Linden, K. G. (2004). UV disinfection of indigenous aerobic spores: Implications for UV reactor validation in unfiltered waters. *Water Research*, *38*(12), 2898–2906. https://doi.org/10.1016/j.watres.2004.03.035

Mamane-Gravetz, H., & Linden, K. G. (2005). Relationship between physiochemical properties, aggregation and u.v. Inactivation of isolated indigenous spores in water. *Journal of Applied Microbiology*, *98*(2), 351–363. https://doi.org/10.1111/j.1365-2672.2004.02455.x

Mamane-Gravetz, H., Linden, K. G., Cabaj, A., & Sommer, R. (2005). Spectral Sensitivity of *Bacillus subtilis* Spores and *MS2 Coliphage* for Validation Testing of Ultraviolet Reactors for Water Disinfection. *Environmental Science & Technology*, *39*(20), 7845–7852. https://doi.org/10.1021/es048446t

Masschelein, W. J., & Rice, R. G. (2002). *Ultraviolet light in water and wastewater sanitation* (1st ed.). CRC Press.

Medema, G. J., Schets, F. M., Teunis, P. F. M., & Havelaar, A. H. (1998). Sedimentation of Free and Attached *Cryptosporidium* Oocysts and *Giardia* Cysts in Water. *Applied and Environmental Microbiology*, *64*(11), 4460–4466. https://doi.org/10.1128/aem.64.11.4460-4466.1998

Mi, H., Fagherazzi, S., Qiao, G., Hong, Y., & Fichot, C. G. (2019). Climate change leads to a doubling of turbidity in a rapidly expanding Tibetan lake. *Science of The Total Environment*, *688*, 952–959. https://doi.org/10.1016/j.scitotenv.2019.06.339

Mofidi, A. A., Rochelle, P. A., Chou, C. I., Mehta, H. M., Linden, K. G., & Malley, J. P. (2002). *Bacterial Survival After Ultraviolet Light Disinfection: Resistance, Regrowth and Repair*. American Water Works Association Water Quality and Technology Conference, Seattle.

Mukundan, R., Scheerer, M., Gelda, R. K., & Owens, E. M. (2018). Probabilistic Estimation of Stream Turbidity and Application under Climate Change Scenarios. *Journal of Environmental Quality*, *47*(6), 1522–1529. https://doi.org/10.2134/jeq2018.06.0229

Nieminski, E. C., Bellamy, W. D., & Moss, L. R. (2000). Using surrogates to improve plant performance. *Journal - American Water Works Association*, *92*(3), 67–78. https://doi.org/10.1002/j.1551-8833.2000.tb08910.x

Oguma, K., Rattanakul, S., & Masaike, M. (2019). Inactivation of health-related microorganisms in water using UV light-emitting diodes. *Water Supply*, *19*(5), 1507–1514. https://doi.org/10.2166/ws.2019.022

Oppenheimer, J., Gillogly, T., Stolarik, G., & Ward, R. (2002). *Comparing the Efficiency of Low and Medium Pressure UV Light for Inactivating Giardia muris and Cryptosporidium*

parvum in Waters with Low and High Levels of Turbidity. American Water Works Association Annual Conference, New Orleans.

Örmeci, B., & Linden, K. G. (2002). Comparison of UV and chlorine inactivation of particle and non-particle associated coliform. *Water Supply*, *2*(5–6), 403–410. https://doi.org/10.2166/ws.2002.0197

Parker, J. A., & Darby, J. L. (1995). Particle-Associated Coliform in Secondary Effluents: Shielding from Ultraviolet Light Disinfection. *Water Environment Research, 67*(7), 1065–1075. https://doi.org/doi.org/10.2175/106143095X133310

Passantino, L., Malley Jr., J., Knudson, M., Ward, R., & Kim, J. (2004). Effect of Low Turbidity and Algae on UV Disinfection Performance. *Journal - American Water Works Association, 96*(6), 128–137. https://doi.org/10.1002/j.1551-8833.2004.tb10786.x

Paul, A., Dziallas, C., Zwirnmann, E., Gjessing, E. T., & Grossart, H.-P. (2012). UV irradiation of natural organic matter (NOM): Impact on organic carbon and bacteria. *Aquatic Sciences*, *74*, 443–454. https://doi.org/10.1007/s00027-011-0239-y

PerkinElmer, Inc. (2004). *60 mm Integrating Sphere Reflectance Accessory User's Guide*.

Qualls, R. G., Flynn, M. P., & Johnson, J. D. (1983). The Role of Suspended Particles in Ultraviolet Disinfection. *Journal (Water Pollution Control Federation)*, *55*(10), 1280–1285. https://www.jstor.org/stable/25042084 .

Qualls, R. G., Ossoff, S. F., Chang, J. C. H., Dorfman, M. H., Dumais, C. M., Lobe, D. C., & Johnson, J. D. (1985). Factors Controlling Sensitivity in Ultraviolet Disinfection of Secondary Effluents. *Journal (Water Pollution Control Federation)*, *57*(10), 1006–1011. https://www.jstor.org/stable/25042770

Rice, E. W., Baird, R. B., Eaton, A. D., & Clesceri, L. S. (Eds.). (2012). *Standard Methods For the Examination of Water and Wastewater*. American Public Health Association.

Rice, E. W., Fox, K. R., Miltner, R. J., Lytle, D. A., & Johnson, C. H. (1996). Evaluating plant performance with endospores. *Journal - American Water Works Association*, *88*(9), 122–130. https://doi.org/10.1002/j.1551-8833.1996.tb06618.x

Ryan, U., & Hijjawi, N. (2015). New developments in *Cryptosporidium* research. *International Journal for Parasitology*, *45*(6), 367–373. https://doi.org/10.1016/j.ijpara.2015.01.009

Setlow, P. (2001). Resistance of spores of *Bacillus* species to ultraviolet light. *Environmental and Molecular Mutagenesis*, *38*(2–3), 97–104. https://doi.org/10.1002/em.1058

Severin, B. F., Suidan, M. T., & Engelbrecht, R. S. (1983). Kinetic modeling of U.V. disinfection of water. *Water Research*, *17*(11), 1669–1678. https://doi.org/10.1016/0043-1354(83)90027-1

Soleimanpour Makuei, M., Ketabchi, F., & Peleato, N. (2022). Impact of water characteristics on UV disinfection of unfiltered water. *Water Quality Research Journal*, *57*(4), 247–261. https://doi.org/10.2166/wqrj.2022.006

Sommer, R., & Cabaj, A. (1993). Evaluation of the Efficiency of a UV Plant for Drinking Water Disinfection. *Water Science and Technology*, *27*(3–4), 357–362. https://doi.org/10.2166/wst.1993.0375

Tan, T. C., Azimi, Y., & Farnood, R. R. (2017). Tailing propensity in the ultraviolet disinfection of trickling filter and activated sludge wastewater treatment processes. *Water Science and Technology: A Journal of the International Association on Water Pollution Research*, *76*(3–4), 623–632. https://doi.org/10.2166/wst.2017.242

Templeton, M. R., Andrews, R. C., & Hofmann, R. (2005). Inactivation of particle-associated viral surrogates by ultraviolet light. *Water Research*, *39*(15), 3487–3500. https://doi.org/10.1016/j.watres.2005.06.010

Templeton, M. R., Andrews, R. C., & Hofmann, R. (2008). Particle-Associated Viruses in Water: Impacts on Disinfection Processes. *Critical Reviews in Environmental Science and Technology*, *38*(3), 137–164. https://doi.org/10.1080/10643380601174764

Templeton, M. R., Cantwell, R. E., Quinn, C., Hofmann, R., & Andrews, R. C. (2009). Pilot-scale assessment of the impacts of transient particulate water quality events on the UV disinfection of indigenous total coliform bacteria in drinking water treatment. *Journal of Water Supply: Research and Technology - AQUA*, *58*(1), 11–20. https://doi.org/10.2166/aqua.2009.082

USEPA. (2006). *Ultraviolet Disinfection Guidance Manual for the Final Long Term 2 Enhanced Surface Water Treatment Rule*. United States Environmental Protection Agency.

Winward, G. P., Avery, L. M., Stephenson, T., & Jefferson, B. (2008). Ultraviolet (UV) disinfection of grey water: Particle size effects. *Environmental Technology*, *29*(2), 235–244. https://doi.org/10.1080/09593330802030069

Wright, H., Heath, M., & Bandy, J. (2011). *Yikes! What the UVDGM Does Not Address on UV Disinfection*. IUVA World Congress, Paris.

Yong, D. H. N., Cairns, W., Mao, T., & Farnood, R. R. (2008). Bench-Scale Evaluation of Sonication as a Pretreatment Process for Ultraviolet Disinfection of Wastewater. *Water Quality Research Journal*, *43*(1), 37–45. https://doi.org/10.2166/wqrj.2008.005

Zhang, X., Wan, H., Zwiers, F. W., Hegerl, G. C., & Min, S.-K. (2013). Attributing intensification of precipitation extremes to human influence. *Geophysical Research Letters*, *40*(19), 5252–5257. https://doi.org/10.1002/grl.51010

Appendix

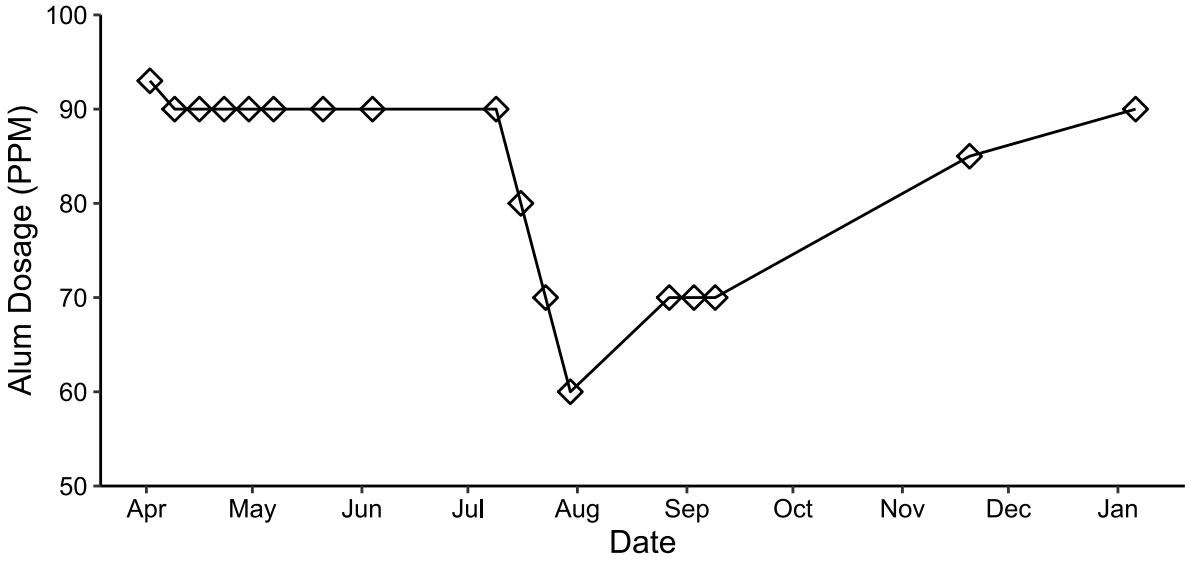

Figure A 1. Alum dosing values at Dublin Road Water Treatment Plant when samples were taken for control experiments and UV inactivation/water quality characterisation experiments.

Text A 1. Flocculated water and softened water samples have particles that must be suspended for consistency when taking measurements. For routine testing, employees at DRWP plant used a jar test setup and mix for 20 seconds at 300 rpm, then six minutes at 120 rpm, then 12 minutes at 60 rpm, and then 12 minutes at 30 rpm to simulate the water flowing through the channel and is based on their calculated G-value. A stir plate was evaluated because a jar test set-up was unavailable. Stir plate mixing rate was determined by measuring turbidity at rates of 60, 125, and 350 rpm (the three lowest settings available on the stir plate). 350 rpm was too turbulent and did not represent the flow of the flocculated and softened water in the channel where samples were collected, while 60 rpm allowed particle settling. The coefficient of variation for turbidity was lowest for 125 rpm (Table A 1) and was chosen as the mixing rate.

Table A 1. Turbidity values of flocculated and softened water at variable stirring rates and times

Type	Biological Replicate	Time (min)	Turbidity		Coefficient of Variation	
			60 rpm	125 rpm	60 rpm	125 rpm
Floc	1	5	131	126	5.47%	1.66%
		10	129	123		
		15	120	125		
		20	117	128		
	2	5	135	131	1.60%	0.73%
		10	132	133		
		15	136	131		
		20	137	132		
Soft	1	5	551	547	40.72%	2.33%
		10	372	550		
		15	253	541		
		20	240	522		

Text A 2. The pour plate method, spread plate method, “swirl” method, spot and filter membrane method were compared to determine which plating method to use that maximized recovery of spores.

For the pour plate method, the nutrient agar was made by combining Tryptic Soy Broth (TSB) (BD, 211825) and 1.5% agar (BD, 214010) in DI water. After dissolving the agar, the medium was autoclaved for 45 minutes at 121°C. After cooling the nutrient agar to 55°C, approximately 25 mL of the nutrient agar was added to an inoculated plate with 1 mL of sample in the center of a disposable 100 cm petri dish (VWR, 25384-342). The petri dish was swirled and tilted to mix the sample and the nutrient agar.

For the spread plate method, 25 mL of the same nutrient agar was added to the petri dishes and solidified completely. Afterwards, 1 mL of sample was added to the surface of the solid medium. Using a glass spreader bar (ethanol and flame sterilized), the sample was spread evenly over the surface of the medium.

For the “swirl” method, the petri dishes were prepared in the same way as the spread plate method, however, after the sample was added to the surface of the medium a swirl motion was used to spread the sample instead of using a spreader bar.

For the filter membrane method, a filter vacuum apparatus set up was used. 100 mL of sample or diluted sample was put in the funnel and the vacuum was applied. The 0.45 µm sterile filter membrane (Fisherband, 09-719-555) captured the spores. The filter membrane was then placed on a sterile absorbent pad (Millipore, AP10045S0) soaked with 1.4 mL of sterile TSB in a 60 mm petri dish.

For all methods of plating, the plates were incubated at 35°C for 22-24 hours (Barbeau et al., 1997; Mamane-Gravetz & Linden, 2005). Plates were manually counted on a Reichert Quebec Colony Counter.

Due to the number of samples that needed to be plated in one experiment, it was determined that filter membrane plating would not be feasible. When comparing the pour, spread, and swirl method, the pour method yielded the highest spore concentrations (Table A 2). For the listed methods, using a t-test statistical analysis, the P-value indicated that the means for these methods were significantly less than the pour method.

Table A 2. Comparison between different plating methods for flocculated water. P-value obtained from t-Test between the pour method and the other methods.

Plating Method	Type	SFU/mL	Average	P-value
Pour	Floc 1	1450	1320	
		1190		
	Floc 2	1380		
		1260		
Spread	Floc 1	840	1045	2.99E-02
		970		
	Floc 2	1070		
		1300		
Swirl	Floc 1	860	767.5	1.47E-04
		650		
	Floc 2	750		
		810		

Table A 3.Comparison of different extraction methods prior to pour-plate enumeration of flocculated water. All methods are compared through t-Test analysis to the control: manually shaking the tube. The mean value of the control is in parantheses.

Particle suspension method	Mean	Mean compared to manual shaking	P-Value
30s vortex	725 (690)	>	0.351
30s vortex	2375 (2350)	>	0.490
45s vortex	533 (690)	<	0.047
45s vortex	5450 (7150)	<	0.176
60s vortex	548 (690)	<	0.004
60s vortex	2570 (2350)	>	0.421
90s vortex	585 (690)	<	0.029
90s vortex	2200 (2350)	<	0.161
Manual shaking + 0.05% SDS	618 (690)	<	0.047
30s vortex + 0.05% SDS	433 (690)	<	0.006
30s vortex + 0.05% SDS	1000 (1498)	<	0.084
45s vortex + 0.05% SDS	538 (690)	<	0.003
60s vortex + 0.05% SDS	375 (690)	<	0.002
60s vortex + 0.05% SDS	1274 (1498)	<	0.239
90s vortex + 0.05% SDS	415 (690)	<	0.000
90s vortex + 0.05% SDS	1085 (1498)	<	0.108
30s tissue homogenizer (15000 rpm)	4850 (7150)	<	0.143
60s tissue homogenizer (15000 rpm)	6450 (7150)	<	0.335
60s tissue homogenizer (15000 rpm)	6100 (6750)	<	0.310
120s tissue homogenizer (15000 rpm)	5000 (6750)	<	0.165
60s tissue homogenizer (30000 rpm)	6450 (6750)	<	0.404
60s tissue homogenizer (30000 rpm)	4500 (7150)	<	0.124
120s tissue homogenizer (30000 rpm)	4850 (6750)	<	0.156
5s sonication	2130 (2350)	<	0.271
10s sonication	2185 (2350)	<	0.341
15s sonication	2300 (2350)	<	0.089
30s sonication	1890 (2350)	<	0.184
60s sonication	2400 (2350)	>	0.481
60s grinder	6450 (7150)	<	0.325

Table A 4. Pearson correlation coefficients between measurements from turbidity and total suspended solids for each water type. Turbidity and total suspended solids have a significantly strong, positive linear relationship.

Water type	r	p-value
Unsettled raw river water	0.992	3.40E-10
Unsettled flocculated water	0.996	5.59E-12
Unsettled softened water	0.948	2.74E-06

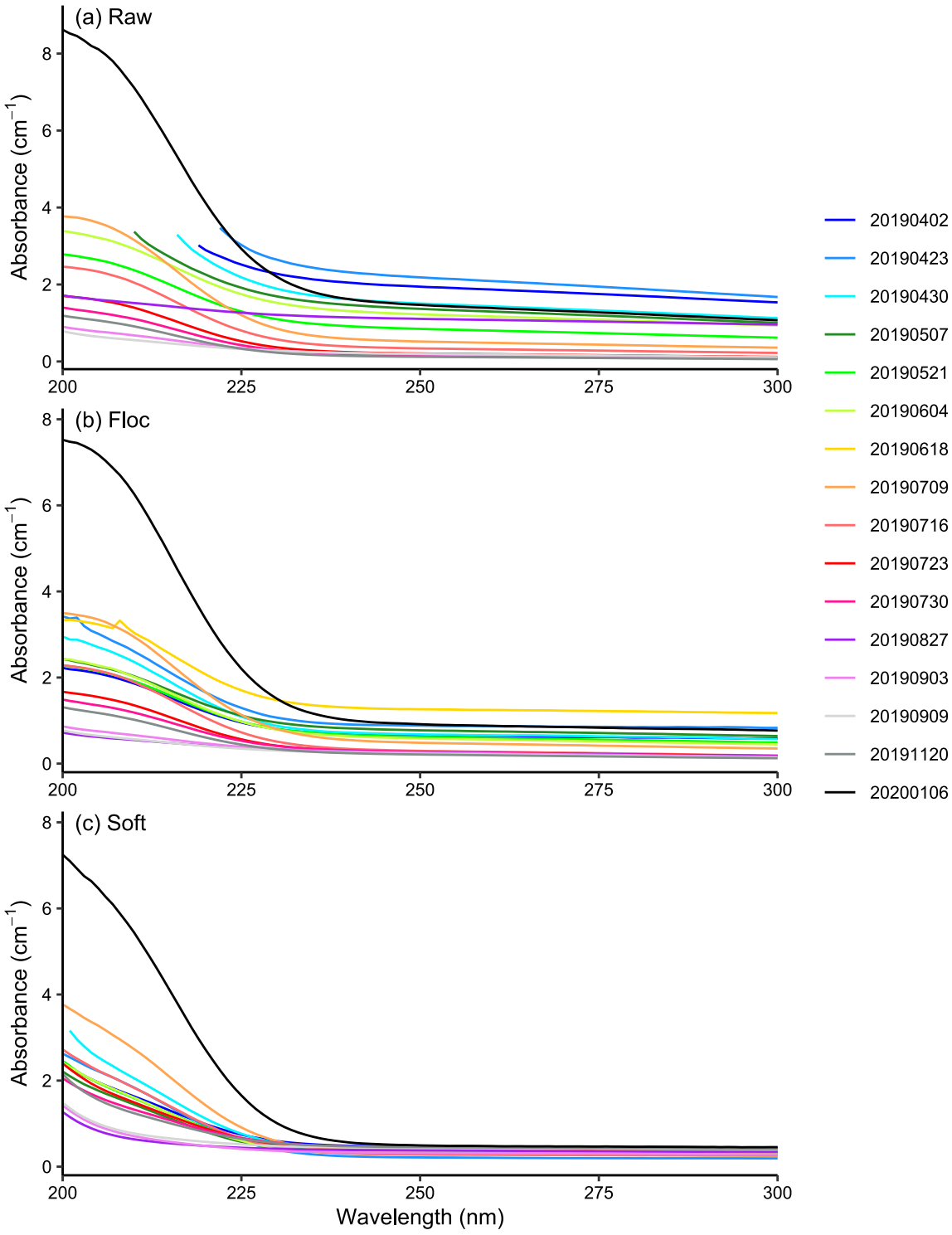

Figure A 2. Absorbance scans for (a) unsettled raw river water, (b) unsettled flocculated water, and (c) unsettled softened water. Data points from 300 – 350 nm are not shown because the full trend can be seen from 200 to 300 nm. Lines represent the average of four total technical replicates from two biological replicates for each water type on each collection date. Absorbance measurements beyond the dynamic range were omitted.

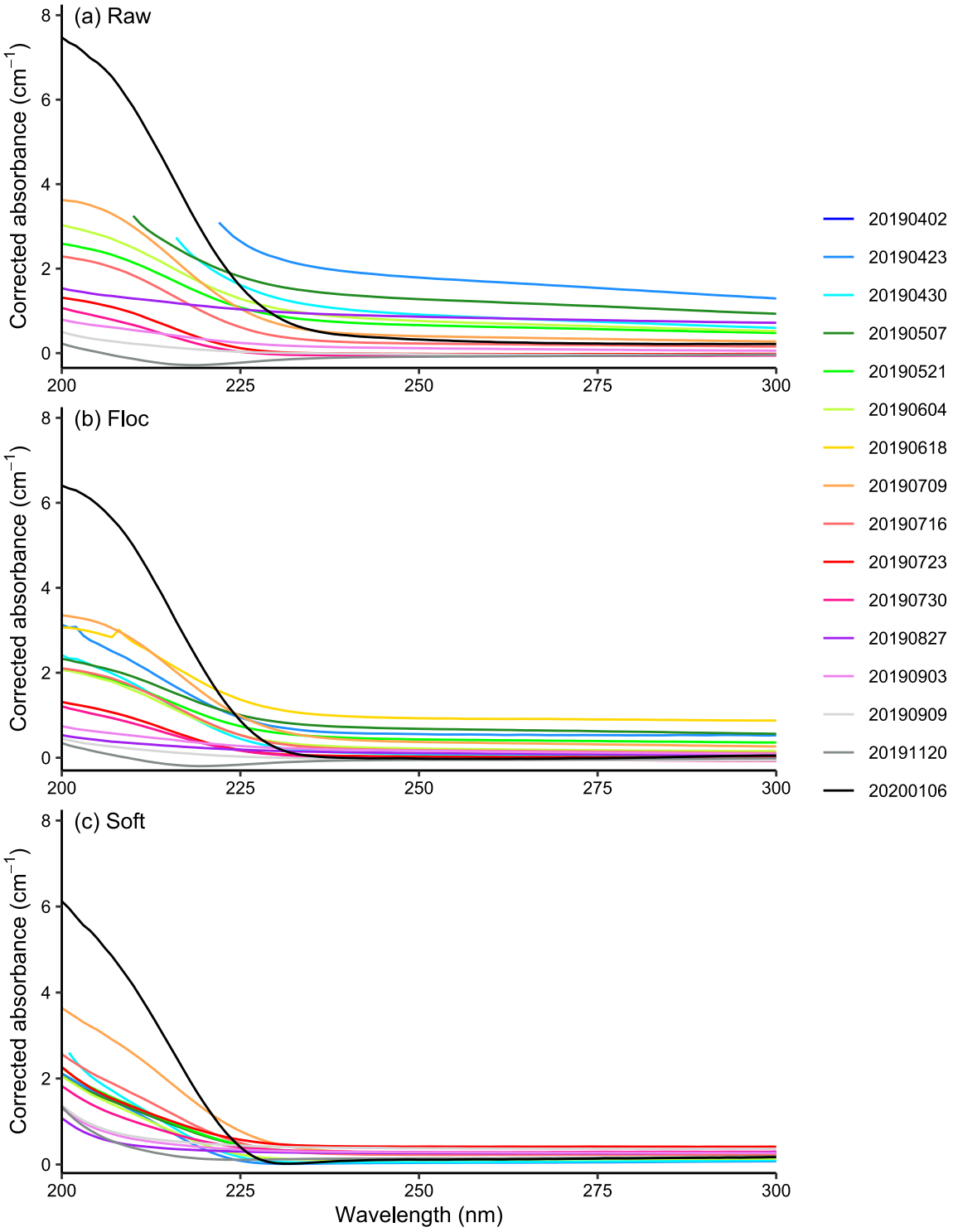

Figure A 3. Absorbance scans for (a) unsettled raw river water, (b) unsettled flocculated water, and (c) unsettled softened water. Data points from 300 – 350 nm are not shown because the full trend can be seen from 200 to 300 nm. Lines represent the average of four total technical replicates from two biological replicates for each water type on each collection date. Absorbance measurements beyond the dynamic range were omitted.

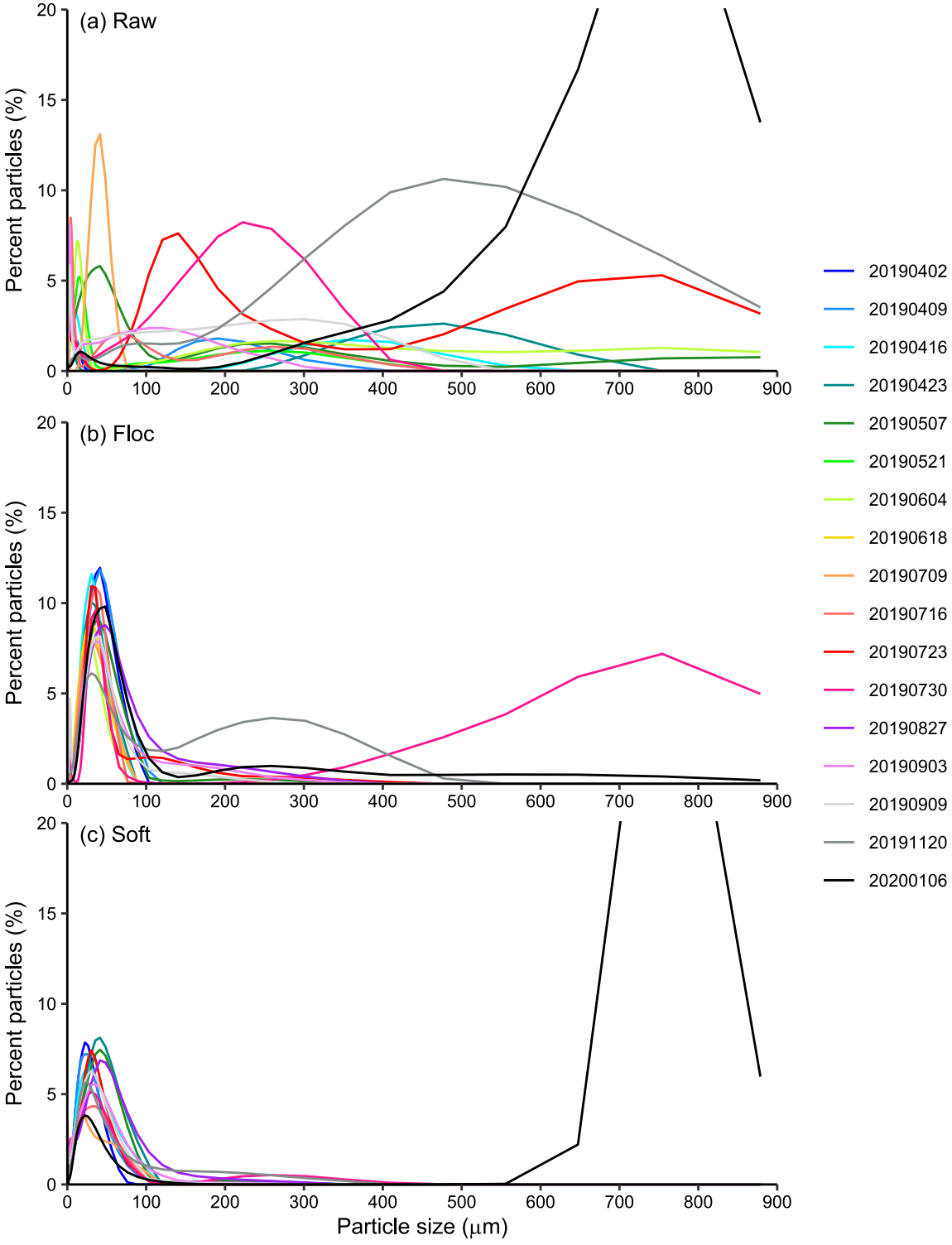

Figure A 4. Percent of total particles for (a) unsettled raw river water, (b) unsettled flocculated water, and (c) unsettled softened water. Lines represent the average of four total technical replicates from two biological replicates for each water type on each collection date.

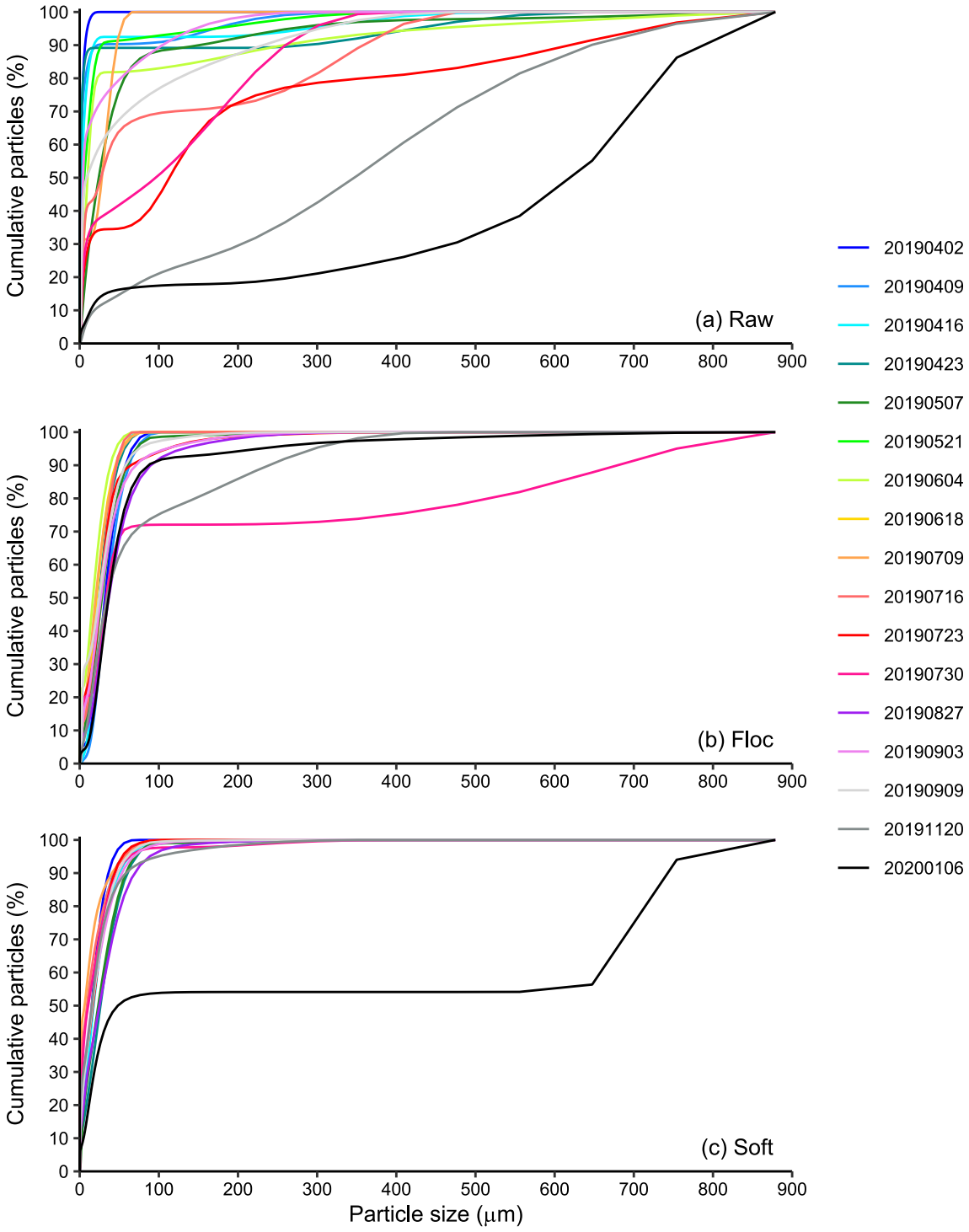

Figure A 5. Cumulative percent of particles for (a) unsettled raw river water, (b) unsettled flocculated water, and (c) unsettled softened water. Lines represent the average of four total technical replicates from two biological replicates for each water type on each collection date.

Table A 5. P-value from Pearson's r correlation coefficient between water quality characteristics (highlighted green indicates P-value < 0.05)

		TSS	Turbidity	DOC	UVA254	UVA254 IS	UVA254 C	SUVA	D[4,3]	D[3,2]	D(v,0.1)	D(v,0.5)	D(v,0.9)
Raw	Turbidity	5E-09											
	DOC	3E-04	4E-04										
	UVA254	2E-04	9E-14	2E-04									
	UVA254 IS	5E-02	2E-05	7E-02	4E-05								
	UVA254 C	2E-03	2E-02	6E-05	1E-02	6E-01							
	SUVA	2E-02	4E-10	1E-03	7E-13	4E-05	1E-02						
	D[4,3]	1E-01	8E-02	9E-01	1E-01	4E-03	5E-01	1E-01					
	D[3,2]	4E-02	8E-01	2E-01	7E-01	7E-01	1E-01	7E-01	8E-03				
	D(v,0.1)	4E-02	4E-01	6E-01	5E-01	2E-01	4E-01	5E-01	5E-04	2E-06			
	D(v,0.5)	2E-01	2E-02	6E-01	4E-02	1E-03	9E-01	3E-02	6E-08	1E-02	3E-04		
	D(v,0.9)	2E-01	3E-01	7E-01	4E-01	3E-02	2E-01	3E-01	5E-07	1E-02	7E-03	2E-04	
Floc	Turbidity	5E-03											
	DOC	6E-01	3E-03										
	UVA254	2E-02	9E-13	3E-04									
	UVA254 IS	3E-01	2E-05	1E-01	4E-04								
	UVA254 C	5E-02	9E-01	1E-01	5E-01	4E-02							
	SUVA	1E-03	9E-12	6E-03	4E-12	4E-04	6E-01						
	D[4,3]	5E-02	8E-01	9E-01	7E-01	5E-01	1E-01	6E-01					
	D[3,2]	4E-02	1E-01	1E-01	6E-02	7E-01	8E-02	6E-02	6E-02				
	D(v,0.1)	6E-01	2E-02	6E-01	7E-02	1E-03	4E-02	7E-02	9E-01	1E-01			
	D(v,0.5)	3E-02	8E-01	1E+00	1E+00	3E-01	1E-01	1E+00	3E-05	6E-04	7E-02		
	D(v,0.9)	5E-02	6E-01	1E+00	5E-01	6E-01	9E-02	4E-01	3E-13	6E-02	1E+00	1E-04	
	Alum	3E-02	3E-02	7E-02	2E-02	3E-01	1E-01	2E-02	7E-02	4E-02	3E-01	2E-01	7E-02
Soft	Turbidity	7E-07											
	DOC	5E-01	7E-01										
	UVA254	3E-05	3E-07	8E-01									
	UVA254 IS	8E-02	2E-01	8E-01	7E-03								
	UVA254 C	6E-02	4E-02	6E-01	4E-01	7E-03							
	SUVA	2E-01	1E-03	3E-02	1E-04	2E-02	7E-01						
	D[4,3]	1E-01	9E-01	8E-01	3E-01	2E-02	7E-02	7E-01					
	D[3,2]	1E-02	7E-01	9E-01	6E-01	9E-02	1E-01	8E-01	8E-06				
	D(v,0.1)	3E-02	9E-01	9E-01	3E-01	2E-02	7E-02	7E-01	0E+00	2E-06			
	D(v,0.5)	3E-01	1E+00	8E-01	3E-01	4E-02	1E-01	6E-01	8E-07	8E-09	4E-07		
	D(v,0.9)	5E-01	9E-01	8E-01	3E-01	2E-02	6E-02	7E-01	0E+00	1E-05	0E+00	1E-06	
All	Turbidity	0E+00											
	DOC	7E-03	3E-04										
	UVA254	8E-02	2E-02	5E-03									
	UVA254 IS	8E-03	5E-01	4E-03	5E-09								
	UVA254 C	1E-02	7E-06	8E-01	8E-04	5E-02							
	SUVA	4E-06	6E-13	1E-02	3E-07	5E-02	4E-05						
	D[4,3]	5E-02	2E-01	3E-02	7E-02	3E-05	1E-02	5E-01					
	D[3,2]	2E-04	2E-04	5E-01	2E-01	2E-01	5E-05	2E-03	4E-06				
	D(v,0.1)	7E-04	2E-02	2E-01	3E-01	1E-04	2E-03	3E-01	2E-07	1E-15			
	D(v,0.5)	2E-02	2E-01	6E-03	4E-03	2E-05	2E-01	8E-01	9E-15	3E-06	1E-09		
	D(v,0.9)	6E-02	8E-02	7E-02	5E-01	8E-04	9E-04	2E-01	0E+00	4E-05	5E-05	3E-08	

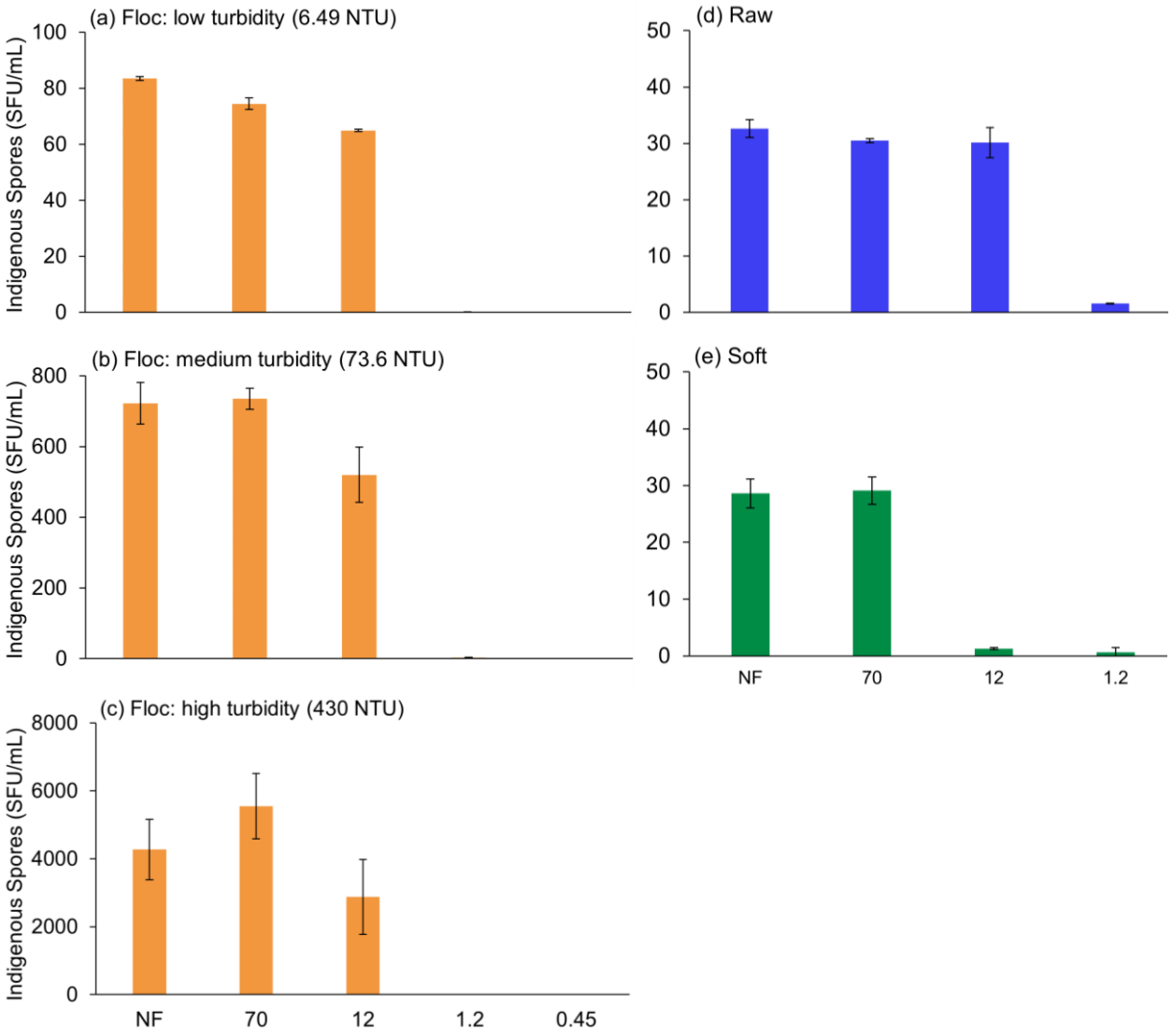

Figure A 6. Spore forming units per milliliter for water filtrate through various filter sizes (microns). NF stands for "No Filter." Three filtrate experiments were performed on flocculated water with variable turbidity values: (a) November 20, 2019, (b) June 4, 2019, and (c) June 18, 2019. On November 20, 2019, filtrate experiments were also performed on (d) raw and (e) softened water. The bar graph represents the average of two enumeration replicates each from two technical filtration replicates (four total replicates for each bar), except for November 20, 2019, with only two enumeration replicates from one filtration sample. Error bars represent standard deviation values between the replicates.

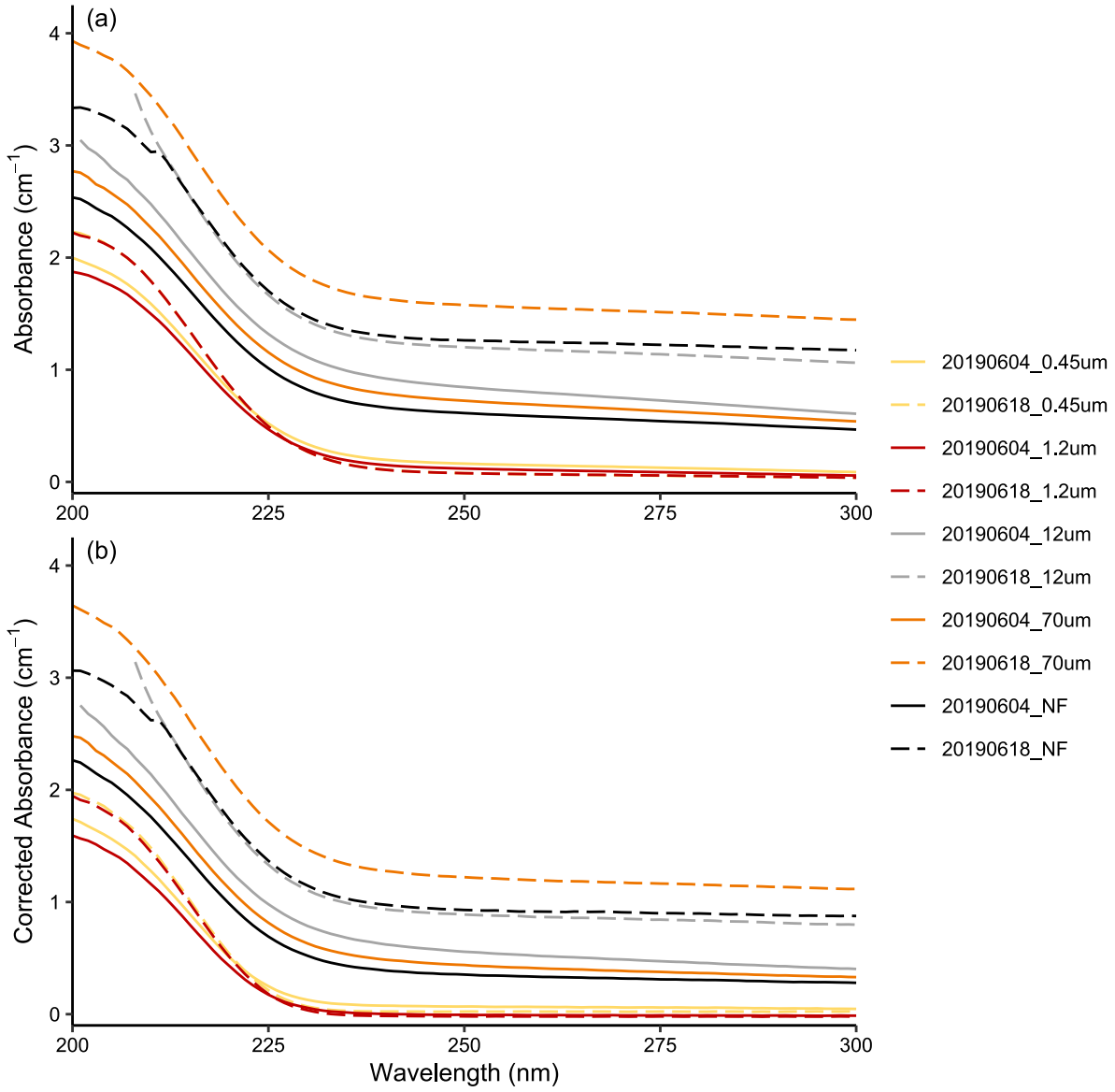

Figure A 7. (a) Aborbance measurements and (b) corrected absorbance measurements for the different filtrate levels from the filtrate experiment for June 4, 2019 (turbidity < 100 NTU) and June 18, 2019 (turbidity > 400 NTU). Lines represent the average between three replicates from each filtrate Absorbance measurements beyond the dynamic range were omitted.

Table A 6. Geeraerd tail model parameters for each water type, calculated with the average of each biological replicate for each water type and collection date (Figure 4.10). Values are from GInaFiT (Geeraerd et al., 2005)

Geeraerd Tail Model Parameter	Water Type & Dose Calculation	Parameter Values	Standard Error
k_{max} (1/dose)	Raw	0.027	0.004
	Raw (corrected)	0.026	0.004
	Floc	0.021	0.004
	Floc (corrected)	0.020	0.004
	Soft	0.030	0.003
	Soft (corrected)	0.028	0.003
N_{res} (SFU/mL)	Raw	1.168	1.887
	Raw (corrected)	1.722	1.519
	Floc	7.081	1.561
	Floc (corrected)	8.892	1.382
	Soft	0.216	1.297
	Soft (corrected)	0.225	1.305
N_0 (SFU/mL)	Raw	134.0	1.186
	Raw (corrected)	137.9	1.200
	Floc	200.6	1.134
	Floc (corrected	203.2	1.141
	Soft	15.50	1.124
	Soft (corrected)	15.40	1.130

Table A 7. Quadratic model parameters for each water type, calculated with the average of each biological replicate for each water type and collection date (Figure 4.10).

Quadratic Model Parameter	Water Type & Dose Calculation	Parameter Values	Standard Error
Linear coefficient ($SFU \cdot mL^{-1} \cdot fluence^{-1}$)	Raw	1.31E-02	7.15E-04
	Raw (corrected)	1.27E-02	4.97E-04
	Floc	8.97E-03	4.85E-04
	Floc (corrected)	7.92E-03	3.13E-04
	Soft	1.40E-02	7.27E-04
	Soft (corrected)	1.34E-02	6.40E-04
Quadratic coefficient ($SFU \cdot mL^{-1} \cdot fluence^{-2}$)	Raw	-1.53E-05	4.06E-06
	Raw (corrected)	-1.84E-05	2.15E-06
	Floc	-1.05E-05	2.72E-06
	Floc (corrected)	-8.35E-06	1.41E-06
	Soft	-2.45E-05	4.18E-06
	Soft (corrected)	-2.28E-05	3.38E-06

Table A 8. Goodness of fit between Geeraerd-tail and quadratic models shown in Figure 4.10

	Water Type	RMSE		R^2		adjusted R^2	
		Geeraerd-tail	Quadratic	Geeraerd-tail	Quadratic	Geeraerd-tail	Quadratic
Uncorrected	Raw	0.456	0.177	0.702	0.976	0.696	0.976
	Floc	0.345	0.129	0.665	0.974	0.659	0.973
	Soft	0.321	0.191	0.810	0.968	0.806	0.967
Corrected	Raw	0.484	0.205	0.664	0.968	0.657	0.968
	Floc	0.362	0.128	0.631	0.974	0.624	0.973
	Soft	0.337	0.194	0.790	0.967	0.786	0.966

Table A 9. Geeraerd shoulder-tail and quadratic model parameters for each water type and PBS during the spiking experiment

Model	Model Parameter (units)	Water Type	Parameter Values	Standard Error
Geeraerd shoulder-tail	k_{max} (1/fluence)	Raw	2.40E-01	6.20E-02
		Floc	1.22E-01	1.29E-02
		Soft	1.63E-01	1.27E-02
		PBS	2.41E-01	3.52E-02
	SI (fluence)	Raw	9.60E+00	7.84E+00
		Floc	1.17E+01	6.65E+00
		Soft	8.97E+00	4.85E+00
		PBS	1.53E+01	3.75E+00
	N_{res} (SFU/mL)	Raw	1.20E+02	1.74E+00
		Floc	2.20E+02	1.37E+00
		Soft	1.24E+01	1.40E+00
		PBS	3.85E+01	1.27E+00
	N_0 (SFU/mL)	Raw	5.84E+06	2.49E+00
		Floc	6.23E+06	1.49E+00
		Soft	5.93E+06	1.56E+00
		PBS	3.67E+06	1.42E+00
Quadratic	Linear coefficient ($SFU \cdot mL^{-1} \cdot fluence^{-1}$)	Raw	7.04E-02	7.98E-03
		Floc	4.80E-02	6.09E-03
		Soft	6.92E-02	8.17E-03
		PBS	7.62E-02	9.36E-03
	Quadratic coefficient ($SFU \cdot mL^{-1} \cdot fluence^{-2}$)	Raw	-2.34E-04	4.53E-05
		Floc	-1.26E-04	3.46E-05
		Soft	-2.06E-04	4.64E-05
		PBS	-2.62E-04	5.32E-05

Table A 10. Average water quality data after samples were spiked with *B. subtilis*. Initial concentration includes indigenous spores and spiked *B. subtilis* spores.

Water Type	Turbidity (NTU)		abs254 (cm^{-1})		D[4,3] (µm)		D[3,2] (µm)		D(v,0.1) (µm)		D(v,0.5) (µm)		D(v,0.9) (µm)		Initial Concentration (SFU/mL)	
	$\bar{x}$	σ	$\bar{x}$	σ	$\bar{x}$	σ	$\bar{x}$	σ	$\bar{x}$	σ	$\bar{x}$	σ	$\bar{x}$	σ	$\bar{x}$	σ
Raw	156	1.73	1.93	0.04	68.9	2.47	3.47	0.03	2.58	0.10	28.9	0.47	208	5.60	5.20E+06	1.50E+05
Floc	192	7.55	1.27	0.07	55.5	1.46	35.2	1.65	20.8	1.18	46.6	0.29	97.6	5.18	5.70E+06	7.00E+05
Soft	470	4.58	0.95	0.02	57.1	0.70	4.11	0.16	5.98	0.20	42.0	0.22	123	2.72	4.95E+06	1.50E+05
PBS	17.1	0.44	0.74	0.01	216	32.3	9.69	1.26	6.93	0.97	165	30.6	516	67.2	3.88E+06	6.25E+05

Table A 11. P-values from ANOVA and tukey analysis (highlighted green indicates P-value < 0.05)

	Comparison	k_{max}	N_{res}	N_0	Linear coef	Quad coef
Uncorrected	raw-floc	5E-03	6E-03	9E-01	8E-04	6E-01
	soft-floc	6E-05	4E-05	7E-02	3E-05	2E-02
	soft-raw	4E-01	3E-01	2E-01	7E-01	2E-01
Corrected	raw-floc	2E-02	6E-03	9E-01	3E-03	7E-01
	soft-floc	3E-05	4E-05	7E-02	2E-05	1E-02
	soft-raw	1E-01	3E-01	2E-01	3E-01	1E-01

Table A 12. P-values from nested ANOVA and Tukey analysis between corrected and uncorrected models for each water type

Comparison	kmax	Nres	N0	Linear coef	Quad coef
raw:uncorrected - raw:corrected	6E-01	1E+00	1E+00	7E-01	1E+00
floc:uncorrected - floc:corrected	9E-01	1E+00	1E+00	9E-01	1E+00
soft:uncorrected - soft:corrected	9E-01	1E+00	1E+00	1E+00	1E+00

Table A 13. P-values for Pearson's r correlation coefficient between the water quality characteristics and parameters from the uncorrected modeled dose response (P-value < 0.05 highlighted in green, n = 8 for TSS, n = 15 for raw, and n = 17 floc and soft for other characteristics)

	Model and Parameter	TSS	Turbidity	DOC	abs254 Direct	abs254 IS	abs254 Corrected	SUVA	D[4,3]	D[3,2]	D(v,0.1)	D(v,0.5)	D(v,0.9)
Raw	k_{max}	8E-02	6E-02	1E-03	3E-02	6E-01	1E-04	3E-02	3E-01	7E-02	3E-01	5E-01	1E-01
	N_{res}	5E-06	3E-08	1E-03	2E-07	2E-04	2E-02	1E-06	2E-01	7E-01	5E-01	6E-02	5E-01
	N_0	2E-08	0E+00	3E-04	1E-14	3E-05	1E-02	2E-10	1E-01	8E-01	4E-01	3E-02	3E-01
	Linear coef	8E-02	4E-01	3E-02	3E-01	1E+00	1E-02	3E-01	9E-02	2E-02	6E-02	2E-01	4E-02
	Quad coef	6E-03	5E-01	2E-01	4E-01	1E+00	1E-01	4E-01	2E-01	2E-01	3E-01	2E-01	8E-02
Flocculated	k_{max}	8E-01	1E-01	3E-02	6E-02	7E-01	5E-02	8E-02	1E-01	4E-02	6E-01	1E-01	4E-02
	N_{res}	4E-02	1E-04	3E-04	8E-06	9E-02	4E-02	4E-05	5E-01	5E-02	5E-01	6E-01	3E-01
	N_0	2E-02	6E-15	1E-03	7E-12	5E-05	8E-01	9E-10	7E-01	1E-01	2E-02	8E-01	5E-01
	Linear coef	6E-01	1E-01	4E-02	6E-02	9E-01	2E-02	7E-02	1E-01	2E-02	3E-01	8E-02	4E-02
	Quad coef	9E-01	5E-01	2E-01	3E-01	6E-01	3E-02	4E-01	3E-01	8E-02	6E-02	1E-01	2E-01
Softened	k_{max}	1E-01	7E-01	6E-01	8E-01	6E-01	8E-01	5E-01	3E-01	8E-02	3E-01	2E-01	3E-01
	N_{res}	7E-01	4E-02	8E-01	2E-03	1E-03	4E-01	4E-03	3E-01	8E-01	3E-01	4E-01	3E-01
	N_0	4E-01	6E-01	8E-01	1E-01	2E-03	6E-02	2E-01	1E-03	1E-03	1E-03	5E-04	1E-03
	Linear coef	4E-02	1E+00	9E-01	8E-01	8E-01	6E-01	9E-01	2E-01	5E-02	2E-01	9E-02	2E-01
	Quad coef	5E-02	4E-01	9E-01	4E-01	4E-01	9E-01	4E-01	4E-01	6E-02	3E-01	2E-01	4E-01
All	k_{max}	1E-01	1E-03	8E-01	6E-02	9E-01	4E-03	9E-03	3E-01	7E-03	9E-02	9E-01	1E-01
	N_{res}	1E-01	3E-02	8E-03	1E-04	1E-04	7E-01	3E-01	6E-01	4E-01	6E-02	3E-01	9E-01
	N_0	2E-02	3E-01	7E-05	1E-10	2E-11	7E-01	7E-02	9E-02	7E-01	5E-03	1E-02	4E-01
	Linear coef	2E-01	4E-03	4E-01	1E-01	6E-01	2E-03	6E-02	1E-01	6E-04	1E-02	5E-01	6E-02
	Quad coef	5E-02	4E-03	8E-01	1E-01	7E-01	6E-03	1E-02	6E-02	8E-03	3E-02	2E-01	3E-02

Table A 14. P-values for Pearson's r correlation coefficient between the water quality characteristics and parameters from the corrected modeled dose response (P-value < 0.05 highlighted in green, n = 8 for TSS, n = 15 for raw, and n = 17 floc and soft for other characteristics)

	Model and Parameter	TSS	Turbidity	DOC	abs254 Direct	abs254 IS	abs254 Corrected	SUVA	D[4,3]	D[3,2]	D(v,0.1)	D(v,0.5)	D(v,0.9)
Raw	k_{max}	6E-02	4E-01	4E-01	5E-01	1E-02	3E-02	5E-01	5E-04	6E-02	3E-02	2E-03	3E-04
	N_{res}	5E-06	3E-08	1E-03	2E-07	2E-04	2E-02	1E-06	2E-01	7E-01	5E-01	6E-02	5E-01
	N_0	2E-08	0E+00	3E-04	1E-14	3E-05	1E-02	2E-10	1E-01	8E-01	4E-01	3E-02	3E-01
	Linear coef	4E-02	5E-01	3E-01	7E-01	6E-02	5E-02	7E-01	1E-03	2E-02	1E-02	3E-03	8E-04
	Quad coef	1E-03	1E+00	3E-01	9E-01	4E-01	1E-01	9E-01	3E-02	1E-01	2E-01	5E-02	2E-02
Flocculated	k_{max}	8E-01	7E-01	3E-01	9E-01	9E-02	3E-03	1E+00	1E-01	1E-01	5E-02	9E-02	8E-02
	N_{res}	4E-02	1E-04	3E-04	8E-06	9E-02	4E-02	4E-05	5E-01	5E-02	5E-01	6E-01	3E-01
	N_0	2E-02	6E-15	1E-03	7E-12	5E-05	8E-01	9E-10	7E-01	1E-01	2E-02	8E-01	5E-01
	Linear coef	6E-01	9E-01	2E-01	6E-01	2E-01	1E-03	7E-01	1E-01	5E-02	2E-02	5E-02	6E-02
	Quad coef	9E-01	1E+00	3E-01	7E-01	2E-01	1E-02	7E-01	3E-01	1E-01	2E-02	1E-01	2E-01
Softened	k_{max}	1E-01	9E-01	9E-01	7E-01	6E-01	8E-01	1E+00	1E-01	4E-02	1E-01	1E-01	2E-01
	N_{res}	7E-01	4E-02	8E-01	2E-03	1E-03	4E-01	4E-03	3E-01	8E-01	3E-01	4E-01	3E-01
	N_0	4E-01	6E-01	8E-01	1E-01	2E-03	6E-02	2E-01	1E-03	1E-03	1E-03	5E-04	1E-03
	Linear coef	3E-02	6E-01	8E-01	3E-01	5E-01	1E+00	4E-01	1E-01	2E-02	9E-02	4E-02	1E-01
	Quad coef	6E-02	8E-01	6E-01	9E-01	1E+00	9E-01	1E+00	3E-01	3E-02	3E-01	1E-01	3E-01
All	k_{max}	8E-02	2E-03	6E-01	9E-01	1E-02	4E-04	1E-01	2E-02	2E-03	4E-03	1E-01	1E-02
	N_{res}	1E-01	3E-02	8E-03	1E-04	1E-04	7E-01	3E-01	6E-01	4E-01	6E-02	3E-01	9E-01
	N_0	2E-02	3E-01	7E-05	1E-10	2E-11	7E-01	7E-02	9E-02	7E-01	5E-03	1E-02	4E-01
	Linear coef	1E-01	4E-03	1E+00	9E-01	1E-02	3E-04	3E-01	9E-03	2E-04	5E-04	7E-02	5E-03
	Quad coef	3E-02	5E-03	6E-01	5E-01	1E-01	2E-03	6E-02	1E-02	4E-03	7E-03	5E-02	6E-03

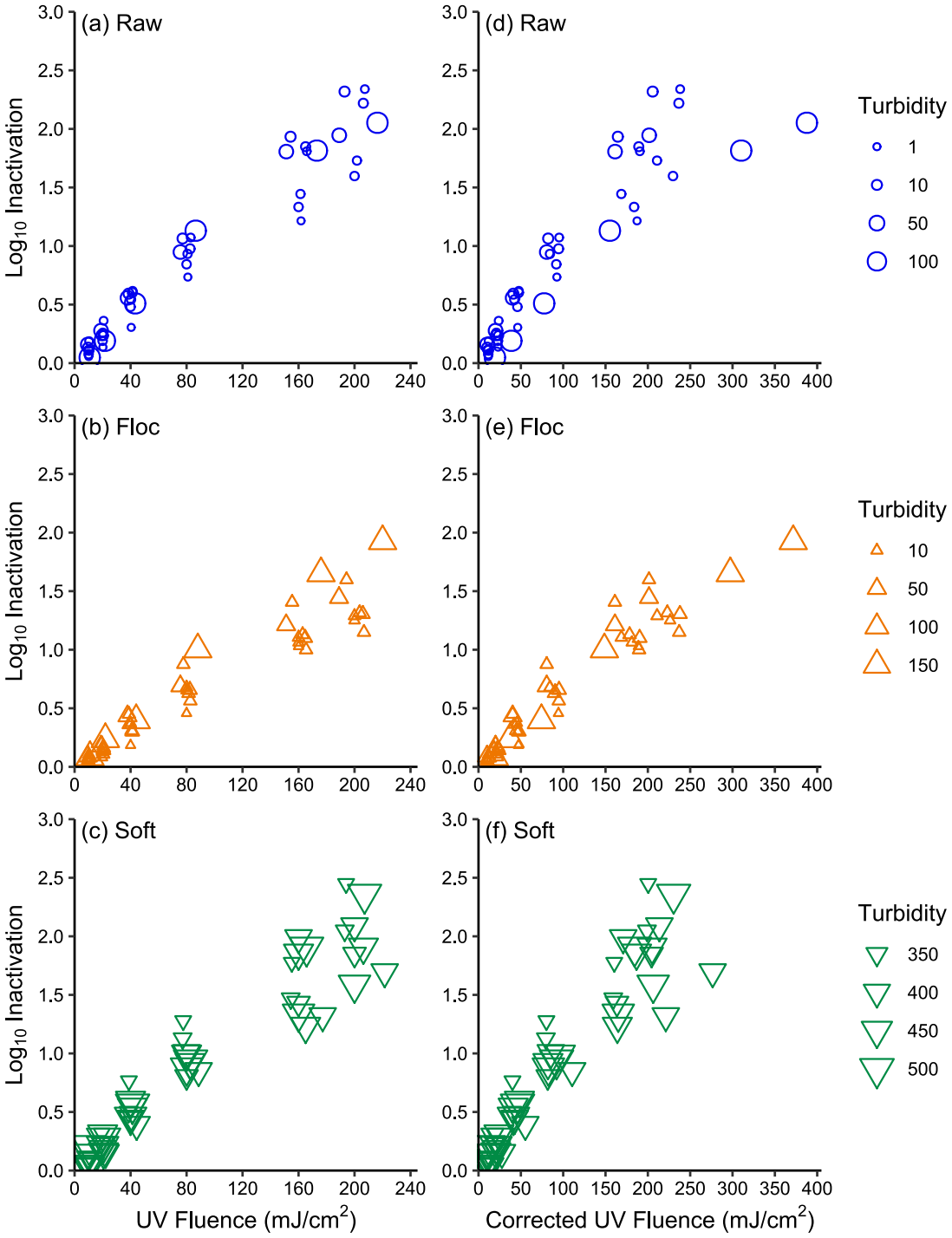

Figure A 8. Log inactivation graphs with point sizes that correspond to turbidity measurements (NTU) of that sample. For subfigures a – c on the left, the legend sizes are the same. For subfigures d – f on the right, the legend sizes are dependent on the size range of the respective water type. Softened water has the highest turbidity but a similar dose response to raw river water and a better dose response than flocculated water. Both flocculated water and raw river water plots show that samples with high turbidity did not have the worst dose response. Correlation between turbidity and UV inactivation is not visually apparent.

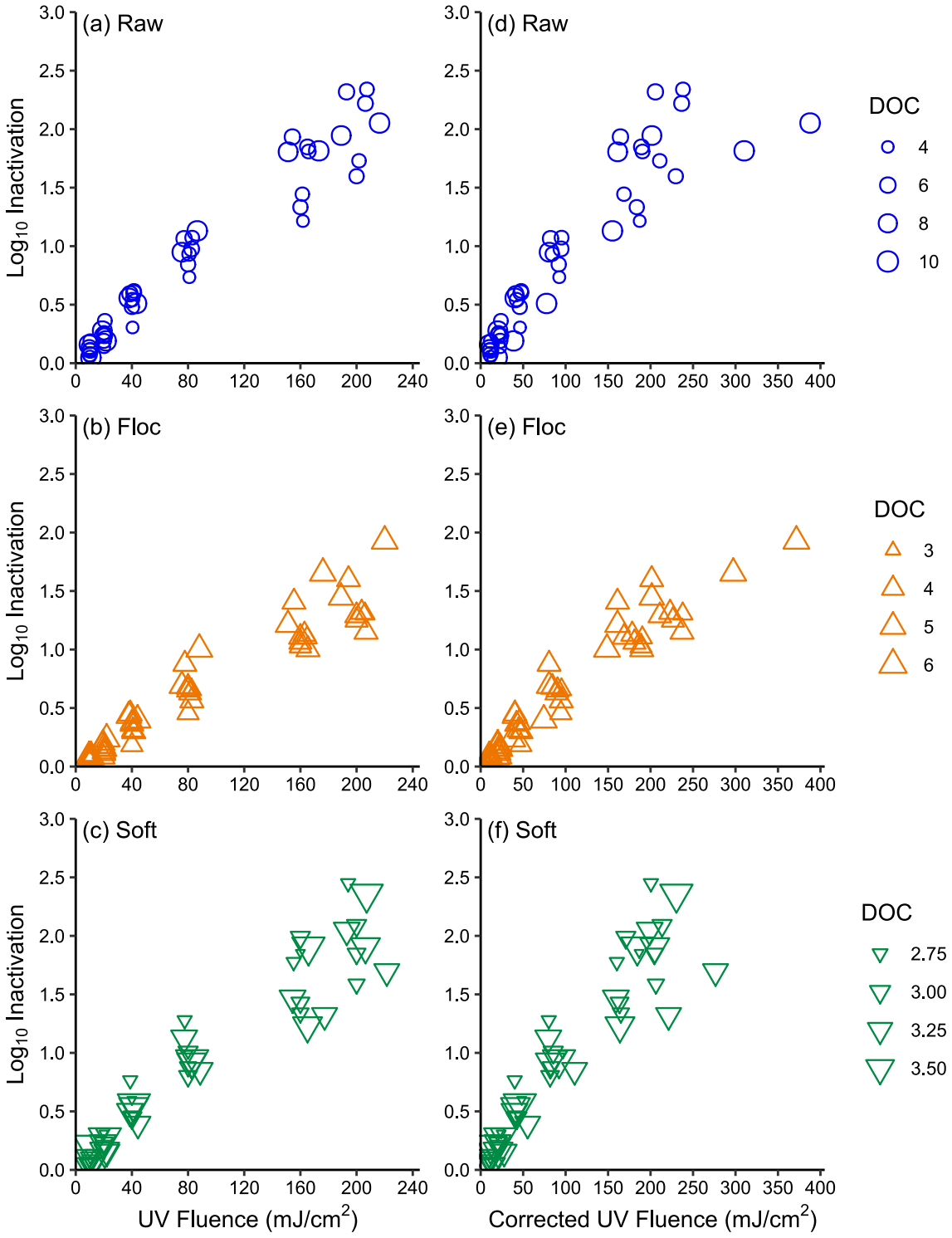

Figure A 9. Log inactivation graphs with point sizes that correspond to dissolved organic carbon measurements (mgC/L) of that sample. For subfigures a – c on the left, the legend sizes are the same. For subfigures d – f on the right, the legend sizes are dependent on the size range of the respective water type. Raw river water has the highest DOC and unsettled softened water has the lowest DOC.

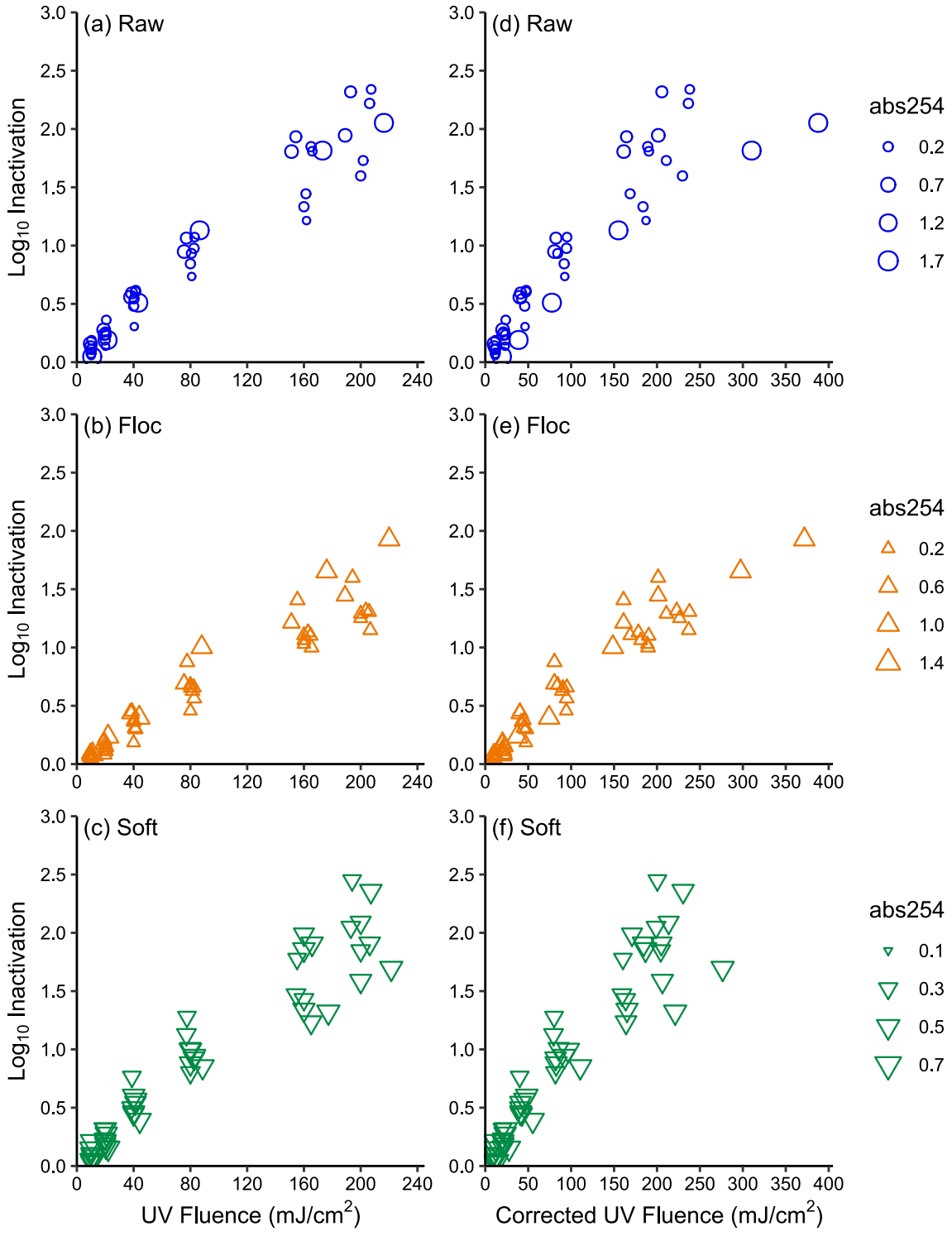

Figure A 10. Log inactivation graphs with point sizes that correspond to the UV absorbance at 254 nm measurements of that sample. For subfigures a – c on the left, the legend sizes are the same. For subfigures d – f on the right, the legend sizes are dependent on the size range of the respective water type.

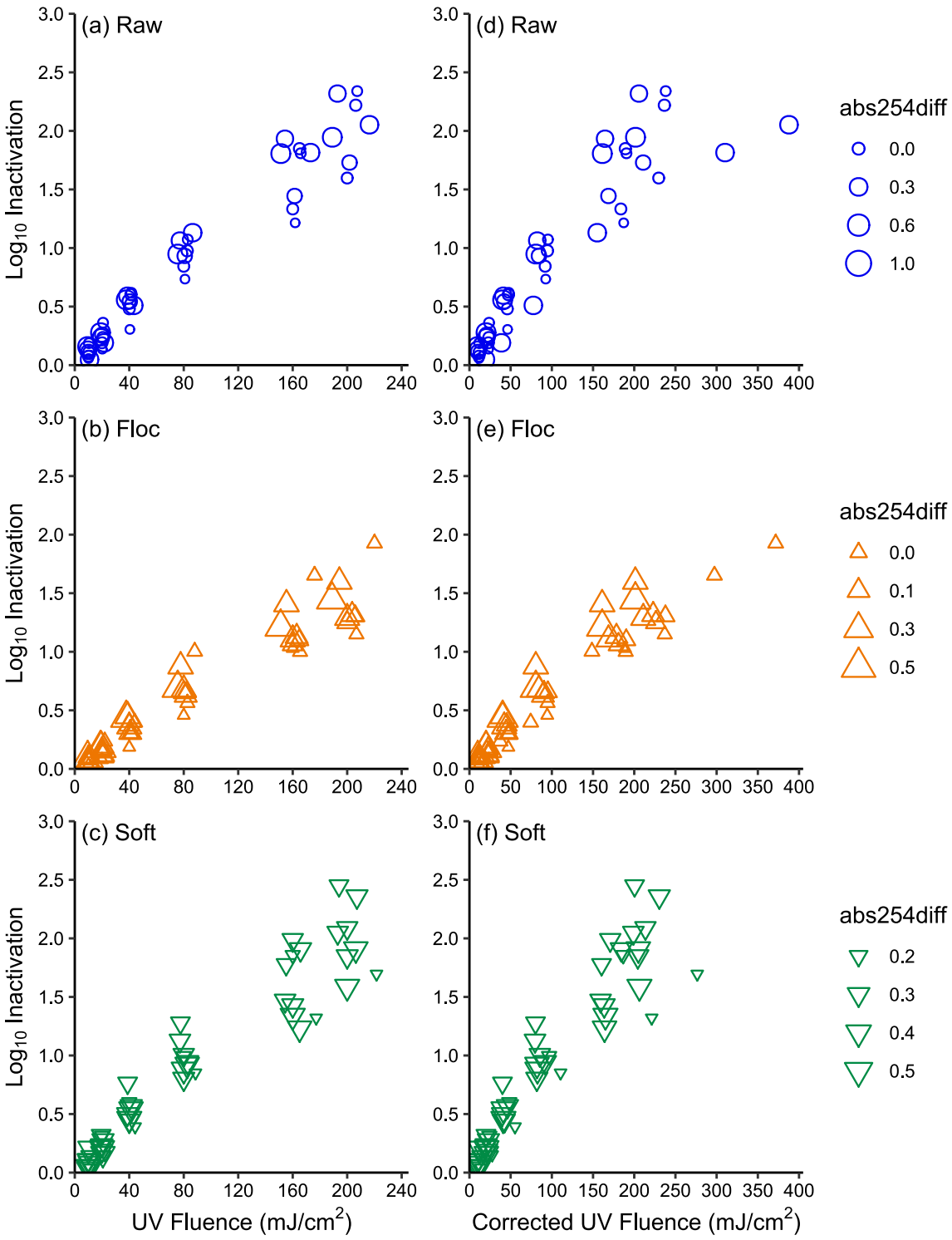

Figure A 11. Log inactivation graphs with point sizes that correspond to the corrected absorbance: the difference in UV absorbance measurements at 254 nm and the integrating sphere UV absorbance measurements at 254 nm of that sample. For subfigures A – C on the left, the legend sizes are the same. For subfigures D – F on the right, the legend sizes are dependent on the size range of the respective water type.

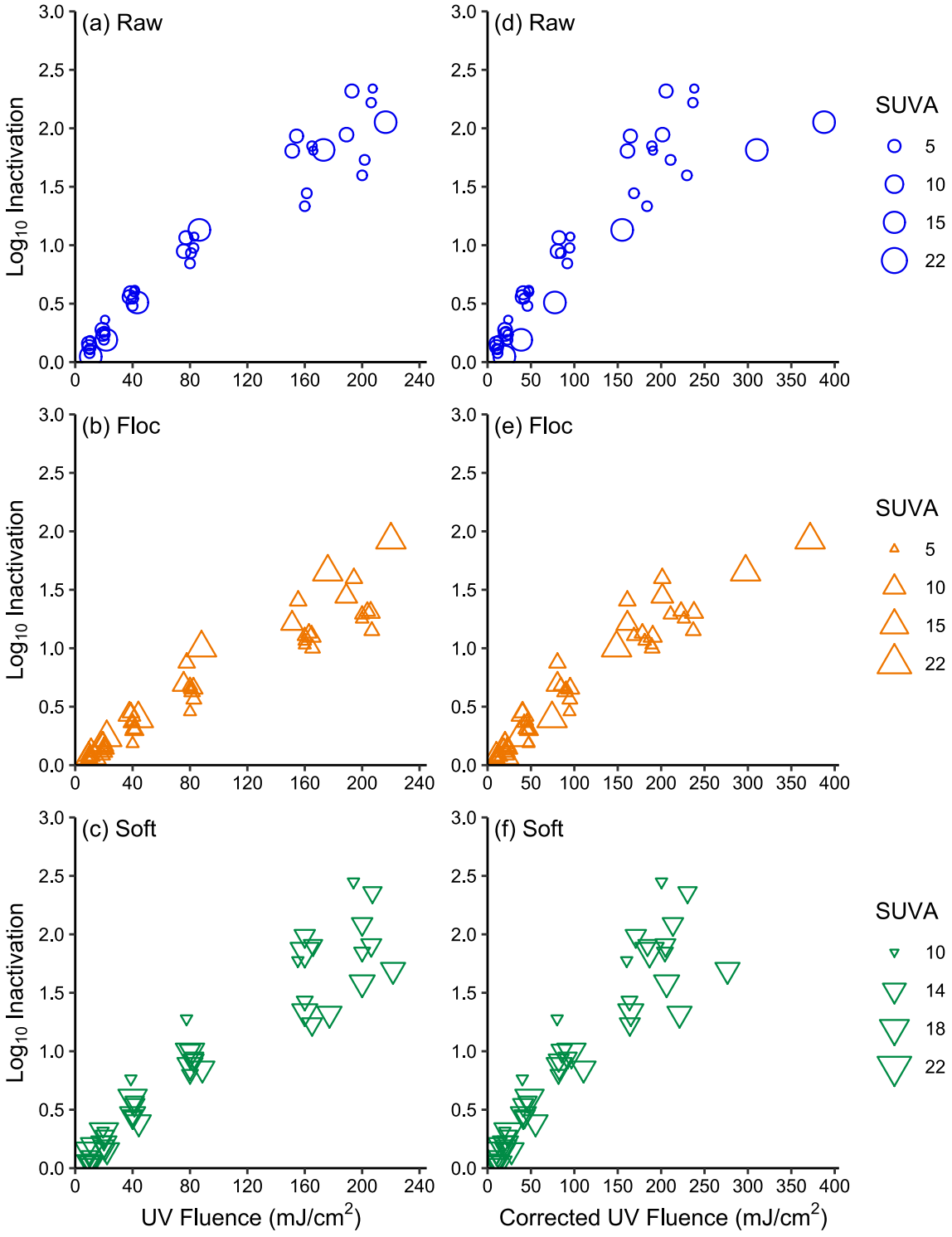

Figure A 12. Log inactivation graphs with point sizes that correspond to the SUVA calculations of that sample. For subfigures A – C on the left, the legend sizes are the same. For subfigures D – F on the right, the legend sizes are dependent on the size range of the respective water type.

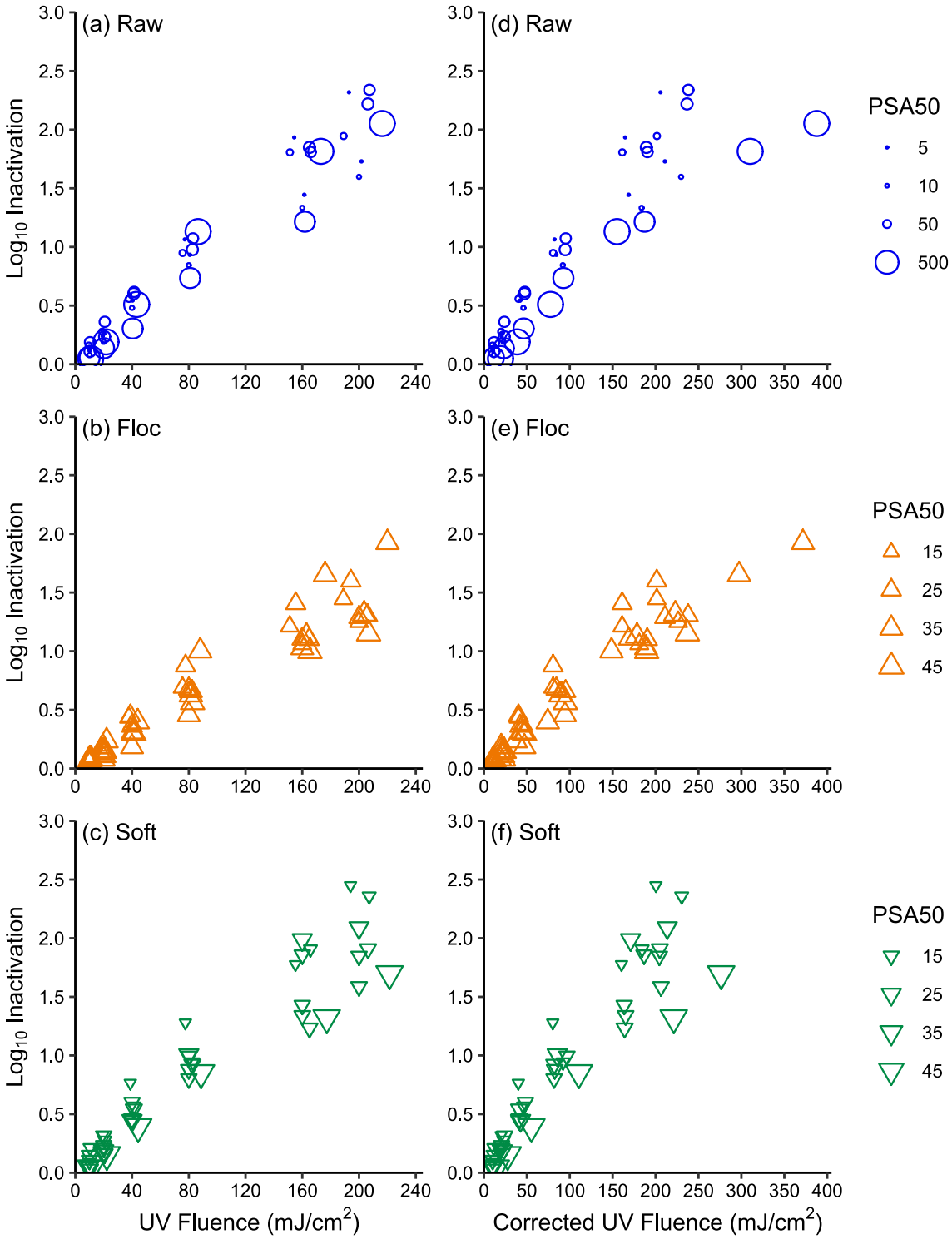

Figure A 13. Log inactivation graphs with point sizes that correspond to the median particle size (PSA50) of that sample. For subfigures A – C on the left, the legend sizes are the same. For subfigures D – F on the right, the legend sizes are dependent on the size range of the respective water type. Flocculated water has a larger median particle size than softened water.